Intrathecal B cells in multiple sclerosis

Doctoral thesis by

Justyna Polak

UiO : Faculty of Medicine
University of Oslo

Department of Molecular Medicine

Institute of Basic Medical Sciences

University of Oslo

2024

Series of dissertations submitted to the
Faculty of Medicine, University of Oslo

ISBN 978-82-348-0382-6

Cover: UiO.
Print production: Graphic center, University of Oslo.

Table of contents

1. Summary

English

Multiple sclerosis is a chronic, inflammatory, neurodegenerative disease that affects the central nervous system and has no known cure. The development of the disease is likely influenced by a combination of genetic, environmental, and stochastic factors. The pathology of the disease is characterized by immune cell infiltration of the central nervous system, and B cells seem to play a significant role in this process. Specifically, B cells have been shown to form tertiary lymphoid structures in the meninges; they may produce cytokines and neurotoxic factors and could act as antigen-presenting cells and activate pathogenic T cells. Moreover, B cells are known to differentiate into antibody-secreting cells that produce intrathecal IgG, which is a hallmark of MS.

The main goal of this thesis was to gain insights into the mechanisms underlying B-cell responses in both treated and treatment-naïve multiple sclerosis patients. To this end, we characterized the B-cell receptor repertoire, clonal relationships, and transcriptional profiles of B-lineage cells found in the cerebrospinal fluid of multiple sclerosis patients. Utilizing techniques such as flow cytometry index-sorting and single-cell full-length mRNA sequencing, we conducted a detailed study of B-lineage cells, dissecting their phenotypes and revealing specific patterns of paired heavy- and light-chain gene usage. Next, by combining paired heavy- and light-chain variable region data with mass spectrometry analysis of IgG from cerebrospinal fluid and serum samples, we found that the intrathecal IgG-producing B cells are heterogenous and include highly proliferating cells as well as more differentiated cells primarily focused on immunoglobulin production. Finally, we also examined the B cell composition and phenotypes in the cerebrospinal fluid of multiple sclerosis treated with dimethyl fumarate. Our results support the theory that memory B cells are a potential mechanistic target of dimethyl fumarate.

This work sheds light on the role of B cells in the context of the intrathecal immunoglobulin repertoire in multiple sclerosis. It also discusses the consequences of our results in light of immunomodulatory treatment options for patients suffering from multiple sclerosis.

Norsk

Multipel sklerose er en kronisk, inflammatorisk og nevrodegenerativ sykdom som skader sentralnervesystemet. Sykdommen har i dag ingen kur. Man antar at sykdommen skyldes en kombinasjon av genetiske, miljømessige og stokastiske faktorer. Patologien kjennetegnes av en infiltrasjon av immunceller i sentralnervesystemet, og B-celler ser ut til å spille en vesentlig rolle i denne prosessen. Det er vist at B-celler danner tertiære lymfoide strukturer i hjernehinnene, de kan produsere cytokiner og nevrotoksiske faktorer og de kan fungere som antigenpresenterende celler og aktivere patogene T-celler. Dessuten kan B-celler differensiere til antistoffproduserende celler og skille ut IgG i spinalvæsken, som er et kjennetegn på multipel sklerose.

Formålet med denne studien var å få innsikt i mekanismene som ligger til grunn for B–celleresponser hos både behandlede og ubehandlede pasienter med multippel sklerose. Vi benyttet oss av metoder som flowcytometri og enkeltcelle fullengde mRNA-sekvensering for å utforske ulike fenotyper av B-celler og analysere bruk av spesifikke mønstre av sammenkoblet tung- og lettkjede. Deretter kombinerte vi data fra de sammenkoblede tunge og lette kjedene med massespektrometri-analyse av IgG fra cerebrospinalvæske og serum. Gjennom denne analysen fant vi at de intratekale IgG-produserende B-cellene er noe heterogene og spenner fra svært prolifererende celler til mer differensierte celler som hovedsakelig fokuserer på produksjon av antistoffer. Til slutt analyserte vi B-cellesammensetningen og fenotypene i cerebrospinalvæsken hos pasienter med multippel sklerose som er behandlet med dimetylfumarat. Resultatene gir støtte til teorien om at hukommelses-B-celler er et potensielt terapeutisk mål for dimetylfumarat.

Dette arbeidet gir innsikt i B-celle-repertoaret i cerebrospinalvæsken hos pasienter med multippel sklerose. Videre drøfter avhandlingen konsekvensene av våre funn i lys av nåværende og fremtidige behandlingsmuligheter.

2. Acknowledgments

The present work was conducted at the Department of Immunology and Transfusion Medicine, University of Oslo, at the Oslo University Hospital Rikshospitalet from 2017–2022. The work was funded by a grant from Norske Kvinders Sanitetsforening, contributions from the University of Oslo, and a research award from Novartis. For this support, I express my sincere gratitude.

First, I would like to thank my main supervisor, Andreas Lossius, who made this thesis possible. Thank you for giving me the opportunity, guiding me through the process, letting me experience science in all its colors, and believing in me even when I did not. You have taught me many things, but your love for science has always been the most inspiring. I am also profoundly grateful for the supervision, guidance, support, and critical thinking of co-supervisors Trygve Holmøy and Ludvig M. Sollid. This thesis is a result of your expertise and ability to ask the most important questions. Thank you all for granting me a chance to learn and grow.

This work heavily relied on close collaboration. Ida Lindeman, thank you for greatly contributing to processing and analyzing large amounts of data, giving valuable input, and shaping the entirety of my work. Silje Torsetnes, thank you for the teamwork and for sharing your knowledge and ideas in mass spectrometry. Thanks to colleagues from the MS research group, first and foremost Frode Vartdal, who always provided constructive discussion and deep insight into allotypes and immunology as a whole. I am grateful for your expertise in and out of the laboratory, as well as the financial support that allowed us to complete this project. Alina Tomescu-Baciu, Rune Høglund, Egil Røsjø, and Johanna Henny Wagnerberger, our collaborations, discussions, and brainstorming sessions were truly enjoyable and helpful. You created a supportive scientific environment and were a great help in writing this thesis. Rune, thank you for every “pick-me-up” along the way; they always made me feel like I belonged. Johanna, your patience and enthusiasm in the data jungle were greatly appreciated. Egil, never change your scientific honesty policy. Last but not least, Alina, I am so grateful for the memes, dark humor, and amazingly supportive friendship. They will stay with me forever.

I would also like to thank Shuo-Wang Qiao for providing me the tools to uncover the mysteries of Smart-seq2. Łukasz Wyrożemski, you taught me how to perform the protocol

and made the entire process infinitely easier in the laboratory and the lunchroom. Marc McGowan, thank you for showing the light at the tunnel's end.

Additionally, I want to express gratitude for the ways I benefited from the knowledge and facilities of the Functional Immunogenetics group and the KG Jebsen Coeliac Disease Research Centre. I am also grateful to all members of the Gutfeeling group, especially the research technicians Bjørg Simonsen and Marie K. Johannesen, for their invaluable help and readiness to answer all questions, even the most mundane.

Studies like this would never be possible without patients' willingness o; therefore, a heartfelt thank you to all who shared samples with us. I also thank all the doctors at the Departments of Neurology at Akershus University Hospital and Ullevaal Oslo University Hospital who participated in the tedious patient recruitment process.

Most importantly, I want to thank my Polish and Norwegian families for their unwavering support and faith in me. I am grateful to my Norwegian family for inviting me in and showing me the beauty of this country, its traditions, and its culture. This work would have been immensely more difficult without my partner Jonas's advice and programming skills. But the biggest thank you goes to my mother and sister for showing me what is possible.

Justyna Polak

Oslo, 2023

3. Abbreviations

ADCC	Antibody-dependent cell-mediated cytotoxicity
APC	Antigen-presenting cells
ASC	Antibody-secreting cell
BAFF	B-cell survival factor
BBB	Blood-brain barrier
BCR	B-cell receptors
BTK	Bruton's tyrosine kinase
C	Constant region
CDR	Complementarity-determining region
CH	Constant heavy region
CIS	Clinically isolated syndrome
CNS	Central nervous system
CSF	Cerebrospinal fluid
CSR	Class-switch recombination
CXCL	C-X-C motif chemokine ligand
CXCR	C-X-C motif chemokine receptor
D	Diversity
DC	Dendritic cell
DMF	Dimethyl fumarate
DMT	Disease-modifying therapies
EAE	Autoimmune encephalomyelitis
EBV	Epstein-Barr virus
Fab	Antibody-binding fragment
Fc	Crystallizable fragment
FcR	Fc receptor
FcRn	Neonatal Fc receptor
FDC	Follicular dendritic cell
FR	Framework region
Fv	Variable fragment
GC	Germinal centers
GWAS	Genome-Wide Association Studies
HIV	Human immunodeficiency virus
HLA	Human leukocyte antigen
iBAQ	Intensity-based absolute quantification
IEF	Isoelectric focusing
IgH	Immunoglobulin heavy chain
IgL	Light chain
Igκ	Kappa light chain
Igλ	Lambda light chain
IL	Interleukin
J	Joining
mAb	Monoclonal antibodies
MHC	Major histocompatibility complex
MMF	Monomethyl fumarate
MRI	Magnetic resonance imaging
MRZ	Measles, rubella, varicella-zoster virus
MS	Multiple sclerosis
NK	Natural killer
OCB	Oligoclonal bands
PB	Plasmablasts
PC	Plasma cells
PPMS	Primary progressive multiple sclerosis
RRMS	Relapsing-remitting multiple sclerosis
SHM	Somatic hypermutation
SNP	Single nucleotide polymorphism
SPMS	Secondary progressive multiple sclerosis
T_{fh}	T follicular helper cell
T_h	T helper cell
TLS	Tertiary lymphoid structures
TPM	Transcript per million
T_{reg}	T regulatory cell
t-SNE	T-distributed stochastic neighbor embedding
UMAP	Uniform manifold approximation and projection
UVB	Ultraviolet B
V	Variable

4. Publications

Paper I - Lindeman I*, Polak J*, Qiao SW, Holmøy T, Høglund RA, Vartdal F, Berg-Hansen P, Sollid LM, Lossius A. *Stereotyped B-cell responses are linked to IgG constant region polymorphisms in multiple sclerosis*. Eur J Immunol. 2022;0:1-16. doi:10.1002/eji.202149576

**Shared first authorship*

Paper II - Polak J, Wagnerberger JH, Torsetnes SB, Lindeman I, Høglund RA, Vartdal F, Sollid LM, Lossius A. *Single-cell transcriptomics combined with proteomics of intrathecal IgG reveal transcriptional heterogeneity of oligoclonal IgG-secreting cells in multiple sclerosis.* Front Cell Neurosci. 2023;17(June):1-7. doi:10.3389/fncel.2023.1189709

Paper III - Høglund RA, Polak J, Vartdal F, Holmøy T, Lossius A. *B-cell composition in the blood and cerebrospinal fluid of multiple sclerosis patients treated with dimethyl fumarate.* Mult Scler Relat Disord. 2018;26:90-95. doi:10.1016/j.msard.2018.08.032

5. Introduction

5.1. Innate and adaptive immune responses

The human immune system, traditionally divided into the innate and adaptive immune systems, protects the body from a multitude of pathogens and foreign substances. Often described as the first line of defense, the innate immune system distinguishes self from non-self and identifies danger-associated molecular patterns. This identification of danger initializes an immediate reaction against a broad spectrum of invading pathogens and other threats to an organism's homeostasis[1]. In contrast, initial responses in the adaptive immune system develop more slowly, although they are far more efficient at targeting specific foreign antigens than innate immunity responses[2]. An antigen is any substance that causes an adaptive immune response. In subsequent encounters with the same pathogen, the adaptive system responds promptly and more efficiently due to the creation of immunological memory[1]. Thus, adaptive immunity provides long-lasting protection against the pathogen, often for the entire lifespan.

T cells and B cells are the two main cell lineages constituting the adaptive immune system. Both cell types express receptors that recognize antigens and allow for a precise response against a given threat. The B-lineage cells and B-cell receptors (BCRs) are described in greater detail in chapters 5.2 and 5.3. Adaptive responses can be categorized as humoral immunity and cell-mediated immunity. In humoral responses, activated B cells produce antibodies that bind to foreign antigens. This neutralizes the antigen or signals other immune system components to take action. In contrast, cell-mediated immunity destroys cells that show signs of foreign antigens by inducing cell death (apoptosis) or secreting compound signals (cytokines) that are inflammatory indicators for other immune cells[1]. Cells from the B- and T-cell lineages cooperate and further the defensive capabilities of innate immunity to create an efficient and specific system with vast possibilities for protection. However, when these systems malfunction, pathogens are not detected, leading to immunodeficiency or to autoimmunity, in which the body cannot distinguish between healthy self-antigens and foreign tissues[1].

5.2. B cells

The role of B cells is to recognize epitopes (fragments of antigens), produce antibodies, and develop and maintain immunological memory[1]. B cells also possess a regulatory function, in which they alter the behaviors of other cells through cytokine secretion and the modulation of T-cell survival and differentiation. In addition, they can act as antigen-presenting cells (APC), meaning they can process and display on their surface foreign antigens to T cells[3]. B cells acting as APCs are highly specific and can engulf recognized pathogens. In this case, they are also several thousand times more efficient at presenting to T cells than other APCs[4].

5.3. B-cell receptors and immunoglobulins

The B-cell receptor (BCR) is a transmembrane form of an immunoglobulin molecule associated with two signaling chains, CD79 α and β. In the following paragraphs, the term *BCR* refers to membrane-bound immunoglobulin.

The human immunoglobulin heavy-chain (IgH) locus is located on chromosome 14, whereas the kappa light-chain (Igκ) locus is located on chromosome 2 and the lambda light-chain (Igλ) locus is located on chromosome 22[1]. Each heavy- or light-chain locus comprises several gene segments; the human IgH locus harbors nine constant (C) gene segments, while the light-chain loci consist of either one (Igκ) or four (Igλ) C segments. Additionally, the human IgH locus contains at least 51 variable (V) region genes and 25 diversity (D) and joining (J) region genes. IgL loci have 30–40 V genes and 4–5 J genes[5]. Heavy chains typically contain only one D segment; however, V(DD)J recombination has been reported[6]. Some Ig genes can cluster on chromosomes other than the primary immunoglobulin loci[7]. D and J genes are commonly duplicated, deleted, or contain polymorphisms. Many V, D, and J genes are pseudogenes and, therefore, are non-functional. In addition, the immunoglobulin locus is highly repetitive and homologous[8]. All these factors render whole-genome sequencing studies ineffective for accurate and detailed locus mapping. Nonetheless, a continuous effort has been made to identify new alleles and haplotypes to understand germline variation and its effect on naïve antibody repertoire[9].

Before assembling a functional BCR in bone marrow, the V, D, and J genes must rearrange[1]. RAG1/RAG2 enzymes mediate this rearrangement. First, the heavy chain

undergoes recombination by deleting all nucleotides between D and J segments and joining segments together (Figure 1a). Next, the following V gene segment is added, thus forming the VDJ gene segment. Then, all remaining gene segments between V and D are deleted, DNA is transcribed, and the sequences between VDJ and constant gene segments are removed.

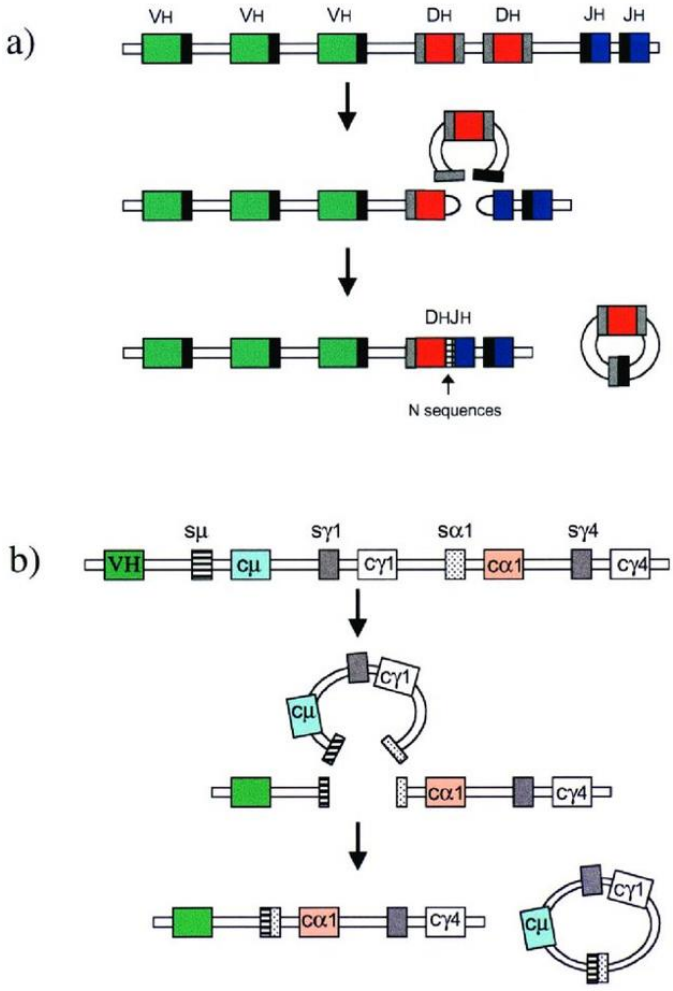

Figure 1. VDJ recombination of the IgH locus and class-switch recombination (CSR). *a) In VDJ, recombination DNA is cleaved at sequences flanking the rearranged D, J, and, subsequently, V segments. The formation of hairpin structures allows for the ligation of joins between gene segments. Before gene segments are joined, semi-random non-germline nucleotides are deleted and inserted. b) DNA is cut upstream of the recombining C-region genes in CSR. The 5' end of the C-region is reconnected to the 3' end of downstream gene segments, thereby replacing the previously expressed C-segment gene with a new gene (here, μ is replaced with α1).* Adapted with permission from Springer Nature Customer Service Centre GmbH: Nature Publishing Group, Mechanisms of chromosomal translocations in B cell lymphomas. Küppers, R. & Dalla-Favera, R., copyright (2001)

The same steps occur in rearranging Igκ and Igλ loci; however, the light-chain loci lack a D segment. Most commonly, Igλ rearrangement occurs if Igκ rearrangement fails to produce a functional light chain. Around one in three sequences makes productive joins. Each

B cell can express only one active light chain from either Igκ or Igλ loci (isotypic exclusion). Moreover, only one heavy chain and one light chain from two possible alleles for each immunoglobulin locus are chosen (allelic exclusion) [1]. However, the expression of two functional chains (especially Igλ) has been previously reported[10].

The assembly of a functional heavy chain and one of the light chains produces a membrane-bound form of the BCR. A functional BCR is necessary for B-cell survival; if the BCR of a B cell does not bind to its ligand, the B cell cannot receive the proper survival signal, and its development ceases. This process is referred to as positive selection and happens in both immature and mature BCRs[11]. In contrast, negative selection is a mechanism for the elimination of self-reactive B cells. If a B cell binds to its own antigen, it is either eliminated by apoptosis (clonal deletion), ceases to respond to its antigen (becomes anergic), ignores other signals and continues development, or most commonly, edits the receptor to change the specificity and rescue the B cell[12]. The concept of central tolerance is based on the elimination of T and B cells that react to self-peptides. For B cells, this process happens in the bone marrow. As mentioned, however, some B cells continue to develop despite being self-reactive. Therefore, a secondary mechanism exists (peripheral tolerance) in which peripheral B cells require cognate T cells' help to activate correctly. When self-reactive T cells are deleted in the thymus, the autoreactive B-cells do not receive the second signal. This results in B-cell tolerance by anergy, deletion, or signaling via inhibitory receptors[12].

In the bone marrow, B cells assemble their BCRs independently of antigen presence. When B cells leave the bone marrow, they are still immature and must migrate to secondary lymphoid organs to complete maturation[13]. The spleen and lymph nodes are considered the main secondary lymphoid organs. The next developmental step occurs in temporary structures called germinal centers (GCs), which are localized within the secondary lymphoid organs. Prior to the formation of GCs, during the initial T-cell-B-cell interaction, the process of class-switch recombination (CSR) begins with an exchange of the current constant segment genes of the heavy chain (μ or δ) with the following downstream exon. This process produces specialized isotypes (Figure 1b) [14]. CSR occurs between highly repetitive and evolutionary-conserved switch sequences. Transcription of μ promoter (resulting in IgM expression) is constitutive, whereas transcription of other promoters is inducible by extracellular signals (i.e., cytokine, antigen)[15].

Secondary lymphoid organs process a constant stream of antigens presented to mature B cells by follicular dendritic cells (FDC). B cells bind to these antigens via their BCR. Some antigens can stimulate both mature and immature B cells and become activated; however, for other antigens, primary B-cell activation requires T-cell help[16]. An activated B cell begins to proliferate and undergo somatic hypermutation (SHM), which mainly introduces point mutations in the cell's DNA (primarily in the V-region genes), produces many clones, and leads to BCR affinity maturation. One enzyme, activation-induced cytidine deaminase (AICDA), single-handedly initiates both CSR and SHM[17]. SHM begins when AICDA converts cytosines to uracils, thereby creating mismatches in the immunoglobulin's V(D)J sequence. These mismatches can either be repaired or produce transition mutations to thymine during replication[18]. Cells expressing BCR with the highest affinity for the antigen receive T-cell help in the form of survival signals and are selected to mature further within the GC. B cells that develop BCR with lower affinity will become apoptotic. To select the B cells with the highest affinity, the processes of proliferation, SHM, T-cell help, and positive selection can occur several times. Maturing B cells will eventually receive a signal to leave the GC. At this stage, the B cells differentiate into either memory or antibody-secreting cells (ASCs) and undergo clonal expansion. The populations of ASCs are traditionally divided into plasmablasts (PBs) and plasma cells (PCs). PBs burst with antibodies and are cleared from circulation in days. They can either become apoptotic or migrate to the bone marrow and become PCs, with a lifespan exceeding decades[19]. Both PBs and PCs secrete large amounts of soluble antibodies with the same specificity as the BCR.

5.3.1. Immunoglobulin structure

The term "antibody" is used when the membrane-bound immunoglobulin portion of the B-cell receptor complex is produced and secreted in soluble form by ASCs. Antibodies are relatively large Y-shaped proteins (150 kDa)[1]. Each antibody comprises two heavy chains and two light chains connected by disulfide bonds, and each chain contains C- and V-regions (Figure 2a)[20]. Additionally, in the C-region of the IgH, three to four separate domains can be distinguished (CH1…CH4).

An antibody consists of an antibody-binding fragment (Fab) and a crystallizable fragment (Fc). The Fc contains a structural pattern recognized by cells that express the Fc receptor (FcR) that can trigger a downstream response in those cells[21]. In addition, Fc is used

for selective antibody transport and contains conserved glycosylation sites[22]. The Fab region consists of heavy- and light-chain V-regions, the CH1 domain of heavy chains, and the C-domain of light chains. The V-region is encoded by genes that have undergone affinity maturation; therefore, the Fv fragment is highly mutated and is responsible for antigen recognition of linear or conformational epitopes. The V-domains comprise three complementarity-determining regions (CDRs), which are flanked by four framework regions (FR) of beta-sheets that support loops created by the CDRs (Figure 2a and b). CDRs are immunoglobulin regions most prone to SHM as they contain several hotspots for introducing point mutations, whereas FRs tend to be more conserved[23]. FRs include hotspots for AICDA activity, and if the mutation is found in the region, it might be selected against since it can interfere with the structural stability of the V-domain[24]. In a native state, CDRs are located near the surface of the antibody, and three CDRs from each heavy and light chain form an antibody-binding site.

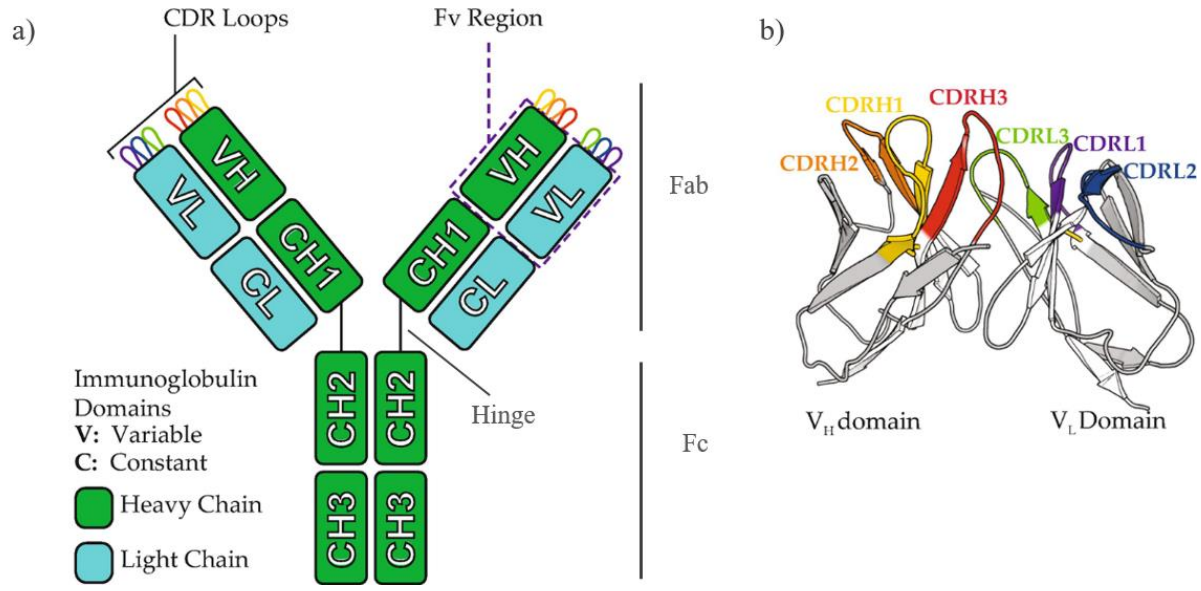

Figure 2. Antibody structure. *a) Two pairs of heavy and light chains form a Y-shaped antibody structure, with a series of domains creating variable (V) and constant (C) regions. The structure can be divided into a crystallizable fragment (Fc)—an effector part of an antibody, and an antigen-binding fragment (Fab). Fab contains a variable fragment (Fv), which is created by combining V domains of heavy and light chains. On the tip of the Fv fragment are situated CDR loops, which form most of the antigen-binding site. The hinge region connects the FC and Fab. b) A variable fragment of an antibody with three CDR regions for each heavy and light chain forming an antigen-biding site*. Adapted with permission from Springer Nature Customer Service Centre GmbH: Humana Press, New York, NY Methods in Molecular Biology by Leem J. & Deane C. M, copyright (2019).

The C domain of the heavy chain of an antibody contains one of nine germline-encoded genes corresponding to the antibody's isotype and subgroup: μ, δ, γ1, γ2, γ3, γ4, α1, α2, and ε. Isotypes determine the structure and function of antibodies. For example, antibodies with IgG, IgD, and IgE isotypes maintain a basic molecular Y-shaped structure, while other isotypes can be found in multimeric forms (IgM as a pentamer and IgA1 and IgA2 as dimers) depending on location and environmental conditions[1].

5.3.2. Immunoglobulin repertoires

The heterogeneity of immunoglobulin repertoires demonstrates the number and distribution of different BCRs throughout the population. In healthy people, this repertoire is diverse and polyclonal, whereas in some pathological conditions, such as MS, the response tends to become clonally restricted and dominated by a few expanded clones.

The first mechanism leading to a versatile immunoglobulin gene repertoire is gene rearrangements through V(D)J recombination. If one V, one D, and one J gene recombine in a semi-stochastic fashion and random nucleotides are inserted and deleted from junctions, this can result in 10^{13} different theoretical variants of BCR[25].

Diversity obtained by V(D)J recombination does not directly translate to an observed variety in the naïve B-cell repertoire. In the peripheral blood of healthy adult humans, the number of B cells is $5x10^9$, which is only a portion of the total B-cell count. A significant portion of the B-cell population is located in the primary and secondary lymphoid organs and different tissues, for instance, in the gut (MALT*). The estimated number of B cells is also merely a fraction of theoretically possible B cells[26]. Not all heavy- and light-chain pairings are due to structural incompatibilities but are likely mostly random[27]. Mechanisms protecting the body from autoreactive immune cells, such as central tolerance, prevent many cells from entering circulation, further decreasing possible BCR diversity. Additionally, some V, D, and J-genes and gene families occur more frequently; thus, some V, D, and J combinations are more commonly found[28]. Almost 50% of all IgH repertoire in peripheral blood consists of *IGHV3* family genes, followed by *IGHV1* (20%) and *IGHV4* (15%)[29].

* MALT - mucosa-associated lymphoid tissue

The next step in repertoire diversification occurs when mature naïve B cells respond to an antigen. The CSR mechanism allows activated B cells to switch isotypes and subclasses of antibodies, thereby changing their structure and effector functions. Further, the SHM process causes activated B cells to acquire mutations 10^6 times faster than a normal cell[30]. As a result, activated B cells produce a vast array of immunoglobulins to achieve higher affinity.

5.3.3. Antibody-antigen interactions

Antibodies interact with antigens through spatial complementarity. The region of the antibody that directly interacts with the antigen is often referred to as a paratope. Most commonly, an antigen contains several different epitopes on its surface. However, not every site on the surface of the antigen has the same potential to invoke immunity; therefore, epitopes are arranged discontinuously, and the dominant epitope is referred to as the determinant[31]. An antibody binds to an epitope through not only weak and non-specific forces (electrostatic and van der Waals forces) but also mainly hydrogen bonds and hydrophobic interactions[13,32]. Binding by weak forces makes the interaction reversible, meaning that antibodies can cross-react with many antigens depending on their relative affinities.

Only 20–33% of the CDR's amino acid sequences participate in epitope binding[33]. The same amino acid sequence can support various conformations and interact with dynamically changing antigens[34]. In both heavy and light chains, CDR3 regions dominate antigen binding[33]. Nevertheless, antigen recognition and binding do not entirely depend on CDRs. Research has demonstrated that residues outside the paratope also play a crucial role in that process. For example, some FR residues near CDRs can actively participate in antigen binding[35]. Those residues that are not directly involved with the epitope help assert the correct structure and orientation of CDRs[24].

The prevailing understanding is that the V- and C-regions of antibodies fulfill their functions independently from each other. However, some reports have suggested that glycosylation and sequence variation can cause configurational allostery—that is, intramolecular regulation between V and C-region[36]. In addition, previous studies have shown that the binding affinity and specificity differ in some IgG molecules with identical antigen-binding sites depending on the subclass of the antibody[32,37]. Therefore, scholars have

hypothesized that the antigen-binding site can undergo conformational changes due to changes in the C-region, leading to differences in antibody affinity and specificity.

5.3.4. Antibody functions

Antibodies' primary function is to initiate responses that either remove the pathogen from the body or hinder the reactivation of latent pathogens (e.g., the herpes virus family). Their first mode of action is neutralization, in which an antibody blocks the pathogen or other particles, such as toxins, rendering them ineffective. An excellent example of this process is binding to viral particles and preventing them from entering the cell or disrupting the formation of biofilm[38]. Multimeric antibodies can also bind many pathogens together, causing them to agglutinate and precipitate, which induces a process of phagocytosis or (on mucosal surfaces) peristalsis, effectively eliminating the antigen[39]. Antibodies can also facilitate phagocytosis through opsonization. In this process, they act as an aid to overcome two negatively charged cell walls that repel each other (macrophage and pathogen), thereby enabling the pathogen's uptake by macrophages and neutrophils[40]. Antibodies interact with macrophages and other immune cells by binding their C regions to FcRs.

Further, antibodies can activate the classical pathway of the complement system by binding to C1q. This results in pathogen lysis and immune cell recruitment to the site. Complement can also be activated in a lectin-dependent manner, in which mannose-binding lectins are recruited to the opsonized material. However, antibodies can also activate complement independent of C1q and lectin[41]. Pathogen clearance can also be promoted through antibody-dependent cell-mediated cytotoxicity (ADCC), in which antibodies act as a bridge between infected cells and effector cells, mainly natural killer (NK) cells. NK cells destroy target cells either by inducing apoptosis or by lysis[21].

The functions of antibodies differ between isotypes and subclasses. The IgG isotype is the most abundant in peripheral blood, constituting up to 80% of all immunoglobulins. IgG has four subclasses, of which IgG1 is the most abundant and IgG4 is the least abundant. IgG molecules can promote mechanisms like ADCC and opsonization by binding to activating FcγRs. They can also bind to different receptor types, such as FcγRII, which has inhibitory properties and plays a vital role in immunomodulation[42]. Each subclass of IgG differs in its

properties; therefore, each subclass binds to particular FcγRs, resulting in functional specialization[42,43].

5.4. Immunosurveillance of the central nervous system

The central nervous system (CNS) comprises the brain and spinal cord. The homeostasis of the CNS is preserved through the meninges, cerebral-spinal fluid (CSF), blood-brain barrier (BBB), blood-leptomeningeal barrier, and blood-CSF barrier (Figure 3). The meninges are the outermost barrier that is the most permissive to immune cell trafficking. The meninges consist of three layers that surround the brain and the CSF: dura mater, arachnoid mater, and pia mater. Møllgård et al. recently identified a fourth layer called the subarachnoid lymphatic-like membrane, which divides the subarachnoid space into two compartments[44]. However, its existence still needs to be confirmed.

Meninges surround the CNS and provide physical protection for brain tissue. They are also gaining attention as an active immune system in which circulating lymphocytes conduct constant immune surveillance[45]. Immune surveillance at the borders of the CNS mainly involves subsets of T cells and macrophages. However, a plethora of cell types and phenotypes have recently been described, including B cells, NK cells, neutrophils, dendritic cells (DC), granulocytes, border-associated macrophages, and monocyte-derived cells[46–48]. The meningeal lymphocytes come from circulating blood, although not exclusively. The recently described system of vascular channels between skull bones and meninges enables the migration of myeloid cells directly from the bone marrow into the CNS. Moreover, in mice CNS, multiple studies have identified clusters of immature B cells and have even indicated skull bones as a hematopoietic niche for most meningeal B cells, thus challenging the hypothesis that meningeal lymphocytes come from blood alone[49–51]. The meninges are also a site where circulatory T cells interact with local APCs and sample CNS antigens, accumulating around the dural sinuses and creating a niche. This site promotes a change in the phenotypes and effector functions of immune cells within the meninges[52]. Below the pia mater, the basal lamina of brain blood vessels and astrocyte endfeet form the glia limitans barrier, which controls T-cell trafficking (Figure 3a).

Understanding of the brain's lymphatic system has recently evolved[53,54]. The extracellular CNS fluid is drained into the CSF, which then drains lymphatic vessels in the

meninges. Next, it drains into deep cervical lymph nodes and, in mouse models, partially into superficial cervical lymph nodes[53,54]. The meningeal lymphatic system transports immune cells and antigens between the CNS and the periphery nervous system. Immune cells from the blood typically enter the CNS compartment via the BBB, blood-meningeal barrier, or choroid plexus[45]. The BBB and blood-CSF barriers rely on tight junctions but have varying levels of permeability and composition (Figures 3b and 3c)[55].

Under homeostatic conditions, the CNS is inspected by a large number of innate resident macrophages, called microglia, which are restricted to the brain parenchyma and do not interact with T cells. Additionally, a few immune cells can cross the BBB, mainly CD4+ T cells and macrophages, which inspect for signs of foreign elements[56]. Typically, they remain within the CSF and perivascular spaces; however, tissue-resident memory T cells have recently been discovered in white brain matter and the meninges[57].

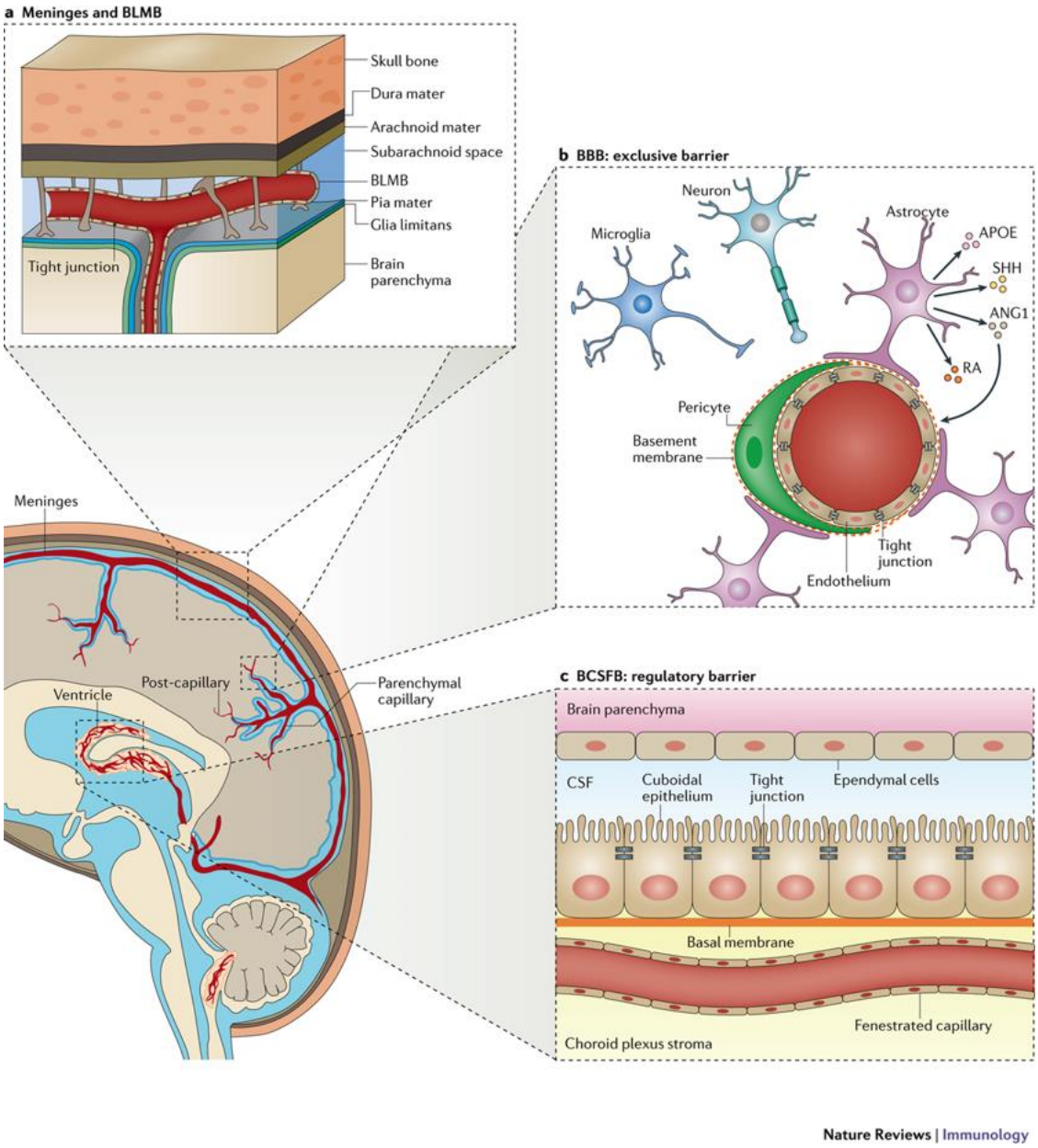

Figure 3. ***Protective barriers of the CNS***. *"a | The meninges (comprising the dura mater, arachnoid mater, and pia mater) form the outermost barrier that protects the brain parenchyma. The meningeal microvessels in the subarachnoid space are composed of a non-fenestrated endothelium that contains tight junctions but is not ensheathed by astroglial endfeet. The pia mater surrounds these blood vessels to form the blood–leptomeningeal barrier (BLMB), which is permeable to solutes and immune cells. b | The blood–brain barrier controls the transport of solutes and fluids and the extravasation of immune cells into the CNS parenchyma. The BBB consists of capillary endothelial cells, astrocyte endfeet and pericytes. Sonic hedgehog (SHH), angiopoietin 1 (ANG1), apolipoprotein E (APOE) and retinoic acid (RA) are produced by astrocytes and promote BBB integrity. c | The cuboidal epithelial cells of the choroid plexus form the blood–cerebrospinal fluid (CSF) barrier (BCSFB). These epithelial cells are connected by tight junctions and have a polarized distribution of numerous transporters. The endothelium of the choroid plexus does not form a barrier but is permeable to allow the delivery of water from the blood to the epithelium, which is necessary for CSF production."* Figure and abbreviated text from Spadoni et al.[55]. Reprinted with permission from Springer Nature Customer Service Centre GmbH: Humana Press, New York, NY. Organ-specific protection mediated by cooperation between vascular and epithelial barriers. Spadoni, I., Fornasa, G. & Rescigno, M. Nature Reviews Immunology, 17 761–773, copyright (2017)

The discovery of routes by which immune cells to enter and exit the CNS has improved the understanding of how immune cells interact with the periphery and maintain an optimal environment for nerve cells. All the barriers provide a stable environment for cells within the CNS while limiting the access of peripheral blood cells and preventing the secretion of CNS-specific molecules into systemic circulation. The presence of immune cells within the CNS has far-reaching consequences for the brain's protection from external and internal threats.

5.5. Multiple sclerosis

Symptoms compatible with multiple sclerosis were described long ago, but the disease was first characterized by Jean-Martin Charcot in 1868[58]. MS is a chronic, inflammatory, neurodegenerative disease of the CNS with an unknown etiology and no known cure. MS typically onsets in adults between 20–40 years of age, although 1.7–5.6% of all MS cases affect children[59]. Worldwide, the prevalence of MS tends to be higher in high-income countries, varying between 50 and 300 per 100,000 people[60]. Around 2–3 million people are estimated to suffer from this disease, although this number is likely considerably higher given the lack of data from developing countries. Furthermore, the trend in prevalence is increasing globally, and females are affected twice as often as males[61].

Thus far, the etiologic agent causing MS has not been identified. However, many known risk factors contribute to the disease's development. A combination of environmental, genetic, and stochastic factors (i.e., seemingly bad luck) plays a vital role in the processes and pathways that result in the onset of MS. The genetic factors, which play a significant role in MS development, will be discussed in Chapter 5.8. Migration studies of different populations have demonstrated how important the environmental factors are in the pathogenesis of MS. For example, adult migrants from low-risk MS countries who move to a high-risk country are at low risk of developing MS. However, their children inherit the risk of the country to which they move[62]. The most recognized environmental causes of MS are inadequate vitamin D, ultraviolet B (UVB) radiation, smoking, and the Epstein-Barr virus (EBV). The distribution of MS prevalence is strongly correlated with latitude, likely due to differences in exposure to sunlight[63]; low UVB exposure during childhood, decreased outdoor activity, and low vitamin D intake and levels have all been implicated in later development of MS[64]. Another lifestyle

risk factor is smoking tobacco, which can increase the risk of developing MS by 50% in adults[65].

EBV infections typically occur during childhood or adolescence, are asymptomatic or mildly symptomatic, and lead to viral latency in B cells[66]. The rate of EBV infections is high in the general population; however, EBV is present in nearly 100% of adult MS patients and a large majority of pediatric MS cases[67]. Additionally, reports have suggested that being genuinely EBV-negative seems to protect against developing MS[68], whereas symptomatic infections resulting in mononucleosis increase the risk of MS two-fold[69]. Many other environmental and lifestyle factors may play a role in developing MS by dysregulating the function of the immune system and facilitating pro-inflammatory reactions[70]. One example of this is adolescent and early adulthood obesity[71,72]. Dysregulation of the microbiome[73], dietary factors[74], and disruption of circadian rhythm[75] have also been suggested as risk components.

For most patients, the differential diagnosis of MS begins when the patient presents to the clinic with the first attack, which can involve various symptoms, depending on whether the lesion affects the spinal cord, brain stem, optic nerve, or elsewhere in the CNS. The symptoms also depend on the lesion's size and the disease's progression. Thus, many possible impairments can affect cognitive functions and autonomous, sensory, and motor systems. The symptoms resolve over time; some patients will never experience a second incident, and those patients are defined as having a clinically isolated syndrome (CIS)[76]. However, the majority of cases presenting to the clinic with CIS symptoms and abnormal magnetic resonance imaging (MRI) scans will experience a second attack, which defines clinically definite multiple sclerosis[76]. The wide scope of possible impairments means that the differential diagnosis of MS must be based not only on clinical presentation but also on the patient's history, MRI scans showing demyelination patterns, and laboratory data, including oligoclonal bands (OCB) in CSF. According to the revised 2017 McDonald criteria[77], new MRI findings, the occurrence of contrast-enhancing and non-enhancing lesions at the same time, or the presence of oligoclonal bands in the CSF will also define clinical definite MS[77].

At onset, 90% of MS patients present with relapsing-remitting MS (RRMS), in which they experience an acute attack of neurological dysfunction followed by gradual, partial or full recovery. At first, recovery often seems complete. However, most relapses leave behind irreversible damage. Over time, the progression of the disease accelerates, with periods of

improvement between attacks shortening and slowly disappearing (secondary progressive MS [SPMS]). SPMS manifests as progressive neurodegeneration and disability. If MS is untreated, it usually develops 10–15 years after onset; however, the process can take decades, or in some cases, the disease does not advance to the SPMS stage. The onset and rate of progression can likely be partially attributed to treatment status and efficacy of the treatment[76]. Around 10–15% of patients at onset present with primary progressive MS (PPMS). In PPMS, there are no recovery periods; instead, patients go through a slow accumulation of symptoms and loss of function, often involving one major neuronal system.

5.6. Involvement of B cells in the pathology of multiple sclerosis

Many theories about what drives MS exist, but most focus on autoimmune mechanisms. Furthermore, what propels the condition in chronic diseases like MS can differ from what triggers the disease. Many autoantigens have been proposed, although not agreed upon, by the scientific community. This lack of consensus is peculiar for an autoimmune disease of the CNS; B cell autoantigens have been uncovered for similar disorders, such as neuromyelitis optica (anti-AQP4 antibody[*]), anti-MOG[*] encephalitis, and antineuronal encephalitides (i.e., anti-LGI1[*], anti-NMDAR[*])[78–80].

As shown above, MS is a complex disease. Historically, it was considered a T-cell-driven autoimmune disorder. However, the success of B-cell-targeting therapies shifted that understanding. In MS, only the CNS is affected, suggesting that immune cells are selectively recruited by antigens only found within the compartment. Histopathological studies have shown an abundance of CD8+ T cells and B cells and few CD4+ T cells and macrophages accumulating in perivascular spaces in the CNS, with the addition of infiltrates from meninges on the cortical surface[81–83]. These accumulations can be detected on MRI scans as lesions. B-cell populations within CSF and MS lesions are clonally related and hypermutated, and the immunoglobulins they produce can be found in CSF as OCBs[84–86]. T-B collaboration is necessary for B cells to proliferate and create clones producing antibodies; however, what initiates these interactions and what drives them afterward are unknown.

[*] AQP4 - aquaporin 4; MOG - myelin oligodendrocyte glycoprotein; LGI1 - leucine-rich glioma-inactivated 1 protein; NMDAR - N-methyl-D-aspartate receptor

MS lesions are characterized by demyelination and damage to oligodendrocytes leading to axonal loss[87]. In most cases, axonal transections occur in active lesions before clinical symptoms and shape the onset of the disease[87,88]. Demyelination is not exclusive to white matter, as myelin is also found in gray brain matter[88]. As the disease progresses, irreversible damage accumulates. During the early stages of the disease, active lesions have different immunopathological patterns depending on the patient; these patterns also reflect the composition of the CSF[89,90]. Immune infiltrates have similar content in RRMS and progressive forms of MS, with the exception of the proportion of B cells, which is increased in progressive stages[91].

Autoreactivity is a normal trait within the lymphocyte population. Therefore, two hypotheses exist about how an aberrant autoimmune response is initiated against the CNS[76]. The first hypothesis assumes that events occur inside the CNS. For example, CNS antigens are released into circulation by APC presentation in the meninges or lymphatic drainage into deep cervical lymph nodes. If the environment favors inflammation, an immune response against the antigen is generated, and eventually launches an attack against the CNS. The second hypothesis speculates that a strong immune response against, for example, systemic infection drives autoimmunity against the CNS outside of the CNS. This might happen due to cross-reactivity or general priming of autoimmune reactions in the case of a potent stimulus.

Not only the production of antibodies but also other B-cell functions are crucial in MS pathology. The additional B-cell roles that may influence the pathogenesis of MS include forming tertiary lymphoid structures; producing cytokines, chemokines, and neurotoxic factors; acting as APCs to T cells and driving proliferation; and serving as a reservoir for EBV[92–94].

5.6.1. Trafficking into the central nervous system

As described in Chapter 5.4, the lymphatic system enables the drainage of cells and antigens from the CNS toward deep and (partially) superficial cervical lymph nodes and then to peripheral circulation[53,54]. Circulating immune cells can also enter the CNS via the BBB, subarachnoid spaces, or choroid plexus. During an MS attack, inflammation disrupts the BBB, making it easier for peripheral immune cells to penetrate the CNS compartment[95]. These cells gather in perivascular spaces and move toward the brain parenchyma, furthering

axonal injury and demyelination. B cells in the CNS of MS patients can be found in the CSF, meninges, parenchyma, and lesions, and a portion of these B cells are class-switched, clonally expanded, and hypermutated. This knowledge has been utilized to identify related cells in different compartments within and outside CNS[96,97]. Indeed, cells belonging to the same clonal lineage have been found in the CNS and peripheral blood. Overall, evidence consistently has pointed to a bidirectional exchange between the two compartments. In addition, it has implicated lymphoid structures in the periphery as responsible for maintaining ongoing immune reactions.

Adhesion molecules ICAM-1* and VLA-4* have been shown to be crucial players in trafficking through BBB endothelial cells; in ex vivo studies, BBB migration was successfully inhibited by blocking these proteins[98]. Another essential factor for transmigration is ALCAM*, which is found on brain endothelial cells and promotes the recruitment of pro-inflammatory B cells to the BBB and blood-meningeal barrier[99]. Secretory proteins, such as chemokines, can also regulate trafficking toward the CNS. Chemokines can act as chemoattractants, causing the locomotion of cells to the site. MS patients have elevated chemokines C-X-C Motif Chemokine Ligand 10 (CXCL10), CXCL12, and CXCL13, which suggests frequent migration through BBB. Moreover, the level of CXCL13 in MS correlates with the number of B cells detected in the CSF[100,101].

5.6.2. Ectopic lymphoid structures

During a sustained chronic inflammatory process, immune cells gather in the tissues and organize into GC-like structures called tertiary lymphoid structures (TLS). The function of these structures is similar to that of secondary lymphoid structures: antigen presentation, cell maturation, and proliferation with SHM and CSR. TLSs have been observed in different autoimmune diseases, cancer, graft rejections, and chronic infections[102,103].

In MS, a pro-inflammatory environment inside the CNS, particularly around lesions, stimulates cytokine production, which prompts B-cell activation, homing, and survival[104]. Ectopic lymphoid structures in MS have been observed in the meninges, where T and B cells, FDCs, and PBs create compact inflammatory aggregates[81]. Presence and abundance of TLSs

* ICAM-1 - Intercellular Adhesion Molecule 1 (CD54); VLA-4 – Very Late Antigen-4 (Integrin α4β1); ALCAM - Activated Leukocyte Cell Adhesion Molecule (CD166)

correlate with earlier disease onset and a poor long-term prognosis[81,105]. The location of TLSs is also associated with the vicinity and size of MS lesions and with the degree of neurodegeneration in the cortical region. However, not all neuropathological studies have shown the existence of TLS, and whether they are present in the early stages of the disease is uncertain. Nevertheless, they are possibly one of the primary sources of cytokines, chemokines, and B-cell regulatory factors within the CNS.

Proliferation markers and the lymphoid-homing chemokine CXCL13 have recently gained much interest. CXCL13 controls immune cell localization and activation of the microglia; therefore, it is one of the main factors necessary in the formation of TLS[106]. B cells are involved in establishing TLS and maintaining them using cytokine, chemokine, and lymphotoxin signaling. In patients with chronic active antibody-mediated rejection after kidney transplantation, B cells residing in meningeal TLSs have been shown to survive treatment with anti-CD20 therapies despite complete peripheral B-cell depletion[107]. These cells continuously produce antibodies, likely due to local secretion of survival factors and a lack of expression of the CD20 molecule.

5.6.3. Antibodies in multiple sclerosis

Intrathecal synthesis of IgG is found in 95% of all MS patients. The majority of antibodies are IgGs, and by far, the most commonly found is the IgG1 subclass. Part of the diagnostic workup for MS is visualizing intrathecal IgG using isoelectric focusing (IEF) on an agarose gel. In IEF, antibodies form a pattern of OCBs depending on their electrical charge. Despite reports of the exchange of IgG-producing B cells within CSF, the pattern of OCBs has been shown to persist for decades[108,109]. The presence of OCBs is a part of MS diagnostic criteria, and it correlates with poor disease outcomes. For CIS patients, the present of OCBs is predictive of conversion to MS[110,111]. However, recent studies have shown that this association may be partially attributed to intrathecal IgM, not only to IgG OCBs; the presence of IgM within the CSF has been linked with a more aggressive course of the disease[112].

OCBs are not unique to MS. Intrathecal antibodies are produced in many chronic CNS infections in which they target etiological agents[113–115] and in autoimmune diseases involving the CNS that lack certain etiology and have unknown antigens. The search for

possible antigens in MS has been ongoing for decades, and antibodies against EBV and myelin-associated epitopes have been found frequently[116–118]. However, the need for reproducibility has prevented a consensus on intrathecal IgG targets[119,120]. Within intrathecal IgGs, there is a group of well-established polyspecific antibodies that are found in most MS patients and are directed against a broad group of neurotropic viruses[121]. Of these, the most frequently found are anti-measles, rubella, and varicella-zoster virus antibodies. The phenomenon is referred to as the MRZ reaction. MRZ is an MS marker and, if found, significantly increases the likelihood of being diagnosed with MS[122].

The presence of OCB in CSF still remains a mystery. Studies have shown that OCBs are produced by intrathecal clonally expanded B cells[85,118]. CSF B cells have been found to match B cells from the brain and periphery[123,124], but whether and how they are involved in the pathology of MS is unknown. The OCB pattern persists despite successful anti-CD20 therapies that result in patient clinical improvements. Therefore, OCBs likely do not contribute to the direct cause of the symptoms but rather play a different role in MS[125]. Another reason for the observed clinical improvement in treated MS patients despite antibody presence could be that the effect of antibodies within the CNS requires an environment that involves other immune cells and complement. These co-factors are removed if a patient is treated efficiently; therefore, the pathogenic antibodies would not be able to cause harm.

5.6.4. B cells as APCs in multiple sclerosis

Previous research has established the role of B cells as APCs in various autoimmune and infectious diseases[126,127]. In MS patients, specific memory B cells can recognize soluble and conformational epitopes. Theoretically, B cells could bind their antigens with BCR, then internalize, process, and present the antigen on the surface alongside the major histocompatibility complex (MHC) to CNS-specific T cells. Based on data from MS patients and a mouse model of autoimmune encephalomyelitis (EAE), Th12, Th1, Tfh, and Tfh-like cell populations have been implicated as pathogenic. These cells are activated in deep cervical lymph nodes, where they cooperate with APC B cells that drive the immunopathogenesis of EAE and MS, resulting in disease progression. Recent data have shown that Th17, Tfh, and Tfh-like cells produce interleukin 21 (IL-21), which stimulates B cells to produce antibodies and drives the aberrant B-cell response within the CNS of MS

patients. The outcome of this interaction is increased disease severity and disease progression[128].

B cells in the CNS also express CD40, CD80, and CD86 molecules, which are co-stimulators that effectively induce activation, expansion, and differentiation of pathogenic T cells in MS[129]. Furthermore, the expression of the co-stimulatory proteins is higher in MS patients' B cells than in those of healthy controls, particularly in active disease (CD80+ B cells)[130]. Memory B cells from MS patients can efficiently present myelin-associated epitopes to T cells. Moreover, the memory B-cell population specific for CNS antigens is significantly elevated in MS patients[131,132]. One of the explanations for failed tolerance might be incorrect autoantigen processing by peripheral B cells. This could cause autoreactive T cells to migrate to the CNS, become activated by APCs, and trigger neuroinflammation. Jelcic et al. found that peripheral B cells activate T cells, causing them to migrate into the CNS[133]. This migration of activated T cells could be the starting point of demyelination, and the depletion of B cells could mitigate this effect.

5.6.5. Cytokines and the production of neurotoxic factors

A crucial component of antigen presentation in B cells to T cells is the CD40-CD40L interaction[134]. In MS, the number of CD4+ T cells expressing the CD40L increases, indicating more frequent T-B collaboration. Activation of B cells results in neuroinflammation through several mechanisms. First, immune cells are recruited to the CNS through upregulation of cell adhesion protein expression. Then, the expression of MHCII is elevated, along with co-stimulatory molecules and B-cell proliferation markers. Finally, B cells secrete antibodies and cytokines and activate the Nf-κB* pathway through CD40, causing further memory B-cell proliferation and increased production of pro-inflammatory IL-6[134].

MS lesions contain persistent B cells with upregulated expression of B-cell survival factor (BAFF), which stimulates the production of cytokines. BAFF regulation is critical for the regulation of pro-inflammatory B-cell activity[135]. Using anti-CD20 therapies in MS patients results in significantly lower pro-inflammatory responses from T cells and myeloid

* Nf-κB - Nuclear factor kappa-light-chain-enhancer of activated B cells;

cells[136]. Conversely, an increase in the production of pro-inflammatory compounds by B cells can activate other cells and advance MS progression[137].

In the correct environment, B cells have been shown to produce anti-inflammatory molecules with a protective effect on the CNS of MS patients. Among protective cytokines, IL-10 gained the most attention. In MS patients, expression of IL-10 by B cells is downregulated compared to healthy controls, implying that MS patients are not as capable of attenuating immune responses[138]. Clinical trials have shown that, after B-cell depleting therapies, the new population of reconstituting B cells differs from the population in untreated patients. In treated patients, the new population presents more anti-inflammatory characteristics, such as higher secretion of IL-10[136]. However, the production of IL-10 by activated B cells is impaired in patients with RRMS and SPMS[139,140]. Anti-inflammatory cytokine expression is an attempt to counteract the pro-inflammatory environment. The production of pro- and anti-inflammatory factors is less balanced and controlled in more severe forms of disability in progressive MS[141].

5.7. Treatment of multiple sclerosis

Medical care for MS patients includes the treatment of acute relapses, disease-modifying therapies (DMTs), psychological help, physical therapy, symptom relief, and comorbidity management through lifestyle changes. The role of DMTs is to suppress or modulate the immune system, thus reducing the recurrence of relapses and delaying disease progression. The first DMT used in MS was interferon-β; many new DMTs have been approved, and numerous clinical trials are ongoing. DMTs can be personalized depending on the mechanism of action, efficacy, and administration routes. The range of DMT mechanisms includes depletion of immune cells, a shift in cytokine profile, alteration of Th1/Th2 proportions, DNA synthesis obstruction in lymphocytes, and isolation of lymphocytes outside of CNS/within primary lymphoid organs[142]. These mechanisms all result in diminished neuroinflammation; some also seem to slow neurodegeneration.

DMTs commonly target B cells and T cells. An emerging group of B-cell-directed drugs used in MS is Bruton's tyrosine kinase (BTK) inhibitors. Several BTK inhibitors are currently being studied as a treatment option in MS, and early reports have shown moderate efficacy[143,144], although not as extensive as achieved by the most prevalent group among B-

cell targeting therapies—anti-CD20 mAbs (rituximab, ocrelizumab, ofatumumab, and ublituximab). Anti-CD20 antibodies cause a rapid and thorough depletion of circulating cells and preserve early precursors and PCs; thus, most of the pre-existing humoral immunity is conserved. Furthermore, the majority of T cells are also saved. The preservation of immunity and T cells might be the reason for the limited side effects and low frequency of infections while receiving anti-CD20 therapy. Moreover, in animal models, a population of antigen-experienced CD20+ cells has been shown to persist within secondary lymphoid organs despite total depletion of anti-CD20+ cells in the periphery[145]. Therefore, another approach to MS treatment is small-molecule therapies capable of reaching and targeting the CNS, where particles can get across the BBB and modulate inflammation (cladribine, fingolimod, dimethyl fumarate [DMF], and teriflunomide).

5.7.1. Mechanism of action of dimethyl fumarate

The mechanism of action of many DMTs is not fully understood, and DMF is one such example. DMF is a first-line drug for RRMS, and when taken daily, it significantly reduces relapse rates and improves MRI outcomes[146,147]. DMF is hydrolyzed in the small intestine to monomethyl fumarate (MMF), which is considered to be the main active metabolite tied to the therapeutic effect of DMF. In addition, part of DMF intake reacts with glutathione, forming a long-lived, biologically active conjugate[148].

DMF likely exerts an immunomodulatory effect on different immune cell types by modulating NF-κB pathways (stress response, i.e., cytokine production), activating HCAR2* (anti-inflammatory signaling, inhibition of NF-κB), and upregulating Nrf2* (managing oxidative stress)[149]. As a result, DMF therapy decreases the total count of T cells, although various T-cell populations are affected differently. For example, DMF can alter the phenotype of T cells, causing a shift from T_h1 to T_h2. T_h1 cells secrete proinflammatory modulators, such as IFN-γ and IL17, which play an important role in the pathogenesis of MS. Additionally, fumarates can halt the differentiation of naïve T cells into reactive T_h1 and T_h17 cells by stopping antigen presentation and maturation of DCs. This results in decreased expression of adhesion molecules and inhibits immune cell recruitment[150]. Furthermore, fumarates increase the ratio of CD4/CD8 and naïve/memory T-cells. T_{fh} cells, which drive

* HCAR2 – Hydroxycarboxylic Acid Receptor 2; Nrf2 - nuclear factor erythroid 2–related factor 2

the development of TLS in the CNS of progressive MS, are simultaneously depleted[151]. Effector T cells in MS patients have also been shown to regain sensitivity to T_{reg} inhibitory signals, possibly through the downregulation of receptors for IL-6 on T cells[152]. DMF downregulates the expression of different chemokines necessary for T-cell migration and blocks T-cell binding to ICAM, preventing the effector cells from crossing the BBB[153].

B cells are also affected by DMF treatment, and induction of apoptosis and diminished T cell help are thought to be the primary mechanisms through which DMF depletes B cell count and their function[154]. Similarly to T cells, various populations of B cells are affected differently. Memory B cells are considered to be the main target population. While this memory population is depleted, the naïve B cell population is enriched in MS patients as a result of DMF treatment[155]. B cells can also be influenced through cytokine and immunoglobulin production modulation and costimulation[151,156]. In DMF-treated MS patients, Longbreak et al. detected reduced CD80 expression in circulating memory B cells, while in mice studies, DMF has been shown to reduce MHC class II expression on B cells[157].

DMF strikes both adaptive and innate components of the immune system. Depletion of DCs was recorded in patients treated with DMF compared to a placebo[158]. DMF also displays a regulatory effect on the maturation of DCs by lowering MHC class II expression and promoting an anti-inflammatory cell phenotype[149,159]. Monocytes, macrophages, and neutrophils are also believed to be affected[160,161]. Another effect of DMF on innate immunity is increased cytotoxicity of NK cells[162]. Additionally, DMF has neuroprotective effects by downregulating the production of proinflammatory cytokines in activated astrocytes[163], balancing iron metabolism in the brain, and shifting microglia toward a more anti-inflammatory state[164].

5.8. Immunogenetics of multiple sclerosis

MS is a complex disease; not one environmental or genetic factor solely causes its pathology. However, very early epidemiological and genetic studies recognized the heritable nature of the disease. The risk of developing MS is about 0.1% in the general population, yet the risk rises to 2–4% in families in which close relatives are affected. Genetic contribution is even more apparent between monozygotic twins, for whom concordance is 25–30%[165].

5.8.1. HLA associations

The first genetic component to be identified as increasing the risk of MS was the human leukocyte antigen (HLA) gene cluster on chromosome 6, which encodes variants of crucial receptors responsible for distinguishing foreign and self-antigens[166]. The most significant of these genes are *HLA-DRB1*15:01* and other genes in strong linkage disequilibrium with *HLA-DRB1*15:01*. Carrying the *HLA-DRB1*15:01* allele places the odds ratio for heterozygotes at ~ 3 and ~ 6 for homozygotes. Additionally, genome-wide association studies (GWAS) have identified more than 200 common genetic variants that increase the risk of MS, and many other risks and protective alleles have been found in addition to HLA genes[167,168]. However, the odds ratio for other polymorphisms is substantially smaller (1.1–1.2). According to the authors of the largest GWAS, the extended MHC region contains at least 32 associations, including MHC class I genes and non-classical HLA[168].

Most autoimmune and infectious diseases are associated with the HLA gene cluster[166]. In MS, the HLA locus contributes 20–30% of the genetic susceptibility[169]. Why *HLA-DRB1*15:01* plays such a significant role in the development of MS is unknown; however, it is hypothesized that the importance lies in antigen presentation[166].

In addition to risk variants, protective alleles have also been identified within HLA class I and II clusters. Most notable is the effect of *HLA-A*02:01*, which was observed independently of all class II associations in multiple studies[167,170]. Similarly, protective effects have been observed in the class I cluster for *HLA-B*44:02* and *HLA-C*05*, which remain in strong linkage disequilibrium[171,172]. Within class II alleles, *DRB1*14:01* is most commonly associated with protection against MS[173]; however, smaller studies have also identified *HLA-DRB1*01*, *DRB1*11*[174], and *DRB1*13 ~ DQB1*06:03* as protective[175]. Furthermore, DNA methylation of the HLA genes has been shown to mediate the risk of MS[176].

5.8.2. Non-HLA genetic risk variants

Most single nucleotide polymorphisms (SNPs) are associated with immune pathway genes, furthering the argument that MS is an autoimmune disease originating in dysregulation

of the peripheral immune system. Moreover, no association has been found between loci of CNS tissues, and the only significant CNS-linked enrichment was identified in microglial cells, the resident macrophages of CNS[168]. Furthermore, Factor et al. used an outside variant approach to identify risk variants closely interacting with genes previously connected to MS risk and found cell populations in which given variants were used[177]. According to Factor et al., most MS loci acted in T and B cells as expected, but myeloid cells of the innate immune system were also condemned. Additionally, they found six loci that they predicted to exert a function in the CNS. In addition, a GWAS found a novel susceptibility variant in chromosome X, which might be significant in the future since MS is overrepresented in females[168].

A GWAS also identified susceptibility variants that explain up to 50% of heritability. The GWAS approach has successfully organized the genetic architecture of MS; however, these studies are not designed to identify rare variants with an allele frequency lower than 1%.

Furthermore, many environmental factors both influence and are influenced by genetic contributions. For example, 12 genes related to vitamin D in MS susceptibility have been discovered. A Mendelian randomization study also showed that genetically elevated body mass is associated with a risk of MS[178,179]. Furthermore, the gut microbiome has been shown to be partially heritable[180]. As mentioned previously, the microbiome is one of the MS risk factors and regulators of the immune system. A microbiome GWAS found multiple significant associations between the microbiome and gene variants involved in metabolism and immunity[180]. Recently, the reactivity of 107 EBV peptides has been shown to be heritable, and a few have been associated with variants in MHC class II locus[181].

Successful studies have associated genetic risk factors with clinical outcomes. Recently, one such study showed genetic differences between RRMS and PPMS not seen in previous GWAS studies, and these differences were confirmed by gene transcription profiling[182]. Furthermore, several low-frequency variants have been correlated with a number of relapses in treated and treatment-naïve MS patients[183–185]. These data point toward a shared genetic background with individual heterogeneity and could help predict the outcome of the disease.

One of the essential loci that have not been thoroughly investigated in previous GWAS studies is *IGH*. The *IGH* locus is highly complex, with abundant polymorphisms, repetitive motifs, and copy number variations. Due to technical reasons, accurately assembling IGHV in large-scale, high-throughput studies has been impossible. However, there has been an effort to characterize the association between immunoglobulin genes and MS.

The IgG index has also been strongly associated with polymorphisms in *IGHC* locus[186], as confirmed by Gasperi et al.[187]. The authors described two regions—the *IGHC* locus and the MHC region—associated with lower levels of intrathecal IgM and IgA as well as higher levels of intrathecal IgG in MS or CIS patients. The effect was attributed to a group of 10 SNPs. The most robust association was found in a variant in the *IGHG3* gene (rs12897751). However, for the purpose of this thesis, the most important variant they studied was variant rs1071803, which they reported to be in strong linkage disequilibrium with rs12897751 and heavily associated with IgG production. The rs1071803 variant determines the G1m17 allotype on the CH1 domain of the IgG1 molecule.

5.8.3. G1m allotypes

Allotypes are amino acid variations in immunoglobulin's constant region. Traditionally, they have been defined by serology with antibodies directed against structural differences in constant regions[43]. Due to the allelic exclusion process, one B cell in a heterozygous person can only express one of two C-region alleles, never both. If a person is homozygous, they will only produce antibodies of one kind; however, heterozygotes will make antibodies of two different allotypes. Following the rule of allelic exclusion in heterozygous individuals, half of all B cells express one heavy chain allele, while the remaining half express the other inherited allele.

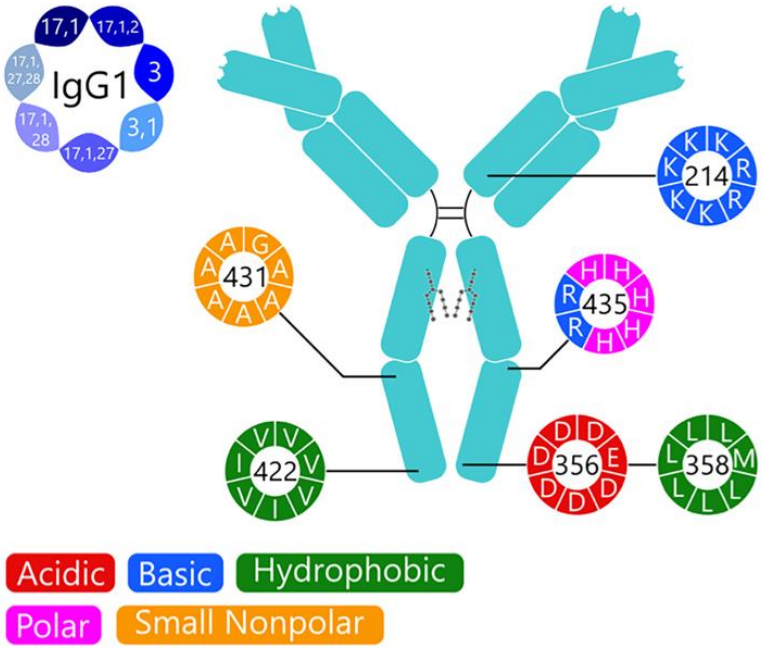

Figure 4. IgG1 allotypes*. Schematic representation of the IgG1 heavy chain with the displayed positions of known allotype-encoding polymorphisms. Each amino acid's location corresponds to the allotype designated at the same point on the wheel surrounding IgG1.* Adapted with permission from Springer Nature Customer Service Centre GmbH: Nature Publishing Group. Functional consequences of allotypic polymorphisms in human immunoglobulin G subclasses Andrew R. Crowley et al., copyright (2023).

Depending on immunoglobulin isotypes and subtypes, several different allotypes exist in heavy and light chains. However, in the context of MS, particular interest lies in the CH domain of IgG1. IgG1 has distinctive amino acids in positions 214 of the CH1 domain and 356, 358, and 431 of the CH3 domain (Figure 4 and Table 1)[188]. If arginine is in position 214 (R120)[*] on CH1, it is classified as a G1m3 allotype, while lysine in the same location (K120) defines G1m17. Within the CH3 domain, aspartate at position 356 (D12) and leucine at 358 (L14) determine G1m1. If glutamate (E12) and methionine (M14) are found at the same positions, the determined allotype is G1m-1. G1m-1 can also be denoted as nG1m1 and is an isoallotype, meaning the same polymorphism is found on IgGs of other subtypes. Glycine at position 431 (G110) defines the G1m2 allotype, and the absence of G1m2 equals the presence of alanine (A110) in this position. A110 is found across many alleles in different subtypes of IgG. Consequently, only one allele, *IGHG1*07p*, encodes the G1m2 allotype[188]. Strong linkage disequilibrium in Caucasians exists between allotypes in the CH1 and CH3 regions of IgG1; therefore, they are inherited together as a haplotype—G1m1 with G1m17

[*] Positions according to IMGT unique numbering for constant domain

and G1m3 with G1m-1. In the Caucasian population, around 43% are heterozygous for G1m1/G1m3, 45% are G1m3 homozygous, and 11% are G1m1 homozygous[189].

Table 1. Human G1m allotypes

Allotypes	IGHG1 alleles	Amino acid positions (IMGT numbering)			
		CH1	CH3		
		120	12	14	110
G1m17,1 G1m17,1,27 G1m17,1,28 G1m17,1,27,28	*IGHG1*01, IGHG1*02* *IGHG1*04* *IGHG1*05p*† *IGHG1*06p*†	Lys (K120)	Asp (D12)	Leu (L14)	Ala (A110)
G1m3 G1m-1	*IGHG1*03*	Arg (R120)	Glu (E12)	Met (M14)	Ala (A110)
G1m17,1,2	*IGHG1*07p*†	Lys (K120)	Asp (D12)	Leu (L14)	Gly (G110)
G1m3,1	*IGHG1*08p*†	Arg (R120)	Asp (D12)	Leu (L14)	Ala (A110)

The importance of G1m allotypes in MS was first reported in 1981 when G1m1 antibodies were described as being most abundant in the CSF of MS patients[190]. A few years later, the same group specified how the synthesis of intrathecal IgG depends on variations in the Ig constant region and MHC loci[191]. After decades of GWAS and studies on the *IGHC* locus, researchers fine-tuned an association between variations in *IGHC* and IgG production[187,192,193], the age of MS onset, and disease risk[193,194]. Additionally, recent flow cytometry studies from our group have demonstrated that an increased ratio of G1m1/G1m3 antibodies in the CSF of heterozygous MS patients uncovered in 1981 was caused by a changed proportion of intrathecal G1m1/G1m3 antibody-secreting cells (ASC)[195]. Accordingly, nearly all intrathecal ASCs expressed the G1m1 allotype, while the ratio remained 50/50 in the blood.

† p – provisional number, alleles are expected but not sequenced at the nucleotide level

G1m allotypes have been shown to impact various immunopathologies. In hepatitis C, the virus core protein mimics the Fcγ receptor and preferentially binds to the G1m3 allotype. Therefore, G1m3 antibodies are mostly scavenged, diminishing the immune system's ability to clear the pathogen[196]. Cytomegalovirus uses decoy Fcγ receptors to evade the immune system that have a higher affinity for G1m1 or G1m3, depending on the type of decoy[197]. A significant association has been found between polymorphisms in the CH1 region of G1m and Alzheimer's disease, where G1m17 leads to increased susceptibility and G1m3 has been connected with a protective role[198]. Furthermore, G1m3 has been reported as a risk factor in different types of cancer[199].

The consequences of allotypes on functions of the immune system are poorly documented. Some allotypes alter the half-life of IgG3 antibodies and can also influence their distribution to particular tissues[200]. They have also been shown to modify secondary mRNA structures and alter the class switching process and the transcription rate[43,201]. Additionally, they correlate with IgG plasma concentrations[202]. IgG1 allotypes have been shown to influence the distribution of antibody subclasses after human immunodeficiency virus (HIV) vaccination[203,204].

6. Aims

The main goal of this thesis is to gain insights into the mechanisms underlying B-cell responses in both treatment-naïve multiple sclerosis patients and those treated with DMF. The aims are as follows:

- The critical point of the study is to characterize the paired immunoglobulin heavy- and light-chain repertoires and phenotypes of B-lineage cells in MS patients. Therefore, we aim to phenotype single cells, describe the variable parts of the heavy and light chains, and identify disease-relevant B-cell clones. The adjacent objective is to examine polymorphisms (allotypes) carried in the IgG constant region in MS (paper I).

- We aim to determine which B cells in the CSF of MS patients are the major intrathecal IgG producers. We investigate whether the most expanded B-cell clones produce the dominant IgG fractions in the CSF. Additionally, we set out to identify the B cell population to which they belong and what phenotypic profile the contributing cells express (papers I and II).

- The relevance of intrathecal B cells in multiple sclerosis is based on the theory that memory B cells reside within the CNS and undergo intrathecal affinity maturation, potentially rendering them an ideal target for MS treatment. Recent studies have shown that memory B cells in the blood are one of the primary targets for all available treatments for multiple sclerosis. Therefore, we aim to uncover whether it holds true for intrathecal B-cell populations and how DMTs with a focus on DMF alter the phenotypes of these populations (paper III).

7. Summary of papers

Paper I

In paper 1, we characterized the intrathecal BCR repertoire, clonal relationships, and transcriptional profiles of intrathecal B-lineage cells. To date, it was the most detailed study of B-lineage cells in the CSF of MS patients. This investigation was achieved by using flow cytometry index-sorting single-cell full-length mRNA-sequencing techniques and various bioinformatics tools. The results revealed biased use of the *IGHV4* gene family and excessive production of the κ-light chain tightly linked to the G1m1 allotype in ASCs, resulting in a pattern of preferential pairing of heavy- and light-chain variable gene segments. In patients homozygous for G1m3, no such patterns were observed. Additionally, the results showed selective enrichment in G1m1 ASCs but not to the same extent in memory cells. We found an accumulation of somatic mutations and large clonal expansions, including clonal relationships between memory cells and ASCs, and thus corroborated previous studies. Moreover, we observed clonally related cells of different isotypes, which indicated an intrathecal isotype switch. These results suggested intrathecal maturation of collected B cells and an intrathecal B-cell response directed against similar epitopes in patients carrying the G1m1 allotype.

Paper II

In paper II, we aimed to establish characteristics of B-lineage cells producing oligoclonal IgG and map how related cells partake in oligoclonal IgG production. We used previously generated paired heavy- and light-chain CDR3 data from a proportion of the patients included in paper I. We combined these data with mass spectrometry of IgG from matching CSF and serum samples of 10 MS patients. Connecting transcriptomic and proteomics data from the CSF of MS patients enabled us to describe true intrathecal IgG-producing single B cells. We showed that intrathecally produced IgG better matches clonally expanded ASCs compared to singletons. The oligoclonal IgG-producing cells represented heterogeneous populations of highly proliferating cells clonally related to a more differentiated, seemingly non-proliferating cell cluster that appeared to focus on immunoglobulin production.

Paper III

Paper III examined differences in blood and CSF B-cell composition in MS patients treated with DMF versus those treated with other therapeutics (GA, IFN) or no drugs. In accordance with previous studies, we found a depleted memory B-cell population in the blood of patients treated with DMF. Furthermore, we also observed that the reduction in memory B-cell numbers was correlated with the duration of the treatment. DMF-treated patients showed a more substantial decrease in the number of intrathecal plasmablasts than any other group, as well as a lower absolute count of intrathecal mononuclear cells. This paper was exploratory and confined by the previous choice of included surface markers, but it supported the theory of B cells as a potential mechanistic target of DMF.

8. Methodological considerations

8.1. Study populations

Subjects were recruited for papers I and II at the Department of Neurology at Akershus University Hospital and the Neurology Department at Ulleval Oslo University Hospital. In paper I, 24 patients were recruited during diagnostic workups. Three patients were excluded during flow cytometry analysis and cell sorting due to the low number of possible ASCs. Prior to inclusion, two patients had been treated with methylprednisolone. No other participants had received corticosteroids or any immunomodulatory treatment that could deplete cell counts and alter the phenotype and composition of B-cell populations in CSF. All patients were of Caucasian ethnicity to ensure a similar genetic profile.

Initially, we discussed whether we should include control patients with other neuroinflammatory diseases. We considered Lyme neuroborreliosis patients as they display neuroinflammation and intrathecal antibody production. Additionally, Lyme neuroborreliosis is caused by a known pathogen and manifests as acute or subacute inflammation, which is typically treated immediately with antibiotics. However, since MS takes years to develop before the first onset of symptoms[205,206], whether diseases presenting with acute neuroinflammation are adequate controls is disputable.

In papers I and II, we used CSF and blood samples from the same patients. For proteomic analysis in paper II we chose participants with the highest number of sorted cells. Considering the limitations of our approach to acquiring ASCs and B cells, we wanted to collect as many BCR sequences as possible to construct a proteomic library. Thus, 10 out of 24 previously included patients were analyzed in paper II.

In paper III, we reanalyzed flow cytometry data based on the treatment status of 28 MS patients recruited at the Departments of Neurology at Akershus University Hospital and Oslo University Hospital[195]. According to the 2010 McDonald criteria, all patients had MS; one was classified as SPMS, and all others had developed RRMS at the time of inclusion[77].

8.2. Flow cytometry

In paper I, single-cell index-sorting was performed on a FACS ARIA III cell sorter equipped with 408, 488, 561, and 633 nm lasers (BD Biosciences) at the flow cytometry core facility at Oslo University Hospital. The staining strategy focused on identifying ASCs and other B-cell subsets; therefore, we used the following anti-human antibodies from BD Biosciences: CD3, CD14, CD16, CD19, CD27, CD38, IgD, and LIVE/DEAD Fixable Violet. Single ASCs and B cells were index-sorted; fluorescence intensity values were recorded for each sorted cell, allowing for more accurate phenotyping of sorted B cells in conjunction with gene expression data. ASCs were the main population of interest but typically constituted only a minor part of the B-cell population. Therefore, other B-cell populations were sorted if we had already obtained a sufficient number of ASCs.

In paper III, a panel of fluorochrome-conjugated antibodies was selected to analyze blood and CSF mononuclear cells, again focusing on ASC identification with the addition of memory and naïve B cells[195]. Therefore, anti-CD19, CD27, CD38, CD138, IgG, Ki-67, and HLA-DR antibodies were utilized in addition to anti-CD3 and CD14 dump-channel antibodies (BD Biosciences). The flow cytometry setup was designed for a different study; therefore, fluorochromes were pre-selected and not optimal for our purpose, which caused us to omit a few markers of interest. For instance, the data did not contain markers for IgD, which would have allowed us to differentiate between class-switched and unswitched memory B cells and determine how these populations within the CSF were affected by DMF.

8.3. Single-cell RNA-sequencing

Due to differences in processing requirements, the B cell and ASCs populations in paper I could not be sorted together. ASCs' transcriptome mostly comprises immunoglobulin genes, unlike other B cells. Consequently, we adjusted the protocol by increasing B cells' PCR cycles by one. This prioritizing approach maximized intrathecal ASC collection, but insufficient CSF remained to sort other B-cell populations in patients with low CSF cell count. Sorting populations into separate plates for separate processing leads to artificial variation due to batch effect rather than biological differences. However, this systemic influence was minimized by normalizing gene expression data[207].

High-throughput sequencing with sensitive PCR methods enhances the understanding of complex transcriptomes. For a long time, the limiting factor of sequencing techniques was the input RNA needed for the analysis. However, in the last decade, single-cell transcriptomic techniques have emerged to study cell-to-cell variability and population heterogeneity. Methods like Drop-seq, InDrop-seq, Seq-Well, and STRT-seq require abundant material and risk losing cells of interest. These methods only capture the 5' or 3' end of each transcript[208]. The 10x Genomics Chromium platform, which sequences either the 5' or 3' part of the transcript, has gained significant interest. The 10X system barcodes and encapsulates single cells in gel beads, enabling downstream processing in a single tube[209]. However, it lacks control over the analyzed cell population and can be influenced by selection biases, potentially distorting or losing rare cell populations. Moreover, it detects fewer genes per cell (500–1,500) compared to Smart-seq2 (~ 4,000–7,000) or MARS-seq (~ 500–3,000)[210].

Aiming to achieve uniform read coverage and quantification of gene expression with high accuracy and sensitivity at minimal losses of scarce material, we chose the Smart-seq2[211] approach to sequence single intrathecal B cells from MS patients. Smart-seq2 enabled us to obtain transcriptomic profiles and full-length paired heavy- and light-chain BCR sequences in papers I and II. The same sequencing depth and a comparable number of analyzed B-lineage cells would not have been achievable using the 10X Genomics protocol.

We implemented the Smart-Seq2 protocol with minor modifications that increased the yield of the reverse transcription reaction, decreased the number of primer-dimers after purification steps, and increased the amplification output. We used SmartScribe RT in reverse transcription instead of Superscript II due to its higher fidelity[212]. In addition, we introduced a modified TSO primer with added 5'-biotin, aiming to produce fewer secondary structures during RT[213]. After RT, the cDNA was amplified, and the final library was prepared using in-house-made Tn5 transposase and dual indexing with Nextera (XT) N7xx and S5xx primers. The final library was sequenced on the Illumina NextSeq500 platform at the Norwegian Sequencing Center. Balancing the cost and depth of sequencing, we chose a sequencing run of 75 bp paired-end reads in high output mode, which gave approximately 400 million reads, effectively producing around 1 million reads per cell. The optimal number of reads depends on cell type, transcripts, the number of known genes, and genome size. Current data from single-cell RNA-seq studies suggest that reaching 1 million reads is nearing saturation of

sequencing depth. Depending on the used protocol and sequencing platform, the vast majority of gene transcripts can be detected at half that depth[208].

8.4. Processing of raw sequencing data

In papers I and II, to quantify the expression of transcripts, we decided to use Salmon[214]. Salmon is a pseudoaligner based on the k-mer model, which uses a lightweight alignment algorithm that works as a mapping model, in which the abundance of transcripts is estimated from equivalence classes rather than an exact match to an index. We built the Salmon index using the human genome GRCh38.94, and the k-mer value of 25 was chosen as optimal. The following steps included collapsing gene-level transcripts and correcting for transcript length, quality, and normalization.

The quality of the reads varied from cell to cell and between libraries. Therefore, the threshold values for each parameter in the quality control phase were established based on the normal distribution observed within libraries. Low-quality reads can be found for several reasons, such as insufficient amounts of mRNA within the cell, problems with amplification, the cell's going into distress while being sorted and becoming apoptotic, cross-contamination between cells, or errors occurring during sorting resulting in no or multiple cells in one well[215]. To interpret our results correctly, we removed low-quality cells based on the following criteria:

- Mapping rate above 40%—low mapping rate points to an empty well or degraded RNA
- Number of detected genes and reads; exact thresholds depending on library—we removed cells with the number falling outside of the range to discard suspected duplicates, spill-overs, and empty wells
- Percent of mitochondrial genes below 8%—this number grows as the cell goes into apoptosis, while genomic mRNA is lost
- Reconstruction of productive BCR heavy chain

After quality control, we obtained single-cell RNA-sequencing data of 2,165 cells from 21 MS patients.

8.5. Transcriptome-based phenotyping and visualization of single-cells

To characterize intrathecal populations of B cells, we looked at three sets of features in paper I: differential gene expression data, flow cytometry surface markers, and properties of expressed BCRs.

To visualize and reduce gene expression data complexity, we used principal component analysis (PCA). PCA is a linear dimensionality reduction technique that retains significant data variation while reducing dimensionality. We then employed uniform manifold approximation and projection (UMAP), a non-linear dimensionality reduction method, for two-dimensional data projection and visualization[216]. For the overall analysis of all cells, we utilized the first 25 principal components. However, only seven components were necessary for the CD19+ B-cell population. This contrast indicated substantial differences in gene expression patterns between ASCs and non-ASC B cells (although fewer differences within the CD19+ B-cell population). An alternative gene data analysis and visualization approach would involve using t-distributed stochastic neighbor embedding (t-SNE). Both methods preserve the local structure, but UMAP better preserves the global structure and topology of the data, making it easier to judge whether differences between cells are important[217].

We adopted a similar approach in paper II, relying on the same data set for gene expression analysis. We also focused on gene expression and pathway enrichment analysis[218]. Pathway enrichment analysis maps gene sets with known biological functions and finds statistically significant enrichments while considering gene or protein interactions and integrating those structures into the analysis. Gene enrichment or gene set enrichment analysis produces lists of up- or down-regulated genes without considering either their function or the topology of cellular interactions. Therefore, focusing on known pathways allowed us to find commonalities in gene expression patterns (phenotypes) among different clusters of IgG-producing ASCs.

8.6. B-cell receptor analysis

While using the SmartSeq2 protocol, we were not limited by primer location in PCR reactions; therefore, we obtained complete heavy-chain gene sequences. BCR sequences were reassembled using BraCeR[219], which generated the full-length, recombined variable regions

of IgH and Igκ/λ. Unfiltered BraCeR output frequently consisted of multiple heavy and light chains per cell in which one pair had a far higher transcript per million (TPM) value than other chains. The additional chains could have been caused by PCR errors, bar-code switching, or cross-contamination from different wells. BraCeR collapsed similar reconstructed sequences in each cell and identified the most highly expressed chains, thus eliminating errors in sequences introduced in PCR reactions. Eliminating PCR errors is a great advantage when performing downstream analysis of mutations, clonal relationships, and lineage tracing.

8.6.1. Mutational load and clonality assessment

In the previous step, we filtered out additional chains constituting a minor part of the cells' transcriptome. However, cells with a high expression of multiple heavy and light chains were retained. We examined each cell individually and manually filtered out suspected doublets. We did not want to exclude any cells truly expressing more than one chain per locus, but removing possible multiplets was necessary as they can interfere with proper clonality assignment. Doublet removal operated on the assumption that cells with two productive recombinants for a locus are rare (expected at 2–5% for IgH and 11% for Igκ in mice[220]). Cells were removed if multiple chains from the same locus significantly differed from each other and/or cells containing multiple chains connected two clone groups.

BraCeR created summary files used to identify clonal relationships between cells and build lineage trees for reconstructed clone groups. Additionally, the mutational load was assessed for the most highly expressed chains. Tracing mutational loads and patterns in the paired full-length variable heavy- and light-chain genes allowed us to follow the clonal evolution of B cells and reconstruct detailed lineage trees.

8.6.2. G1m allotype analysis

Next to the V-, J-, and D-regions, BraCeR reconstructed the CH1 domain for each cell. This provided information about the isotype of BCR but was insufficient to determine the *IGHC* alleles, which correspond to allotypes[188]. Therefore, we also inferred alleles by mapping cell sequences to IMGT allele sequences and CH1, CH2, and CH3 regions. In patients with few cells of the G1m1 allotype, establishing whether the patient was

homozygous for G1m1 or heterozygous for G1m1/G1m3 was impossible, with a strong skewing toward the G1m1 allotype within CSF as previously observed by our group[195].

Allotypes can also be determined by phenotyping IgG1 immunoglobulins in the blood. Therefore, to confirm our findings on the transcriptomic level and differentiate between homozygous G1m1 and heterozygous G1m1/G1m3 patients, we next applied the ELISA method to the serum of the included patients as previously described[195].

8.7. Nano liquid chromatograph-mass spectrometry

The CSF and serum samples from 10 MS patients were matched, and the total IgG was isolated and digested using a mix of trypsin and Lys-C. This mixture has been shown to have greater reproducibility, detect a higher number of products, and achieve more accurate quantification than trypsin alone[221]. Additionally, trypsin specificity matched our needs as it cuts on the C-terminal side of lysine and arginine, which are common in the motifs surrounding predicted CDR3 regions. To increase the number of detected sequences, we used different proteolytic enzymes with specificities. In addition to trypsin/Lys-C, we tried to apply Asp-N protease, which cleaves peptide bonds on the N-terminal side of aspartic and glutamic acids, which are common in BCR sequences surrounding CDR3 fragments. However, in our experimental conditions, Asp-N repeatedly failed to digest IgG.

To detect as many peptides as possible, the digested solution was first run through liquid chromatography (LC). In LC-mass spectrometry, peptide mix fractions are separated on a column prior to detection based on their physical properties. This process significantly increases the sensitivity of mass spectrometry and provides more reproducible results[222].

Output files from the mass spectrometer were processed using MaxQuant. The personalized search libraries consisted of variable region fragments of the BCR database created with the single-cell RNA sequencing from paper I. Peptide hits were filtered based on the obtained intensity-based absolute quantification (iBAQ) values to differentiate between serum and intrathecal IgG. The iBAQ measurement was chosen because it represented the total peak intensity divided by the theoretical peptides identified for one protein; therefore, it was normalized.

An alternative approach to analyzing CSF proteomics is through IEF of matched CSF and serum on IPG strips. This method enables the comparison and selective digestion of CSF-specific bands. While it provides the advantage of preselecting intrathecally produced IgG, it may result in the loss of less-abundant immunoglobulins that do not appear as bands. However, quantifying total IgG using mass spectrometry allows for comparing CSF and serum values, enabling the determination of its origin within or outside the CNS. Additionally, using total IgG is a faster and more cost-effective alternative to IEF.

8.8. Ethical considerations

The sample collection for the studies presented in papers I, II, and III was approved by the Committee for Research Ethics at the South-Eastern Norwegian Health Authority (2009/23). All participants signed an informed consent form before inclusion.

Sample collection for papers I and II occurred during diagnostic lumbar punctures for all but one patient. Lumbar puncture is a standard procedure before MS diagnosis. It is relatively invasive but rarely dangerous. Most commonly, patients can experience spinal headaches after a lumbar puncture; the practice rarely results in bleeding or infections. As the sample collection was part of a standard diagnostic process, donating additional small amounts of CSF and blood did not substantially increase the donors' risk of side effects.

The biological material used in paper III had been the subject of a different study. We reanalyzed already available data, maximizing the output from patient contributions and minimizing the time, labor, and cost associated with patient recruitment and data collection[223]. Samples used in that study were stored in a research biobank at the Department of Immunology and Transfusion Medicine, University of Oslo. All samples were stored in coded containers administered by senior personnel. The Ethical Committee approved the use of this material.

All patients were given identification codes. Code names were used throughout all processing and analysis steps. The identification codes were stored on encrypted and password-protected flash drives in a physical safe. In paper I, all raw sequencing data storage and processing happened within Services for Sensitive Data servers to protect the patients' data further. Services for Sensitive Data is a platform created by UiO to store, analyze, and

collect sensitive data securely. Additionally, we deposited all raw sequencing data output, BCR sequences, and metadata obtained in paper I at the European Genome-Phenome Archive with restricted access. Finally, intrathecal IgG raw mass spectrometry output files from paper II were uploaded to the MassIVE data repository.

8.9. Statistics

In paper I, statistical analysis and graphs were prepared using R and ggpubr. All tests were two-sided, with a significance level set at 0.005. We adopted the non-parametric test (Wilcoxon rank-sum) to compare somatic mutation frequencies between sequences of different isotypes. We also used the Wilcoxon rank-sum test to determine whether differences in Igκ usage and *IGHV4* gene family usage were significant between ASCs expressing G1m1 and G1m3 allotypes. Except for somatic hypermutation frequency, we also tested the median frequency from each patient versus the B-cell population and isotype. This testing was conducted using the Wilcoxon signed-rank test. We applied binomial distribution to determine whether G1m1/G1m3 cells' distribution deviates from 50/50 in ASCs and memory cells from heterozygous patients. A paired t-test was used to examine differences in G1m allotype usage frequencies between different cell populations and between G1m1 and G1m3 cells in G1m1/G1m3 heterozygotes.

For the second paper, all graphs except pathway enrichment analysis were completed utilizing R packages: ggplot2, ggbreak, and ggpubr. The pathway enrichment analysis was visualized using Cytoscape. All statistical analyses were performed in R version and scanpy, and all tests were two-tailed with a significance level of 0.005. To diminish the influence of clonal expansion on the analysis, all clonally related cells were collapsed into a single unit and treated as one. We used the Wilcoxon signed-rank test to compare intrathecal IgG matches between different B-cell populations and the proportion of matches between clonally expanded cells and singletons. Differential gene expression ranking was constructed based on Wilcoxon rank-sum test results.

In the third paper, because of the non-normal distribution of the data, which had only two groups and few samples, we used the two-sample Wilcoxon exact test to compare groups of patients treated with different drugs or without any treatment. As before, we set the significance level at 5%, and the tests were two-tailed. We did not perform any corrections

for multiple tests. Paper III was an exploratory investigation conducted as part of a different study with a highly heterogeneous control group. Additionally, our findings reflected what has previously been found in the blood. Therefore, a conservative multiple testing correction that accounts for dependent variables for multiple testing would be considered too strict[209].

9. Discussion

9.1. Allotypes correlating with immune repertoires

Antibody-secreting cells and memory cells are the main subsets of the intrathecal B-cell population in MS patients[93]. Many known yet unconfirmed specificities of intrathecal immunoglobulins suggest targeting several possible antigens. Previous studies have primarily focused on autoantigens associated with oligodendrocytes, neurons, astrocytes, cellular debris, adhesion molecules, and viruses[118,120,122,224]. However, these findings have not been confirmed by independent studies[117,225]. B cells in CNS are somatically hypermutated, clonally related, and, along with OCBs, persistent over time[109,123]. Preferential use of the *IGHV4* gene family has also been previously reported, along with the acquisition of specific mutations[226,227]. Collectively, characteristics of B cells in the CNS of MS patients are hallmarks of an ongoing, antigen-driven immune response. However, the understanding of intrathecal immunity in MS is still incomplete. Below, I present our results and those of others to fill in knowledge gaps and form new hypotheses that may provide insights into the role of B cells in MS.

In paper I, we utilized the single-cell RNA-seq technique to obtain paired heavy- and light-chain genes of CSF B cells in treatment-naïve MS patients. We confirmed previous reports that the isotype is heavily skewed toward the IgG1 subclass among ASCs. Moreover, we showed on a transcriptional level that IgG1 ASCs preferentially use the G1m1 allotype in heterozygous G1m1/G1m3 patients. In paper I, we also exposed restriction patterns across study subjects. First, *IGHV4* gene segment bias was found only in patients carrying the G1m1 allotype. Previous studies have not found *IGHV4* bias in all MS cases when the G1m carrier status was not defined[86,226]. We also reanalyzed previously published data from intrathecal B cells of MS patients with known G1m carrier status and verified results showing the restriction of *IGHV* gene usage depending on G1m allotype[86,109].

Furthermore, G1m1-expressing ASCs mainly used κ-light chain, whereas in several G1m3 homozygous patients, ASCs showed a κ/λ ratio lower than expected from healthy individuals[228]. The shifted κ/λ ratio was also of interest because κ and λ free light chains are gaining attention as a valuable diagnostic tool in MS. Based on our results, patients with the G1m1 allotype could potentially have higher free κ light chain measurements in CSF

depending on the portion of B cells expressing κ light chain due to the link to the G1m allotype. Another discovery was an association between the G1m1 allotype in ASCs and the preferential pairing of heavy and light variable segments. These repertoire restrictions were more pronounced in ASCs than in the memory-cell population. These results suggest that some ASCs might be directed against similar epitopes.

In paper I, we also provided a more detailed description of clonal relationships between intrathecal B-lineage cells than previous studies. Clonality assessment was based on somatic mutations in both heavy and light chains. The observed high degree of ASC clonality was in line with previous studies[229,230]. However, we also discovered a more focused immune response, as the lineage trees were considerably smaller than previously reported, with fewer offspring cells and many ASCs containing indistinguishable SHM patterns. This was unexpected, as more mutations are anticipated when considering both heavy and light chains. The accurate characterization of clonal expansion was possible due to the minimization of PCR and sequencing errors inherent to previously used bulk sequencing techniques. PCR errors cannot be easily detected, and correcting them requires unique molecular identifiers and computational methods, which were unavailable until recently[231]. Therefore, studies using bulk sequencing have heavily overestimated the diversity of BCR sequences.

9.1.1. Influence of genetic factors

The mechanism underlying the preferential usage and pairing of variable heavy- and light-chain genes is unknown. The observed light chain preference might result from the differences in variable and constant regions of the heavy chain, causing pairing with a more compatible light chain. Another possible explanation could be the influence of the G1m allotype on the BCRs V-region's specificity and affinity, similar to previously shown effects of the CH region on the V-region[32]. For example, polymorphisms in the constant region could result in conformational changes in the variable region, influencing BCR clustering and signaling, as well as modulating the intracellular transport and antigen presentation on HLA class II molecules. In Caucasians, the G1m1 and G1m17 allotypes are in nearly perfect linkage disequilibrium; therefore, they are inherited together on the same chromosome. Thus, linkage disequilibrium between *IGHG1* alleles encoding allotypes and particular *IGHV* gene segments is another possibility.

The genetic explanation for the connection between variable heavy/light chain segments and the constant region of a heavy chain could be so-called super-haplotypes[232,233]. In that case, a critical role would be played by linkage disequilibrium, which is an association of alleles of different genes that occur together more commonly than expected from their allele frequencies. When found on one chromosome, neighboring alleles of other genes are referred to as haplotypes. The most acknowledged example of a super-haplotype is HLA-ABC, which features a strong linkage disequilibrium between involved HLA-ABC genes. Furthermore, the combination of alleles situated in loci on the HLA super-haplotypes has been stable throughout the evolution of our species and parts of MHC block structure are highly conserved[234,235]. Immunoglobulin genes might also form such extended haplotypes. In this case, different haplotype groups would have distinct C- and V-regions in linkage disequilibrium.

The idea of *IGH* locus influencing immune repertoire formation has been proposed previously. For example, polymorphisms with changes in plenty of the regulatory elements in the *IGH* locus have been suggested as driving changes in locus topology and chromatin conformation, thereby impacting the selection of V, D, and J gene segments[236]. In addition, genetic differences could potentially impact V(D)J recombination. Germline *IGHV* genes are partly responsible for antibody specificity[237] and have been associated with progression and clinical phenotypes in various scenarios, including vaccination, infection, and inflammation[238–240]. Moreover, structural variants and SNPs can modify key regulatory elements, such as promoters and enhancers, through deletions, loss of function SNPs, or the creation of new features. These structural variants could additionally influence the unique configuration of key regulatory elements. Such reorganization would lead to changes in interactions between promoters, enhancers, and their respective structures, which could ultimately change the construction of the locus and influence a selection of V, D, and J genes.

Further, some variants of CH domains could be in linkage disequilibrium with polymorphisms regulating CSR, which could explain the observed variation in IgG subclass distribution depending on the carried *IGHG1* alleles[202]. The frequencies of polymorphisms in HS2.1 enhancers in Caucasians have been correlated with the frequencies of *IGHG1* alleles in the same population, indicating linkage diequilibrium[241]. Comparison of polymorphisms in different people has shown that, for functionally distinct allotypes, allotypes exist defined by

SNPs that display significant inter-population differentiation, possibly due to selection pressure[242].

9.1.2. Functional considerations

The importance of allotypes in immunoglobulin functions cannot be overlooked. The IgG subclass's response to tumor antigens and pathogens varies, and one of the determinants of this response is the FcγR. *FCGR* encodes FcγR, and the gene polymorphisms cause variable affinities in binding to subclasses of human IgG. Particular *FCGR* and *IGHG* alleles potentially interact in the form of epistasis and provide a specific effector response through IgG. Epistasis provides a functional explanation for many associations discovered between FcγR and allotypes in infectious and autoimmune diseases and cancer[43]. Allotypes in the modulation of the immunoglobulin's ability to interact with and trigger FcγR have been investigated for decades, yet the evidence has remained limited. Early studies did not find significant differences in the interactions of various FcγRs with IgG allotypes[243,244]. However, the soluble IgG1 has been shown to possess varying affinities for the neonatal Fc receptor (FcRn), depending on the allotype[245]. The FcRn transports IgG and albumin across barriers (i.e., placenta, BBB) and protects them from intracellular degradation. An abundance of the FcRn is expressed at the BBB, where it is involved in the outflow of IgG from the CNS, as well as IgG's distribution in the brain[246,247]. Moreover, various interactions with other FcγRs could play a role in determining the extent of tissue damage in the CNS through FcγR-driven enrichment of G1m1 allotype B cells. Allotypes may also be significant in interactions with complement factors.

Furthermore, depending on the mAb allotype, FcRn has been shown to influence therapeutic mAb kinetics. In a study by Ternant et al., G1m1 homozygous patients had a higher drug clearance rate caused by a higher affinity of G1m1 IgG1 to FcRn than G1m3[245]. In G1m3 carriers, infliximab surpassed the patients' IgG1, thus using more FcRn recycling, which resulted in the drug's longer half-life. These results confirmed that a change far from the FcRn binding site can influence IgG binding to FcRn[248,249]. Therefore, the G1m1 allotype (D/E12; L/M14 in the CH3 region), located close to the FcRn binding site, may impact FcRn binding. This process could depend on the allotype in the CH1 segment, which through changes in charge distribution, would affect the conformational flexibility of the protein[249]. In the CH1 domain, allotypes defining positively charged arginine/lysin are expected to modify

the charge of the Fab fragment. This should affect FcRn and plasma membrane interactions based on electrostatic force[249,250].

9.2. Speculation about B-cell trafficking and intrathecal maturation

In paper I, we showed clonal expansion of isotypes other than IgG1. We also found clonally expanded IgM, IgA1, IgG2, IgG3, and IgG4, as well as clonal trees containing cells of different isotypes. These isotypes were observed between IgG1 and IgG2, IgG1 and IgA1, and IgM and IgG1. The simplest explanation of the different detected isotypes is intrathecal B-cell maturation. Moreover, we found expanded memory cells; for most patients, memory cells were clonally connected to the ASC population.

B cells in the CNS of MS subjects have been shown to be clonally connected to cells in the periphery[86,96,230]. Recent studies of mice have revealed that meningeal B cells come from the skull bone marrow, and the meningeal compartment provides a lymphopoietic niche for developing B cells[50,51]. In pathological conditions like MS, another place for B-cell maturation within the CNS could be GC-like B-cell follicles found in the meninges of SPMS patients and possibly present at earlier stages of the disease[81]. The CNS can be a favorable microenvironment for GC-like reactions, as shown by the presence of crucial cytokines and chemokines in the CSF of MS patients[251]. Additionally, the BCR mutation patterns specific to GC reinforce the idea that the CNS hosts TLSs[252]. Considering these discoveries, intrathecal B cells in MS may originate within the CNS or its proximity. Furthermore, preferential PB differentiation and selection of the G1m1 allotype may occur within TLSs, leading to our observation of G1m allotype skewing in CSF but not in peripheral blood[195]. The unaffected blood G1m1/G1m3 ratio also suggests that the maturation process in GC does not produce enough cells to detect a change among the overwhelming abundance of peripheral blood cells. As B cells in MS may be continuously exchanged between the CNS and blood[96,109], intrathecal trafficking could be skewed toward the CNS and favor the G1m1 allotype over the G1m3 allotype via an unknown mechanism at the contact interface.

When the cell undergoes CSR and SHM, AICDA is crucial for affinity maturation. Expression of AICDA has been previously reported in intrathecal B cells[253]. We confirmed its presence in a portion of CSF B cells (paper I). We also found a relatively high mutational rate in the IgM ASCs, which confirmed previous observations showing excessive SHM in

IgM found in CSF compared to blood[253]. We also found a similar extensive rate of mutations in IgA ASCs, as well as expanded IgA clones, corroborating earlier research[254]. We did not find any distinct phenotypes of IgA B cells. Probstel et al. proposed that such cells could play a regulatory role[255]. The authors showed a population of IgA producers in the CSF that recognize gut microbiota and could be systemic mediators in MS and other neuroinflammatory diseases. However, in light of clonal connections between IgG1/IgM and IgA1-expressing cells, these cells may have a common origin. Another explanation could be diversified populations of IgA B cells with different lineages and functions in MS pathogenesis.

IGHC contains cis-regulatory elements that regulate the isotype switch and CH gene expression[256]. Polymorphism at the 3' of the *IGHC* locus in the regulatory region controls CH gene transcription[257]. The same polymorphism is associated with IgA deficiency and with IgM concentration[258]. Moreover, human and murine 3′ regulatory and switch regions have been described as including hotspots for estrogen receptor binding. The hotspots in enhancers have been shown to influence CSR and the BCR repertoire depending on gender[259]. The authors hypothesized that these findings could explain differences between antibody repertoires in males and females, thus contributing to the susceptibility of females to particular autoimmune diseases, including MS.

IGHG polymorphisms have been associated with IgG, IgM, and IgA indexes in the CSF of MS patients[187,192–194]. One of these polymorphisms encodes the IgG1 allotype and has been connected with a lower IgG index and poor prognosis[110,187]. Such a polymorphism may affect cis-regulatory elements upstream of *IGHC*, which would modify its expression, or it could interfere with different processes during CSR. The association between IgG production and SNPs in the *IGHC* was found only in MS patients; therefore, chronic low-grade inflammation likely produces an environment in which B cells mature with altered signals, triggering the observed effects. The specific array of cytokines in the CNS of MS patients could be favorable for CSR to the IgG1 isotype, which would explain our observations (as well as others') of the almost absolute dominance of the IgG1 subclass of ASCs in CSF (paper I).

9.3. Stereotyped B-cell responses

The target antigen of the humoral immunity in MS has not yet been found. Multiple studies have discovered a multitude of different epitopes, including CNS-associated antigens, cellular debris, and EBV[118,120,260,261]. However, none of these findings have been replicated in independent studies. Nevertheless, in paper I, we observed a preferential pairing pattern in the BCR—shared between patients—of *IGHV4* with *IGKV1*. This preferential pairing resembled stereotyped B-cell responses, which have been found in other diseases and are directed against causal factors. Pathogens can display a diverse range of antigens, consisting of even more epitopes, and the antibody repertoire generated as a response can thus be vast.

Finding similar sequences and antibody pairings between patients is nevertheless not rare. For example, reports of a restricted and stereotyped repertoire have been published for COVID-19[262]; influenza infection[263]; HIV infection[264]; dengue[265]; Ebola[266]; bacterial infections, such as Streptococcus pneumoniae[267]; and even autoimmune disorders, such as coeliac disease[268]. In addition, when exploring immune responses to individual epitopes, convergent and stereotyped antibody responses are often discovered[269]. This universal tendency suggests that suitability between antibody and epitope dictates the selection of BCRs responding to the antigen.

After immunization, activated B cells undergo affinity maturation; a process in which B cells with the highest affinity for BCR are selected over those with lower affinity. The ability of BCR to bind an antigen in the germline configuration is necessary to raise the B-cell response. Accordingly, genetic germline variation of the BCR sequence strongly influences the outcome of the humoral response[270]. The germline variation could be why we observed a pairing pattern only in G1m1-carrying ASCs, not G1m3-carriers. As the immunoglobulin genes have proven problematic to address in large-scale genetic studies, the occurrence of restricted, convergent antibody responses presents a foundation for genetic effects. Biased use of V-gene segments in antigen-specific and disease-specific BCR repertoires indicates functional implementation of germline variation[271].

9.4. Origin and significance of intrathecally produced immunoglobulins

In paper II, we investigated the cellular source of CSF IgG. Intrathecally synthesized immunoglobulins are a hallmark of chronic inflammation in the CNS. In MS, they can be

detected early in the disease process, even before a definite onset[205,272]. Few instances of OCB appearance after an MS diagnosis are known[273]. CIS patients positive for OCBs are two times more likely to convert to MS, and the time frame for conversion is significantly shorter[274,275]. Additionally, presence of OCBs in MS has been connected to a more aggressive disease course and faster development of disability[276]. Furthermore, OCBs at the time of MS onset are linked to more severe grey-matter pathology, cognitive impairment, and disability compared to patients with no OCBs detected[111].

The restricted nature of OCBs suggests that, within the CNS compartment, a limited number of ASCs, PCs, and PBs remain in their niches and continuously secrete antibodies into the CSF[85,123]. In the CSF, we found a rich population of ASCs, bursting with immunoglobulin gene transcripts (paper I and II) and connecting to intrathecally produced antibodies (paper II). In paper II, we showed that the intrathecal IgG matches the immunoglobulin transcriptome of both proliferating ASCs and cells with phenotypes of more differentiated PCs strictly involved with immunoglobulin production. Moreover, we found that cells of both phenotypes are clonally related, which could suggest common ancestry or evolution from newly produced PBs to more mature phenotypes. A different source of intrathecal antibodies could be TLSs in meninges and subarachnoid spaces[81,106]. TLSs are full of ASCs, and the antibodies can be secreted from TLSs into CSF. A portion of immunoglobulins detected in CSF can also be found in the peripheral blood of MS patients, similar to the B-cell clones that produced them[109,230].

The OCB pattern is unique for each individual but can persist for decades despite efficacious MS therapies. Based on our findings in paper II, MS drugs may need to affect both newly generated and more differentiated ASCs to efficiently target the IgG-producing B cells. Due to their inability to cross the BBB and their primary focus on CD20 (which some PBs and PCs do not express), mAb-based treatments fail to influence OCB status. Nevertheless, some MS drugs can reduce OCBs in a proportion of patients, of which well-documented examples are natalizumab and cladribine[277–279]. Natalizumab is an antibody that blocks the migration of lymphocytes into the CNS. Cladribine, a small-molecule compound with good penetration of the BBB, has been shown to stabilize or decrease OCB levels via lymphocyte depletion in progressive MS and to eradicate OCBs in RRMS. Autologous hematopoietic stem cell transplantation also has been shown to suppress IgM and IgG OCBs and reduce intrathecal immunoglobulin indices[280].

OCBs and an elevated IgG index are among the major characteristics of MS. About 95% of patients display OCBs, and 70% of these patients have an elevated IgG index[281]. However, the presence of OCBs and an elevated IgG index do not merely reflect the diffusion of antibodies from blood to CSF; the patient is only considered OCB-positive if OCBs are absent in the serum. Additionally, elevated free light chains in CSF depict intrathecal production of immunoglobulins[282]. Moreover, serum and CSF antibody concentrations are strongly correlated for most viruses found in the CSF of MS patients[283]. The likely explanation of this correlation is a continuous influx of ASCs from blood to the CNS that synchronously differentiate in the periphery and inside the CNS.

Furthermore, several studies have argued that only a small proportion of intrathecal B cells produce the main fractions of CSF IgG. The stable pattern of OCBs, as contrasted by a restricted clonal overlap of intrathecal B cells over time[108,109], shows the limitations of CSF sampling. A CSF sample only represents a small portion of all intrathecal ASCs. Therefore, any sample will miss disease-relevant ASCs and include random B-cell clones (papers I and II).

Antibodies can stimulate immune responses not only by binding a target antigen but also by interacting with the Fc receptor; an interaction that does not depend on the variable region or specificity. Possibly, these two mechanisms operate jointly, causing CNS damage without one specific antigen driving the pathology. This course of action can arise from interaction with activated microglia. Microglia express FcRs, and these cells have been identified as critical players in CNS destruction processes. Locally produced immunoglobulins allow microglia to maintain their activation status and stimulate a secretion of neurotoxic factors. For instance, demyelinating lesions are crowded with activated microglia and astrocytes[284].

Furthermore, activated microglia and astrocytes express CXCL12, a chemokine ligand for C-X-C Motif Chemokine Receptor 4 (CXCR4) found on B cells and PCs. CXCR4 triggers differentiation into PCs and is crucial for their persistence, creating an ever-stimulating loop[100,285]. While CXCL12 can create micro-niches in the parenchyma of PCs, supporting their long-term survival, it can also participate in the migration of end-differentiated PCs to their niche in the bone marrow[285]. Moreover, MS lesions show high CXCL13 expression and strong expression of its receptor (CXCR5) on B cells. The level of CXCL13 also strongly correlates with the production of intrathecal immunoglobulins[100].

Microglia and astrocytes can stimulate B-cell activation and survival of ASCs via the secretion of BAFF, a proliferation-inducing ligand (APRIL), and IL15, which promotes survival and immunoglobulin production[100,286,287]. Therefore, a self-perpetuating loop occurs in which antibodies stimulate activated pathological cells that, in turn, stimulate B cells to produce antibodies.

Furthermore, in gray matter lesions of PPMS, complement activation has been found (classical, lectin, and alternative pathway), indicating antibody-mediated complement activation, which suggests that antibodies contribute to the aggravation of pathology and underlines the irrevocable progression of MS[288]. Studies of demyelinating lesions have described four patterns that are stable for individual patients. However, only one pattern shows antibody-mediated damage[89,289].

The implications of intrathecal immunoglobulins are still under debate. Despite the clear role of intrathecal antibodies in MS, no significant differences have been found in the number of OCBs and IgG index between relapsing and progressive forms of MS and CIS[290]. CSF immunoglobulins could be pathogenic but might also present an active inflammatory process in the CNS. The mechanism of their persistence and the prognostic value of IgG and IgM status are controversial. Intrathecal IgM, like IgG, persists, which is a characteristic feature of MS[108,253]. Furthermore, CNS IgM has a high degree of SHM compared to IgM found in peripheral blood[253]. Moreover, IgM in the CSF of MS patients has been found to target CNS-associated antigens like myelin lipids[291]. How and why CNS B cells are triggered to start SHM and proliferation, resulting in intrathecal IgG and IgM, are indefinite. However, the persistence of the observed antibody production suggests that their production is not caused by a primary immune response.

In summary, identifying the pathological ASC responsible for the production of oligoclonal IgG guides the understanding of the mechanism behind B-cell responses in MS. In contrast to other studies, we showed that intrathecal immunoglobulins in MS patients are produced by heterogenous, but clonally connected populations of ASCs. These cells have phenotypes ranging from newly generated, actively dividing to more differentiated ASCs, possibly stemming from antigen-experienced common ancestors (paper II). This knowledge should reinforce the need for drugs targeting both proliferating and non-proliferating cells and also enable the most relevant B-lineage cells to be identified.

9.5. Peripheral and intrathecal effects of B-cell-mediated MS treatments

The peripheral target of immunomodulatory drugs in MS continues to be disputed. The B-cell exchange between the periphery and the CNS causes potentially pathological cells to enter the CNS compartment; however, mature antigen-experienced memory B cells more frequently enter the CNS or CSF via the BBB when its continuity is not damaged by inflammation[292]. Current immunomodulatory therapies for MS deplete or functionally impair such memory cells in the blood. Moreover, memory B cells are also slower at repopulating the periphery after depletion therapy[293].

The role of memory B cells in MS pathology is poorly understood. However, the key functions are believed to involve antigen presentation and T-cell collaboration. Memory B cells have been shown to cause spontaneous proliferation (autoproliferation) of brain-homing CD4+ memory T cells in MS patients receiving B-cell-depleting therapies[133]. This indicates severely dysregulated T-B collaboration in memory cells and supports the theory that memory cells are an excellent target in MS therapies.

Small molecular compounds used in MS treatment can move efficiently across the BBB. One of them is MMF—the active metabolite of DMF, which we investigated in paper III. MMF in CSF reaches 11% of the plasma concentration, showing robust potential for direct action against intrathecal B-cell populations[294]. DMF has been shown to reduce the number of peripheral memory B cells[151,154,156]. We confirmed these results, and we also observed a significant decline in the number of mononuclear cells and PBs in CSF. Therefore, the effect on the periphery is translated to an outcome inside.

We have also found that blood memory B cells (CD19+CD27+CD38-) in DMF-treated MS patients show decreased expression of HLA-DR molecules compared to untreated subjects. This finding confirmed the results of an animal study in which DMF was shown to reduce MHC class II expression on B cells[157]. Combined with the reported lower expression of co-stimulatory molecules by other researchers, our data suggests that DMF lowers the ability of memory B cells to present antigens[151].

Moreover, immune cells have been shown to respond differently to DMF and MMF depending on the levels of metabolites present in the environment. Due to variations in tissue exposure levels and metabolism rates, plasma levels of MMF exhibit high variability and are influenced by food intake. Furthermore, MMF and DMF are hydrolyzed by monocytes and

lymphocytes, resulting in a greater reduction of drug concentration in the blood compared to serum[295,296]. Therefore, various tissues and immune cell populations may experience distinct activities of fumarates, potentially influencing the drug's mechanism and therapeutic effectiveness. For this reason, determining the extent to which DMF and its metabolites differentially impact biochemical pathways is crucial.

Another approach to immunomodulation in MS is targeting B cells through survival factors. However, in clinical trials, atacicept resulted in an increased frequency of relapses and unaffected lesions[297]. In rheumatoid arthritis, atacicept causes an increase in the memory B-cell population in blood[298]. Likewise, another monoclonal antibody, tabalumab, which targets BAFF, failed to deplete memory B cells as well as clinical trials in various autoimmune diseases[299,300]. The inability to reduce the memory B-cell population might be the reason for the lack of positive clinical outcomes or even the worsening of the disease; nevertheless, further studies are necessary. The results of B-cell-depleting therapies suggest the central role of memory B cells in the efficacy and clinical outcomes of MS drugs. Monitoring the memory B-cell population either in the periphery or CSF could help predict clinical response, as is the case in several other autoimmune diseases[301].

10. Conclusions and future directions

This thesis is one of the most comprehensive analyses to date of B-cell populations in the CSF of MS patients. We demonstrated a distinct connection between the heavy- and light-chain variable region repertoires and the G1m allotype. Hopefully, the thesis will enable a better understanding of immunoglobulin polymorphisms by focusing on allotypes. We expect the interplay between allotypes and variable segments to have biological effects on the humoral response in MS and beyond. Our results also showed the preferential pairing of immunoglobulin's heavy and light chains in MS patients, suggesting that B cells have sustained non-stochastic and unique BCR gene rearrangements typical for antigen-driven immune responses.

The characterization of coupled heavy and light chains provides a basis for further research on specificity. Specific antigenic targets can be found by generating recombinant IgG monoclonal antibodies based on BCRs reconstructed from single-cell data. Additionally, selected sequences should be highly expressed in CSF (based on paper II) and contain preferentially used V-gene regions. Such antibodies can be applied to protein matrixes to pinpoint the antigenic target. If the specificities are known, this could improve the possibility of analyzing antibodies' binding sites and functional capabilities, creating a better understanding of their role in pathological processes within the CNS.

Furthermore, comparing intrathecal proteome and BCR sequences elucidated the major producers of OCBs and their transcriptomic profiles. More comprehensive proteomic profiling of B cells in MS and other autoimmune diseases could be informative regarding the detailed phenotype of cells, especially cells resisting B-cell-depleting therapies. These investigations could be achieved using mass cytometry methods, which allow the detection of numerous different markers, both intracellular and extracellular, thus creating an extensive proteomic map of single cells. Additionally, in this technique, scarce sample material (CSF or rare populations of peripheral blood cells) can be enriched in the cells of interest before analysis, and millions of cells can be analyzed simultaneously.

Another group of cells that requires significantly more detailed characterization is G1m3-expressing B cells in G1m1/G1m3 heterozygous patients. However, a detailed description of these cells would necessitate a large cohort of treatment-naïve MS patients to reach statistical significance. Nonetheless, possible phenotypical differences between G1m1

and G1m3 intrathecal B-cell populations could explain the total dominance of the G1m1 allotype in MS CNS if the studies included differential expression of, for example, survival genes, genes necessary for T-B interaction, or cytokine receptors.

Furthermore, the stereotyped BCR repertoire in G1m1 allotype carriers could be consequential for disease risk and clinical presentation. SNPs in the *IGHC* have been shown to correlate with the IgG index, which is of prognostic value in MS[110,187,194]. Considering the high diversity of the *IGHG* locus between populations, performing disease association studies in large cohorts is crucial. These studies could utilize next-generation sequencing techniques on the entire genome/exome and Sanger sequencing while relying on available SNP data from previous GWAS. Sequencing the complete *IGHG1* allele in a sufficiently sized cohort of MS patients and controls could provide a new understanding of the observed association between *IGHG1* polymorphisms and variable gene segments repertoire. It could also inspire further efforts to determine the consequences of allotypes in other contexts of immunity and autoimmunity. Alternatively, approaches not based on PCR could be implemented to research the immunoglobulin locus. These methods would enable analysis of large genomic fragments of the locus, for instance, through nanopore sequencing, which can provide accurate data; however, it can also be difficult and costly to apply in larger populations.

Genetic variants of IgG may have implications far beyond our current understanding. The extent of variability is still not fully known, including the number of undiscovered polymorphisms and how common they are within and between populations. By providing more detailed data, this thesis changes the view of known phenomena, reveals new aspects of immunogenetics, and underlines the existing knowledge gap in immunoglobulin loci. Allotypes can have functional consequences on IgG expression levels, the half-life of antibodies, FcγR binding, forming oligomers, and the capability for complement activation. This influence translates to a modified immune response and thus holds major consequences for autoimmunity and mAb immunotherapies.

11. References

1. Chaplin, D. D. Overview of the immune response. *J. Allergy Clin. Immunol.* **125**, S3–S23 (2010).
2. Cooper, M. D. & Alder, M. N. The evolution of adaptive immune systems. *Cell* vol. 124 815–822 (2006).
3. Lino, A. C., Dörner, T., Bar-Or, A. & Fillatreau, S. Cytokine-producing B cells: a translational view on their roles in human and mouse autoimmune diseases. *Immunol. Rev.* **269**, 130–144 (2016).
4. Lanzavecchia, A. & Bove, S. Specific B lymphocytes efficiently pick up, process and present antigen to T cells. *Behring Inst. Mitt.* 82–87 (1985).
5. Li, A. *et al.* Utilization of Ig heavy chain variable, diversity, and joining gene segments in children with B-lineage acute lymphoblastic leukemia: implications for the mechanisms of VDJ recombination and for pathogenesis. *Blood* **103**, 4602–4609 (2004).
6. Safonova, Y. & Pevzner, P. A. V(DD)J recombination is an important and evolutionarily conserved mechanism for generating antibodies with unusually long CDR3s. *Genome Res.* **30**, 1547–1558 (2020).
7. E, L. *et al.* Localization, analysis and evolution of transposed human immunoglobulin V kappa genes. *Gene* **69**, 215–223 (1988).
8. Watson, C. T. & Breden, F. The immunoglobulin heavy chain locus: Genetic variation, missing data, and implications for human disease. *Genes and Immunity* vol. 13 363–373 (2012).
9. Khatri, I. *et al.* Population matched (pm) germline allelic variants of immunoglobulin (IG) loci: Relevance in infectious diseases and vaccination studies in human populations. *Genes Immun.* **22**, 172–186 (2021).
10. Shi, Z. *et al.* More than one antibody of individual B cells revealed by single-cell immune profiling. *Cell Discov. 2019 51* **5**, 1–13 (2019).
11. LeBien, T. W. & Tedder, T. F. B lymphocytes: how they develop and function. *Blood* **112**, 1570 (2008).
12. Romagnani, S. Immunological tolerance and autoimmunity. *Intern. Emerg. Med. 2006 13* **1**, 187–196 (2006).
13. Alberts, B. *et al.* B Cells and Antibodies. in *Molecular Biology of the Cell. 4th edition.* (Garland Science, 2002).
14. Roco, J. A. *et al.* Class-Switch Recombination Occurs Infrequently in Germinal Centers. *Immunity* **51**, 337-350.e7 (2019).
15. Rajagopal, D. *et al.* Immunoglobulin switch μ sequence causes RNA polymerase II accumulation and reduces dA hypermutation. *J. Exp. Med.* **206**, 1237–1244 (2009).
16. Yuseff, M. I., Pierobon, P., Reversat, A. & Lennon-Duménil, A. M. How B cells capture, process and present antigens: A crucial role for cell polarity. *Nature Reviews Immunology* vol. 13 475–486 (2013).
17. Muramatsu, M. *et al.* Class switch recombination and hypermutation require activation-induced cytidine deaminase (AID), a potential RNA editing enzyme. *Cell* **102**, 553–563 (2000).
18. Peled, J. U. *et al.* The biochemistry of somatic hypermutation. *Annual Review of Immunology* vol. 26 481–511 (2008).
19. Sanz, I. *et al.* Challenges and opportunities for consistent classification of human b cell and plasma cell populations. *Frontiers in Immunology* vol. 10 2458 (2019).
20. Woof, J. M. & Burton, D. R. Human antibody-Fc receptor interactions illuminated by crystal structures. *Nature Reviews Immunology* vol. 4 89–99 (2004).
21. Dilillo, D. J. & Ravetch, J. V. Fc-receptor interactions regulate both cytotoxic and immunomodulatory therapeutic antibody effector functions. *Cancer Immunol. Res.* **3**, 704–713 (2015).

22. Wang, T. T. & Ravetch, J. V. Functional diversification of IgGs through Fc glycosylation. *Journal of Clinical Investigation* vol. 129 3492–3498 (2019).

23. Yaari, G. *et al.* Models of somatic hypermutation targeting and substitution based on synonymous mutations from high-throughput immunoglobulin sequencing data. *Front. Immunol.* **4**, 358 (2013).

24. Haidar, J. N. *et al.* A universal combinatorial design of antibody framework to graft distinct CDR sequences: A bioinformatics approach. *Proteins Struct. Funct. Bioinforma.* **80**, 896–912 (2012).

25. DeWitt, W. S. *et al.* A public database of memory and naive B-cell receptor sequences. *PLoS One* **11**, e0160853 (2016).

26. Briney, B., Inderbitzin, A., Joyce, C. & Burton, D. R. Commonality despite exceptional diversity in the baseline human antibody repertoire. *Nat. 2019 5667744* **566**, 393–397 (2019).

27. DeKosky, B. J. *et al.* In-depth determination and analysis of the human paired heavy- and light-chain antibody repertoire. *Nat. Med. 2014 211* **21**, 86–91 (2014).

28. Greiff, V. *et al.* Systems Analysis Reveals High Genetic and Antigen-Driven Predetermination of Antibody Repertoires throughout B Cell Development. *Cell Rep.* **19**, 1467–1478 (2017).

29. Boyd, S. D. *et al.* Individual Variation in the Germline Ig Gene Repertoire Inferred from Variable Region Gene Rearrangements. *J. Immunol.* **184**, 6986–6992 (2010).

30. Odegard, V. H. & Schatz, D. G. Targeting of somatic hypermutation. *Nat. Rev. Immunol. 2006 68* **6**, 573–583 (2006).

31. Spuergin, P., Mueller, H., Walter, M., Schiltz, E. & Forster, J. Allergenic epitopes of bovine α(S1)-casein recognized by human IgE and IgG. *Allergy Eur. J. Allergy Clin. Immunol.* **51**, 306–312 (1996).

32. Torres, M. & Casadevall, A. The immunoglobulin constant region contributes to affinity and specificity. *Trends in Immunology* vol. 29 91–97 (2008).

33. Padlan, E. A., Abergel, C. & Tipper, J. P. Identification of specificity-determining residues in antibodies. *FASEB J.* **9**, 133–139 (1995).

34. Liang, Y., Guttman, M., Davenport, T. M., Hu, S.-L. & Lee, K. K. Probing the Impact of Local Structural Dynamics of Conformational Epitopes on Antibody Recognition. *Biochemistry* **55**, 2197–2213 (2016).

35. Raghunathan, G., Smart, J., Williams, J. & Almagro, J. C. Antigen-binding site anatomy and somatic mutations in antibodies that recognize different types of antigens. *J. Mol. Recognit.* **25**, 103–113 (2012).

36. Bowen, A. & Casadevall, A. Revisiting the Immunoglobulin Intramolecular Signaling Hypothesis. *Trends in Immunology* vol. 37 721–723 (2016).

37. Casadevall, A. & Janda, A. Immunoglobulin isotype influences affinity and specificity. *Proceedings of the National Academy of Sciences of the United States of America* vol. 109 12272–12273 (2012).

38. Wang, Y. *et al.* Mouse model of hematogenous implant-related Staphylococcus aureus biofilm infection reveals therapeutic targets. *Proc. Natl. Acad. Sci. U. S. A.* **114**, E5094–E5102 (2017).

39. Chau, P. Y. & Ng, M. H. Differential agglutination of particulate Vi and O antigens by the IgM and IgG class antibodies. *Aust. J. Exp. Biol. Med. Sci.* **56**, 39–45 (1978).

40. Harvey, A. B., Bordin, A. I., Rocha, J. N., Bray, J. M. & Cohen, N. D. Opsonization but not pretreatment of equine macrophages with hyperimmune plasma nonspecifically enhances phagocytosis and intracellular killing of Rhodococcus equi. *J. Vet. Intern. Med.* **35**, 590–596 (2021).

41. Merle, N. S., Church, S. E., Fremeaux-Bacchi, V. & Roumenina, L. T. Complement system part I - molecular mechanisms of activation and regulation. *Frontiers in Immunology* vol. 6 262 (2015).

42. Bournazos, S. & Ravetch, J. V. Diversification of IgG effector functions. *Int. Immunol.* **29**, 303–310 (2017).

43. Vidarsson, G., Dekkers, G. & Rispens, T. IgG subclasses and allotypes: From structure to effector functions. *Front. Immunol.* **5**, 520 (2014).

44. Møllgård, K. *et al.* A mesothelium divides the subarachnoid space into functional compartments. *Science (80-.).* **379**, 84–88 (2023).

45. Alves De Lima, K., Rustenhoven, J. & Kipnis, J. Meningeal Immunity and Its Function in Maintenance of the Central Nervous System in Health and Disease. *Annu. Rev. Immunol.* **38**, 597–620 (2020).

46. Van Hove, H. *et al.* A single-cell atlas of mouse brain macrophages reveals unique transcriptional identities shaped by ontogeny and tissue environment. *Nat. Neurosci.* **22**, 1021–1035 (2019).

47. Mrdjen, D. *et al.* High-Dimensional Single-Cell Mapping of Central Nervous System Immune Cells Reveals Distinct Myeloid Subsets in Health, Aging, and Disease. *Immunity* **48**, 380-395.e6 (2018).

48. Goldmann, T. *et al.* Origin, fate and dynamics of macrophages at central nervous system interfaces. *Nat. Immunol.* **17**, 797–805 (2016).

49. Herisson, F. *et al.* Direct vascular channels connect skull bone marrow and the brain surface enabling myeloid cell migration. *Nat. Neurosci.* **21**, 1209–1217 (2018).

50. Cugurra, A. *et al.* Skull and vertebral bone marrow are myeloid cell reservoirs for the meninges and CNS parenchyma. *Science (80-.).* **373**, (2021).

51. Brioschi, S. *et al.* Heterogeneity of meningeal B cells reveals a lymphopoietic niche at the CNS borders. *Science (80-.).* **373**, eabf9277 (2021).

52. Rustenhoven, J. *et al.* Functional characterization of the dural sinuses as a neuroimmune interface. *Cell* **184**, 1000-1016.e27 (2021).

53. Aspelund, A. *et al.* A dural lymphatic vascular system that drains brain interstitial fluid and macromolecules. *J. Exp. Med.* **212**, 991–999 (2015).

54. Louveau, A. *et al.* Structural and functional features of central nervous system lymphatic vessels. *Nature* **523**, 337–341 (2015).

55. Spadoni, I., Fornasa, G. & Rescigno, M. Organ-specific protection mediated by cooperation between vascular and epithelial barriers. *Nature Reviews Immunology* vol. 17 761–773 (2017).

56. Benarroch, E. E. Microglia: Multiple roles in surveillance, circuit shaping, and response to injury. *Neurology* vol. 81 1079–1088 (2013).

57. Smolders, J. *et al.* Tissue-resident memory T cells populate the human brain. *Nat. Commun.* **9**, (2018).

58. Murray, T. J. The history of multiple sclerosis: the changing frame of the disease over the centuries. *Journal of the Neurological Sciences* vol. 277 (2009).

59. Alroughani, R. & Boyko, A. Pediatric multiple sclerosis: A review. *BMC Neurol.* **18**, 1–8 (2018).

60. Browne, P. *et al.* Atlas of Multiple Sclerosis 2013: A growing global problem with widespread inequity. *Neurology* **83**, 1022 (2014).

61. Walton, C. *et al.* Rising prevalence of multiple sclerosis worldwide: Insights from the Atlas of MS, third edition. *Mult. Scler. J.* **26**, 1816–1821 (2020).

62. Kurtzke, J. F. Epidemiology in multiple sclerosis: a pilgrim's progress. *Brain* **136**, 2904–2917 (2013).

63. Simpson, S. *et al.* Latitude continues to be significantly associated with the prevalence of multiple sclerosis: An updated meta-analysis. *J. Neurol. Neurosurg. Psychiatry* **90**, 1193–1200 (2019).

64. Sintzel, M. B., Rametta, M. & Reder, A. T. Vitamin D and Multiple Sclerosis: A Comprehensive Review. *Neurology and Therapy* vol. 7 59–85 (2018).

65. Zhang, P. *et al.* The risk of smoking on multiple sclerosis: A meta-analysis based on 20,626 cases from case-control and cohort studies. *PeerJ* **2016**, (2016).

66. Balfour, H. H. *et al.* Behavioral, virologic, and immunologic factors associated with acquisition and severity of primary epstein-barr virus infection in university students. *J. Infect. Dis.* **207**, 80–88 (2013).

67. Bjornevik, K. *et al.* Longitudinal analysis reveals high prevalence of Epstein-Barr virus associated with

multiple sclerosis. *Science* **375**, 296–301 (2022).

68. Pakpoor, J. *et al.* The risk of developing multiple sclerosis in individuals seronegative for Epstein-Barr virus: A meta-analysis. *Mult. Scler. J.* **19**, 162–166 (2013).

69. Handel, A. E. *et al.* An updated meta-analysis of risk of multiple sclerosis following infectious mononucleosis. *PLoS One* **5**, 1–5 (2010).

70. Matveeva, O. *et al.* Western lifestyle and immunopathology of multiple sclerosis. *Annals of the New York Academy of Sciences* vol. 1417 71–86 (2018).

71. Hedström, A. K., Olsson, T. & Alfredsson, L. High body mass index before age 20 is associated with increased risk for multiple sclerosis in both men and women. *Mult. Scler. J.* **18**, 1334–1336 (2012).

72. Høglund, R. A. A. *et al.* Association of Body Mass Index in Adolescence and Young Adulthood and Long-term Risk of Multiple Sclerosis: A Population-Based Study. *Neurology* **97**, E2253–E2261 (2021).

73. Wasko, N. J., Nichols, F. & Clark, R. B. Multiple sclerosis, the microbiome, TLR2, and the hygiene hypothesis. *Autoimmun. Rev.* **19**, (2020).

74. Bjørnevik, K., Chitnis, T., Ascherio, A. & Munger, K. L. Polyunsaturated fatty acids and the risk of multiple sclerosis. *Mult. Scler.* **23**, 1830–1838 (2017).

75. Gustavsen, S. *et al.* Shift work at young age is associated with increased risk of multiple sclerosis in a Danish population. *Mult. Scler. Relat. Disord.* **9**, 104–109 (2016).

76. Thompson, A. J., Baranzini, S. E., Geurts, J., Hemmer, B. & Ciccarelli, O. Multiple sclerosis. *Lancet* **391**, 1622–1636 (2018).

77. Thompson, A. J. *et al.* Diagnosis of multiple sclerosis: 2017 revisions of the McDonald criteria. *The Lancet Neurology* vol. 17 162–173 (2018).

78. Wingerchuk, D. M. *et al.* International consensus diagnostic criteria for neuromyelitis optica spectrum disorders. *Neurology* **85**, 177 (2015).

79. Reindl, M. & Waters, P. Myelin oligodendrocyte glycoprotein antibodies in neurological disease. *Nat. Rev. Neurol. 2018 152* **15**, 89–102 (2018).

80. Dalmau, J. & Graus, F. Antibody-Mediated Encephalitis. *N. Engl. J. Med.* **378**, 840–851 (2018).

81. Serafini, B., Rosicarelli, B., Magliozzi, R., Stigliano, E. & Aloisi, F. Detection of ectopic B-cell follicles with germinal centers in the meninges of patients with secondary progressive multiple sclerosis. *Brain Pathol.* **14**, 164–174 (2004).

82. Howell, O. W. *et al.* Meningeal inflammation is widespread and linked to cortical pathology in multiple sclerosis. *Brain* **134**, 2755–2771 (2011).

83. Machado-Santos, J. *et al.* The compartmentalized inflammatory response in the multiple sclerosis brain is composed of tissue-resident CD8+ T lymphocytes and B cells. *Brain* **141**, 2066–2082 (2018).

84. Skulina, C. *et al.* Multiple sclerosis: Brain-infiltrating CD8+ T cells persist as clonal expansions in the cerebrospinal fluid and blood. *Proc. Natl. Acad. Sci. U. S. A.* **101**, 2428–2433 (2004).

85. Obermeier, B. *et al.* Matching of oligoclonal immunoglobulin transcriptomes and proteomes of cerebrospinal fluid in multiple sclerosis. *Nat. Med.* **14**, 688–693 (2008).

86. Johansen, J. N. *et al.* Intrathecal BCR transcriptome in multiple sclerosis versus other neuroinflammation: Equally diverse and compartmentalized, but more mutated, biased and overlapping with the proteome. *Clin. Immunol.* **160**, 211–225 (2015).

87. Trapp, B. D. *et al.* Axonal Transection in the Lesions of Multiple Sclerosis. *N. Engl. J. Med.* **338**, 278–285 (1998).

88. Bø, L., Vedeler, C. A., Nyland, H. I., Trapp, B. D. & Mørk, S. J. Subpial demyelination in the cerebral cortex of multiple sclerosis patients. *J. Neuropathol. Exp. Neurol.* **62**, 723–732 (2003).

89. Metz, I. *et al.* Pathologic heterogeneity persists in early active multiple sclerosis lesions. *Ann. Neurol.*

75, 728–738 (2014).

90. Jarius, S. *et al.* Pattern II and pattern III MS are entities distinct from pattern I MS: Evidence from cerebrospinal fluid analysis. *J. Neuroinflammation* **14**, (2017).

91. Frischer, J. M. *et al.* The relation between inflammation and neurodegeneration in multiple sclerosis brains. *Brain* **132**, 1175–1189 (2009).

92. Lisak, R. P. *et al.* B cells from patients with multiple sclerosis induce cell death via apoptosis in neurons in vitro. *J. Neuroimmunol.* **309**, 88–99 (2017).

93. Schafflick, D. *et al.* Integrated single cell analysis of blood and cerebrospinal fluid leukocytes in multiple sclerosis. *Nat. Commun.* **11**, (2020).

94. Serafini, B., Rosicarelli, B., Veroni, C., Mazzola, G. A. & Aloisi, F. Epstein-Barr Virus-Specific CD8 T Cells Selectively Infiltrate the Brain in Multiple Sclerosis and Interact Locally with Virus-Infected Cells: Clue for a Virus-Driven Immunopathological Mechanism. *J. Virol.* **93**, (2019).

95. Sweeney, M. D., Zhao, Z., Montagne, A., Nelson, A. R. & Zlokovic, B. V. Blood-brain barrier: From physiology to disease and back. *Physiological Reviews* vol. 99 21–78 (2019).

96. Von Büdingen, H. C. *et al.* B cell exchange across the blood-brain barrier in multiple sclerosis. *J. Clin. Invest.* **122**, 4533–4543 (2012).

97. Stern, J. N. H. *et al.* B cells populating the multiple sclerosis brain mature in the draining cervical lymph nodes. *Sci. Transl. Med.* **6**, 1–11 (2014).

98. Yednock, T. A. *et al.* Prevention of experimental autoimmune encephalomyelitis by antibodies against α4βl integrin. *Nature* **356**, 63–66 (1992).

99. Michel, L. *et al.* Activated leukocyte cell adhesion molecule regulates B lymphocyte migration across central nervous system barriers. *Sci. Transl. Med.* **11**, (2019).

100. Krumbholz, M. *et al.* Chemokines in multiple sclerosis: CXCL12 and CXCL13 up-regulation is differentially linked to CNS immune cell recruitment. *Brain* **129**, 200–211 (2006).

101. Kalinowska-Łyszczarz, A., Szczuciński, A., Pawlak, M. A. & Losy, J. Clinical study on CXCL13, CCL17, CCL20 and IL-17 as immune cell migration navigators in relapsing−remitting multiple sclerosis patients. *J. Neurol. Sci.* **300**, 81–85 (2011).

102. Mitsdoerffer, M. & Peters, A. Tertiary lymphoid organs in central nervous system autoimmunity. *Frontiers in Immunology* vol. 7 451 (2016).

103. Pitzalis, C., Jones, G. W., Bombardieri, M. & Jones, S. A. Ectopic lymphoid-like structures in infection, cancer and autoimmunity. *Nature Reviews Immunology* vol. 14 447–462 (2014).

104. Gharibi, T. *et al.* The role of B cells in the immunopathogenesis of multiple sclerosis. *Immunology* vol. 160 325–335 (2020).

105. Magliozzi, R. *et al.* Meningeal B-cell follicles in secondary progressive multiple sclerosis associate with early onset of disease and severe cortical pathology. *Brain* **130**, 1089–1104 (2007).

106. Magliozzi, R. *et al.* Inflammatory intrathecal profiles and cortical damage in multiple sclerosis. *Ann. Neurol.* **83**, 739–755 (2018).

107. Thaunat, O. *et al.* B cell survival in intragraft tertiary lymphoid organs after rituximab therapy. *Transplantation* **85**, 1648–1653 (2008).

108. Walsh, M. J. & Tourtellotte, W. Temporal invariance and clonal uniformity of brain and cerebrospinal IgG, IgA, and IgM in multiple sclerosis. *J. Exp. Med.* **163**, 41–53 (1986).

109. Tomescu-Baciu, A. *et al.* Persistence of intrathecal oligoclonal B cells and IgG in multiple sclerosis. *J. Neuroimmunol.* **333**, 576966 (2019).

110. Gasperi, C. *et al.* Association of Intrathecal Immunoglobulin G Synthesis with Disability Worsening in Multiple Sclerosis. in *JAMA Neurology* vol. 76 841–849 (JAMA Neurol, 2019).

111. Farina, G. *et al.* Increased cortical lesion load and intrathecal inflammation is associated with oligoclonal bands in multiple sclerosis patients: A combined CSF and MRI study. *J. Neuroinflammation* **14**, (2017).

112. Fonderico, M. *et al.* Cerebrospinal fluid igm and oligoclonal igg bands in multiple sclerosis: A meta-analysis of prevalence and prognosis. *Brain Sciences* vol. 11 (2021).

113. VANDVIK, B., NORRBY, E., NORDAL, H. J. & DECRÉ, M. Oligoclonal Measles Virus-Specific IgG Antibodies Isolated from Cerebrospinal Fluids, Brain Extracts, and Sera from Patients with Subacute Sclerosing Panencephalitis and Multiple Sclerosis. *Scand. J. Immunol.* **5**, 979–992 (1976).

114. Vartdal, F., Vandvik, B. & Norrby, E. Intrathecal synthesis of virus-specific oligoclonal IgG, IgA and IgM antibodies in a case of varicella-zoster meningoencephalitis. *J. Neurol. Sci.* **57**, 121–132 (1982).

115. Nagel, M. A. *et al.* The value of detecting anti-VZV IgG antibody in CSF to diagnose VZV vasculopathy. *Neurology* **68**, 1069–1073 (2007).

116. von Büdingen, H. C., Harrer, M. D., Kuenzle, S., Meier, M. & Goebels, N. Clonally expanded plasma cells in the cerebrospinal fluid of MS patients produce myelin-specific antibodies. *Eur. J. Immunol.* **38**, 2014–2023 (2008).

117. Owens, G. P. *et al.* Antibodies produced by clonally expanded plasma cells in multiple sclerosis cerebrospinal fluid. *Ann. Neurol.* **65**, 639–649 (2009).

118. Lanz, T. V. *et al.* Clonally expanded B cells in multiple sclerosis bind EBV EBNA1 and GlialCAM. *Nature* **603**, 321–327 (2022).

119. Opsahl, M. L. & Kennedy, P. G. E. An attempt to investigate the presence of Epstein Barr virus in multiple sclerosis and normal control brain tissue. *J. Neurol. 2007 2544* **254**, 425–430 (2007).

120. Brändle, S. M. *et al.* Distinct oligoclonal band antibodies in multiple sclerosis recognize ubiquitous self-proteins. *Proc. Natl. Acad. Sci. U. S. A.* **113**, 7864–7869 (2016).

121. Jarius, S. *et al.* The intrathecal, polyspecific antiviral immune response: Specific for MS or a general marker of CNS autoimmunity? *J. Neurol. Sci.* **280**, 98–100 (2009).

122. Jarius, S. *et al.* The MRZ reaction as a highly specific marker of multiple sclerosis: re-evaluation and structured review of the literature. *J. Neurol.* **264**, 453–466 (2017).

123. Obermeier, B. *et al.* Related B cell clones that populate the CSF and CNS of patients with multiple sclerosis produce CSF immunoglobulin. *J. Neuroimmunol.* **233**, 245–248 (2011).

124. Bankoti, J. *et al.* In multiple sclerosis, oligoclonal bands connect to peripheral B-cell responses. *Ann. Neurol.* **75**, 266–76 (2014).

125. Roach, C. A. & Cross, A. H. Anti-CD20 B Cell Treatment for Relapsing Multiple Sclerosis. *Frontiers in Neurology* vol. 11 1936 (2021).

126. Molnarfi, N. *et al.* MHC class II-dependent B cell APC function is required for induction of CNS autoimmunity independent of myelin-specific antibodies. *J. Exp. Med.* **210**, 2921–2937 (2013).

127. Li, R. *et al.* Antibody-Independent Function of Human B Cells Contributes to Antifungal T Cell Responses. *J. Immunol.* **198**, 3245–3254 (2017).

128. Gharibi, T. *et al.* IL-21 and IL-21-producing T cells are involved in multiple sclerosis severity and progression. *Immunol. Lett.* **216**, 12–20 (2019).

129. Smets, I. *et al.* Multiple sclerosis risk variants alter expression of co-stimulatory genes in B cells. *Brain* **141**, 786–796 (2018).

130. Fraussen, J. *et al.* B cells of multiple sclerosis patients induce autoreactive proinflammatory T cell responses. *Clin. Immunol.* **173**, 124–132 (2016).

131. Harp, C. T., Lovett-Racke, A. E., Racke, M. K., Frohman, E. M. & Monson, N. L. Impact of myelin-specific antigen presenting B cells on T cell activation in multiple sclerosis. *Clin. Immunol.* **128**, 382–391 (2008).

132. Harp, C. T. *et al.* Memory B cells from a subset of treatment-naïve relapsing-remitting multiple sclerosis patients elicit CD4+ T-cell proliferation and IFN-γ production in response to myelin basic protein and myelin oligodendrocyte glycoprotein. *Eur. J. Immunol.* **40**, 2942–2956 (2010).

133. Jelcic, I. *et al.* Memory B Cells Activate Brain-Homing, Autoreactive CD4+ T Cells in Multiple Sclerosis. *Cell* **175**, 85-100.e23 (2018).

134. Chen, D. *et al.* CD40-Mediated NF-κB Activation in B Cells Is Increased in Multiple Sclerosis and Modulated by Therapeutics. *J. Immunol.* **197**, 4257–4265 (2016).

135. Kannel, K. *et al.* Changes in blood B cell-activating factor (BAFF) levels in multiple sclerosis: A sign of treatment outcome. *PLoS One* **10**, e0143393 (2015).

136. Li, R. *et al.* Proinflammatory GM-CSF-producing B cells in multiple sclerosis and B cell depletion therapy. *Sci. Transl. Med.* **7**, (2015).

137. Korn, T. *et al.* IL-6 controls Th17 immunity in vivo by inhibiting the conversion of conventional T cells into Foxp3+ regulatory T cells. *Proc. Natl. Acad. Sci. U. S. A.* **105**, 18460–18465 (2008).

138. Xiang, W., Xie, C. & Guan, Y. The identification, development and therapeutic potential of IL-10-producing regulatory B cells in multiple sclerosis. *Journal of Neuroimmunology* vol. 354 (2021).

139. Duddy, M. *et al.* Distinct Effector Cytokine Profiles of Memory and Naive Human B Cell Subsets and Implication in Multiple Sclerosis. *J. Immunol.* **170**, 6092–6099 (2007).

140. Knippenberg, S. *et al.* Reduction in IL-10 producing B cells (Breg) in multiple sclerosis is accompanied by a reduced naïve/memory Breg ratio during a relapse but not in remission. *J. Neuroimmunol.* **239**, 80–86 (2011).

141. Donninelli, G. *et al.* Immune Soluble Factors in the Cerebrospinal Fluid of Progressive Multiple Sclerosis Patients Segregate Into Two Groups. *Front. Immunol.* **12**, 428 (2021).

142. McGinley, M. P., Goldschmidt, C. H. & Rae-Grant, A. D. Diagnosis and Treatment of Multiple Sclerosis: A Review. *JAMA - J. Am. Med. Assoc.* **325**, 765–779 (2021).

143. Montalban, X. *et al.* Placebo-Controlled Trial of an Oral BTK Inhibitor in Multiple Sclerosis. *N. Engl. J. Med.* **380**, 2406–2417 (2019).

144. Syed, S., Yonkers, N., LaGanke, D. & et al. Efficacy and safety of tolebrutinib in patients with highly active relapsing MS: subgroup analysis of the phase 2b study (2260). *Neurology* **96**, 2260 (2021).

145. Häusler, D. *et al.* Functional characterization of reappearing B cells after anti-CD20 treatment of CNS autoimmune disease. *Proc. Natl. Acad. Sci. U. S. A.* **115**, 9773–9778 (2018).

146. Liu, Z., Liao, Q., Wen, H. & Zhang, Y. Disease modifying therapies in relapsing-remitting multiple sclerosis: A systematic review and network meta-analysis. *Autoimmun. Rev.* **20**, 102826 (2021).

147. Gold, R. *et al.* Placebo-Controlled Phase 3 Study of Oral BG-12 for Relapsing Multiple Sclerosis. *N. Engl. J. Med.* **367**, 1098–1107 (2012).

148. Rostami-Yazdi, M., Clement, B., Schmidt, T. J., Schinor, D. & Mrowietz, U. Detection of Metabolites of Fumaric Acid Esters in Human Urine: Implications for Their Mode of Action. *J. Invest. Dermatol.* **129**, 231–234 (2009).

149. Peng, H. *et al.* Dimethyl fumarate inhibits dendritic cell maturation via nuclear factor κB (NF-κB) and extracellular signal-regulated kinase 1 and 2 (ERK1/2) and mitogen stress-activated kinase 1 (MSK1) signaling. *J. Biol. Chem.* **287**, 28017–28026 (2012).

150. Vandermeeren, M., Janssens, S., Borgers, M. & Geysen, J. Dimethylfumarate is an inhibitor of cytokine-induced E-selectin, VCAM-1, and ICAM-1 expression in human endothelial cells. *Biochem. Biophys. Res. Commun.* **234**, 19–23 (1997).

151. Longbrake, E. E. *et al.* Dimethyl fumarate induces changes in B- and T-lymphocyte function independent of the effects on absolute lymphocyte count. *Mult. Scler. J.* **24**, 728–738 (2018).

152. Schlöder, J., Berges, C., Luessi, F. & Jonuleit, H. Dimethyl fumarate therapy significantly improves the

responsiveness of T cells in multiple sclerosis patients for immunoregulation by regulatory T cells. *Int. J. Mol. Sci.* **18**, 271 (2017).

153. Mathias, A. *et al.* Impaired T-cell migration to the CNS under fingolimod and dimethyl fumarate. *Neurol. Neuroimmunol. NeuroInflammation* **4**, 401 (2017).

154. Lundy, S. K. *et al.* Dimethyl fumarate treatment of relapsing-remitting multiple sclerosis influences B-cell subsets. *Neurol. Neuroimmunol. NeuroInflammation* **3**, (2016).

155. Smith, M. D., Martin, K. A., Calabresi, P. A. & Bhargava, P. Dimethyl fumarate alters B-cell memory and cytokine production in MS patients. *Ann. Clin. Transl. Neurol.* **4**, 351–355 (2017).

156. Li, R. *et al.* Dimethyl Fumarate Treatment Mediates an Anti-Inflammatory Shift in B Cell Subsets of Patients with Multiple Sclerosis. *J. Immunol.* **198**, 691–698 (2017).

157. Schulze-Topphoff, U. *et al.* Dimethyl fumarate treatment induces adaptive and innate immune modulation independent of Nrf2. *Proc. Natl. Acad. Sci. U. S. A.* **113**, 4777–4782 (2016).

158. Longbrake, E. E. *et al.* Dimethyl fumarate selectively reduces memory T cells in multiple sclerosis patients. *Mult. Scler.* **22**, 1061–1070 (2016).

159. Ghoreschi, K. *et al.* Fumarates improve psoriasis and multiple sclerosis by inducing type II dendritic cells. *J. Exp. Med.* **208**, 2291–2303 (2011).

160. Lin, R., Cai, J., Kostuk, E. W., Rosenwasser, R. & Iacovitti, L. Fumarate modulates the immune/inflammatory response and rescues nerve cells and neurological function after stroke in rats. *J. Neuroinflammation* **13**, 1–15 (2016).

161. Müller, S. *et al.* Dimethylfumarate impairs neutrophil functions. *J. Invest. Dermatol.* **136**, 117–126 (2016).

162. Al-Jaderi, Z. & Maghazachi, A. A. Vitamin D3 and monomethyl fumarate enhance natural killer cell lysis of dendritic cells and ameliorate the clinical score in mice suffering from experimental autoimmune encephalomyelitis. *Toxins (Basel).* **7**, 4730–4744 (2015).

163. Wilms, H. *et al.* Dimethylfumarate inhibits microglial and astrocytic inflammation by suppressing the synthesis of nitric oxide, IL-1β, TNF-α and IL-6 in an in-vitro model of brain inflammation. *J. Neuroinflammation* **7**, 1–8 (2010).

164. Kronenberg, J. *et al.* Fumaric Acids Directly Influence Gene Expression of Neuroprotective Factors in Rodent Microglia. *Int. J. Mol. Sci.* **20**, 325 (2019).

165. Harirchian, M. H., Fatehi, F., Sarraf, P., Honarvar, N. M. & Bitarafan, S. Worldwide prevalence of familial multiple sclerosis: A systematic review and meta-analysis. *Multiple Sclerosis and Related Disorders* vol. 20 43–47 (2018).

166. Muñiz-Castrillo, S., Vogrig, A. & Honnorat, J. Associations between HLA and autoimmune neurological diseases with autoantibodies. *Autoimmunity Highlights* vol. 11 1–13 (2020).

167. Patsopoulos, N. A. *et al.* Fine-Mapping the Genetic Association of the Major Histocompatibility Complex in Multiple Sclerosis: HLA and Non-HLA Effects. *PLoS Genet.* **9**, (2013).

168. Patsopoulos, N. A. *et al.* Multiple sclerosis genomic map implicates peripheral immune cells and microglia in susceptibility. *Science (80-.).* **365**, (2019).

169. Haines, J. L. *et al.* Linkage of the MHC to familial multiple sclerosis suggests genetic heterogeneity. *Hum. Mol. Genet.* **7**, 1229–1234 (1998).

170. Sawcer, S. *et al.* Genetic risk and a primary role for cell-mediated immune mechanisms in multiple sclerosis. *Nature* vol. 476 214–219 (2011).

171. Yeo, T. W. *et al.* A second major histocompatibility complex susceptibility locus for multiple sclerosis. *Ann. Neurol.* **61**, 228–236 (2007).

172. Rioux, J. D. *et al.* Mapping of multiple susceptibility variants within the MHC region for 7 immune-mediated diseases. *Proc. Natl. Acad. Sci. U. S. A.* **106**, 18680–18685 (2009).

173. Dyment, D. A. *et al.* Complex interactions among MHC haplotypes in multiple sclerosis: Susceptibility and resistance. *Hum. Mol. Genet.* **14**, 2019–2026 (2005).

174. Mamedov, A. *et al.* Protective Allele for Multiple Sclerosis HLA-DRB1*01:01 Provides Kinetic Discrimination of Myelin and Exogenous Antigenic Peptides. *Front. Immunol.* **10**, 3088 (2020).

175. Laaksonen, M. *et al.* HLA class II associated risk and protection against multiple sclerosis - A Finnish family study. *J. Neuroimmunol.* **122**, 140–145 (2002).

176. Kular, L. *et al.* DNA methylation as a mediator of HLA-DRB1 15:01 and a protective variant in multiple sclerosis. *Nat. Commun.* **9**, (2018).

177. Factor, D. C. *et al.* Cell Type-Specific Intralocus Interactions Reveal Oligodendrocyte Mechanisms in MS. *Cell* **181**, 382-395.e21 (2020).

178. Scazzone, C., Agnello, L., Bivona, G., Lo Sasso, B. & Ciaccio, M. Vitamin D and Genetic Susceptibility to Multiple Sclerosis. *Biochemical Genetics* vol. 59 (2021).

179. Mokry, L. E. *et al.* Obesity and Multiple Sclerosis: A Mendelian Randomization Study. *PLoS Med.* **13**, (2016).

180. Maglione, A., Zuccalà, M., Tosi, M., Clerico, M. & Rolla, S. Host genetics and gut microbiome: Perspectives for multiple sclerosis. *Genes* vol. 12 1181 (2021).

181. Venkataraman, T. *et al.* Analysis of antibody binding specificities in twin and SNP-genotyped cohorts reveals that antiviral antibody epitope selection is a heritable trait. *Immunity* **55**, 174-184.e5 (2022).

182. Koch, M. W. *et al.* Global transcriptome profiling of mild relapsing-remitting versus primary progressive multiple sclerosis. *Eur. J. Neurol.* **25**, 651–658 (2018).

183. Hilven, K. *et al.* Genetic basis for relapse rate in multiple sclerosis: Association with LRP2 genetic variation. *Mult. Scler. J.* **24**, 1773–1775 (2018).

184. Vandebergh, M. *et al.* Genetic Variation in WNT9B Increases Relapse Hazard in Multiple Sclerosis. *Ann. Neurol.* **89**, 884–894 (2021).

185. Espino-Paisán, L. *et al.* A Polymorphism Within the MBP Gene Is Associated With a Higher Relapse Number in Male Patients of Multiple Sclerosis. *Front. Immunol.* **11**, (2020).

186. Moutsianas, L. *et al.* Class II HLA interactions modulate genetic risk for multiple sclerosis. *Nat. Genet. 2015 4710* **47**, 1107–1113 (2015).

187. Gasperi, C. *et al.* Genetic determinants of the humoral immune response in MS. *Neurol. Neuroimmunol. neuroinflammation* **7**, 827 (2020).

188. Lefranc, M. P. & Lefranc, G. Human Gm, Km, and Am allotypes and their molecular characterization: A remarkable demonstration of polymorphism. *Methods Mol. Biol.* **882**, 635–680 (2012).

189. Oxelius, V. A. & Pandey, J. P. Human immunoglobulin constant heavy G chain (IGHG) (Fcγ) (GM) genes, defining innate variants of IgG molecules and B cells, have impact on disease and therapy. *Clinical Immunology* vol. 149 475–486 (2013).

190. Salier, J. P., Goust, J. M., Pandey, J. P. & Fudenberg, H. H. Preferential synthesis of the G1m(1) allotype of IgG1 in the central nervous system of multiple sclerosis patients. *Science (80-.).* **213**, 1400–1402 (1981).

191. Salier, J. P. *et al.* HLA-DR-dependent variation of intrathecal IgG1 (Gm) allotype synthesis in multiple sclerosis. *J. Immunol.* **134**, 1551–1554 (1985).

192. Buck, D. *et al.* Genetic variants in the immunoglobulin heavy chain locus are associated with the IgG index in multiple sclerosis. *Ann. Neurol.* **73**, 86–94 (2013).

193. Goris, A. *et al.* Genetic variants are major determinants of CSF antibody levels in multiple sclerosis. *Brain* **138**, 632–643 (2015).

194. Delgado-García, M. *et al.* A new risk variant for multiple sclerosis at the immunoglobulin heavy chain locus associates with intrathecal IgG, IgM index and oligoclonal bands. *Mult. Scler.* **21**, 1104–1111

(2015).

195. Lossius, A. *et al.* Selective intrathecal enrichment of G1m1-positive B cells in multiple sclerosis. *Ann. Clin. Transl. Neurol.* **4**, 756–761 (2017).

196. Namboodiri, A. M., Budkowska, A., Nietert, P. J. & Pandey, J. P. Fcγ receptor-like hepatitis C virus core protein binds differentially to IgG of discordant Fc (GM) genotypes. *Mol. Immunol.* **44**, 3805–3808 (2007).

197. Pandey, J. P., Namboodiri, A. M., Radwan, F. F. & Nietert, P. J. The decoy Fcγ receptor encoded by the cytomegalovirus UL119-UL118 gene has differential affinity to IgG proteins expressing different GM allotypes. *Hum. Immunol.* **76**, 591–594 (2015).

198. Pandey, J. P. Immunoglobulin gm genes as functional risk and protective factors for the development of alzheimers disease. *Journal of Alzheimer's Disease* vol. 17 753–756 (2009).

199. Pandey, J. P. Immunoglobulin GM Genes, Cytomegalovirus Immunoevasion, and the Risk of Glioma, Neuroblastoma, and Breast Cancer. *Front. Oncol.* **4**, (2014).

200. Einarsdottir, H. *et al.* H435-containing immunoglobulin G3 allotypes are transported efficiently across the human placenta: Implications for alloantibody-mediated diseases of the newborn. *Transfusion* **54**, 665–671 (2014).

201. Pan, Q., Petit-Frére, C. & Hammarström, L. An allotype-associated polymorphism in the γ3 promoter determines the germ-line γ3 transcriptional rate but does not influence switching and subsequent IgG3 production. *Eur. J. Immunol.* **30**, 2388–2393 (2000).

202. Seppälä, I. J., Sarvas, H. & Mäkelä, O. Low concentrations of Gm allotypic subsets G3 mg and G1 mf in homozygotes and heterozygotes. *J. Immunol.* **151**, 2529–37 (1993).

203. Kratochvil, S. *et al.* Immunoglobulin G1 allotype influences antibody subclass distribution in response to HIV gp140 vaccination. *Front. Immunol.* **8**, (2017).

204. Stickler, M. M. *et al.* The human G1m1 allotype associates with CD4 T-cell responsiveness to a highly conserved IgG1 constant region peptide and confers an asparaginyl endopeptidase cleavage site. *Genes Immun.* **12**, 213–221 (2011).

205. Beltrán, E. *et al.* Early adaptive immune activation detected in monozygotic twins with prodromal multiple sclerosis. *J. Clin. Invest.* **129**, 4758–4768 (2019).

206. Wijnands, J. M. A. *et al.* Five years before multiple sclerosis onset: Phenotyping the prodrome. *Mult. Scler. J.* **25**, 1092–1101 (2019).

207. Tung, P.-Y. *et al.* Batch effects and the effective design of single-cell gene expression studies. *Sci. Reports 2017 71* **7**, 1–15 (2017).

208. Ziegenhain, C. *et al.* Comparative Analysis of Single-Cell RNA Sequencing Methods. *Mol. Cell* **65**, 631-643.e4 (2017).

209. Zheng, G. X. Y. *et al.* Massively parallel digital transcriptional profiling of single cells. *Nat. Commun. 2017 81* **8**, 1–12 (2017).

210. See, P., Lum, J., Chen, J. & Ginhoux, F. A single-cell sequencing guide for immunologists. *Frontiers in Immunology* vol. 9 2425 (2018).

211. Picelli, S. *et al.* Full-length RNA-seq from single cells using Smart-seq2. *Nat. Protoc.* **9**, 171–181 (2014).

212. Bagnoli, J. W. *et al.* Sensitive and powerful single-cell RNA sequencing using mcSCRB-seq. *Nat. Commun. 2018 91* **9**, 1–8 (2018).

213. Turchinovich, A. *et al.* Capture and Amplification by Tailing and Switching (CATS): An ultrasensitive ligation-independent method for generation of DNA libraries for deep sequencing from picogram amounts of DNA and RNA. *RNA Biol.* **11**, 817 (2014).

214. Patro, R., Duggal, G., Love, M. I., Irizarry, R. A. & Kingsford, C. Salmon provides fast and bias-aware

quantification of transcript expression. *Nat. Methods* **14**, 417–419 (2017).

215. Bacher, R. & Kendziorski, C. Design and computational analysis of single-cell RNA-sequencing experiments. *Genome Biology* vol. 17 1–14 (2016).

216. McInnes, L., Healy, J. & Melville, J. UMAP: Uniform Manifold Approximation and Projection for Dimension Reduction. arXiv [preprint], 1802.03426 (2018).

217. Kobak, D. & Berens, P. The art of using t-SNE for single-cell transcriptomics. *Nat. Commun.* **10**, (2019).

218. Kolberg, L., Raudvere, U., Kuzmin, I., Vilo, J. & Peterson, H. gprofiler2 -- an R package for gene list functional enrichment analysis and namespace conversion toolset g:Profiler. *F1000Research* **9**, 709 (2020).

219. Lindeman, I. *et al.* BraCeR: B-cell-receptor reconstruction and clonality inference from single-cell RNA-seq. *Nat. Methods* **15**, 563–565 (2018).

220. Brady, B. L., Steinel, N. C. & Bassing, C. H. Antigen Receptor Allelic Exclusion: An Update and Reappraisal. *J. Immunol.* **185**, 3801–3808 (2010).

221. Saveliev, S. *et al.* Trypsin/Lys-C protease mix for enhanced protein mass spectrometry analysis. *Nat. Methods* **10**, i–ii (2013).

222. Pitt, J. J. Principles and Applications of Liquid Chromatography-Mass Spectrometry in Clinical Biochemistry. *Clin. Biochem. Rev.* **30**, 19 (2009).

223. Sielemann, K., Hafner, A. & Pucker, B. The reuse of public datasets in the life sciences: Potential risks and rewards. *PeerJ* **8**, (2020).

224. Rivas, J. R. *et al.* Peripheral VH4+ Plasmablasts Demonstrate Autoreactive B Cell Expansion Toward Brain Antigens in Early Multiple Sclerosis Patients. *Acta Neuropathol* **133**, 43–60 (2017).

225. Otto, C. *et al.* Intrathecal EBV antibodies are part of the polyspecific immune response in multiple sclerosis. *Neurology* **76**, 1316–1321 (2011).

226. Owens, G. P. *et al.* VH4 Gene Segments Dominate the Intrathecal Humoral Immune Response in Multiple Sclerosis. *J. Immunol.* **179**, 6343–6351 (2007).

227. Rivas, J. R. *et al.* Peripheral VH4+ Plasmablasts Demonstrate Autoreactive B Cell Expansion Toward Brain Antigens in Early Multiple Sclerosis Patients. *Acta Neuropathol* **133**, 43–60 (2017).

228. Koulieris, E. *et al.* Ratio of involved/uninvolved immunoglobulin quantification by Hevylite™ assay: clinical and prognostic impact in multiple myeloma. *Exp. Hematol. Oncol.* **1**, 9 (2012).

229. Owens, G. P. *et al.* Single-Cell Repertoire Analysis Demonstrates that Clonal Expansion Is a Prominent Feature of the B Cell Response in Multiple Sclerosis Cerebrospinal Fluid. *J. Immunol.* **171**, 2725–2733 (2003).

230. Eggers, E. L. *et al.* Clonal relationships of CSF B cells in treatment-naive multiple sclerosis patients. *JCI insight* **2**, (2017).

231. Friedensohn, S. *et al.* Synthetic standards combined with error and bias correction improve the accuracy and quantitative resolution of antibody repertoire sequencing in human naïve and memory B cells. *Front. Immunol.* **9**, 1401 (2018).

232. Mayr, W. R. HLA-A, B, C gene and haplotype frequencies in Vienna - An analysis of family data. *Hum. Genet.* **37**, 41–48 (1977).

233. Lokki, M. L. & Paakkanen, R. The complexity and diversity of major histocompatibility complex challenge disease association studies. *HLA* **93**, 3–15 (2019).

234. Vorechovsky, I. *et al.* Short tandem repeat (STR) haplotypes in HLA: An integrated 50-kb STR/linkage disequilibrium/gene map between the RING3 and HLA-B genes and identification of STR haplotype diversification in the class III region. *Eur. J. Hum. Genet.* **9**, 590–598 (2001).

235. Smith, W. P. *et al.* Toward understanding MHC disease associations: Partial resequencing of 46 distinct

HLA haplotypes. *Genomics* **87**, 561–571 (2006).

236. Kenter, A. L., Watson, C. T. & Spille, J. H. Igh Locus Polymorphism May Dictate Topological Chromatin Conformation and V Gene Usage in the Ig Repertoire. *Front. Immunol.* **12**, 1724 (2021).

237. Yeung, Y. A. *et al.* Germline-encoded neutralization of a Staphylococcus aureus virulence factor by the human antibody repertoire. *Nat. Commun.* **7**, 1–14 (2016).

238. Johnson, T. A. *et al.* Association of an IGHV3-66 gene variant with Kawasaki disease. *J. Hum. Genet.* **66**, 475–489 (2021).

239. Avnir, Y. *et al.* IGHV1-69 polymorphism modulates anti-influenza antibody repertoires, correlates with IGHV utilization shifts and varies by ethnicity. *Sci. Rep.* **6**, 1–13 (2016).

240. Dhande, I. S. *et al.* Germ-line genetic variation in the immunoglobulin heavy chain creates stroke susceptibility in the spontaneously hypertensive rat. *Physiol. Genomics* **51**, 578–585 (2019).

241. Frezza, D. *et al.* Concerted variation of the 3′ regulatory region of Ig heavy chain and Gm haplotypes across human continental populations. *Am. J. Phys. Anthropol.* **171**, 671–682 (2020).

242. Bashirova, A. A. *et al.* Population-specific diversity of the immunoglobulin constant heavy G chain (IGHG) genes. *Genes Immun.* **22**, 327–334 (2021).

243. Brüggemann, M. *et al.* Comparison of the effector functions of human immunoglobulins using a matched set of chimeric antibodies. *J. Exp. Med.* **166**, 1351–1361 (1987).

244. Paterson, T., Innes, J., McMillan, L., Downing, I. & McCann Carter, M. C. Variation in IgG1 heavy chain allotype does not contribute to differences in biological activity of two human anti-Rhesus (D) monoclonal antibodies. *Immunotechnology* **4**, 37–47 (1998).

245. Ternant, D. *et al.* IgG1 Allotypes Influence the Pharmacokinetics of Therapeutic Monoclonal Antibodies through FcRn Binding. *J. Immunol.* **196**, 607–613 (2016).

246. Schlachetzki, F., Zhu, C. & Pardridge, W. M. Expression of the neonatal Fc receptor (FcRn) at the blood-brain barrier. *J. Neurochem.* **81**, 203–206 (2002).

247. Cooper, P. R. *et al.* Efflux of monoclonal antibodies from rat brain by neonatal Fc receptor, FcRn. *Brain Res.* **1534**, 13–21 (2013).

248. Monnet, C. *et al.* Selection of IgG variants with increased FcRn binding using random and directed mutagenesis: Impact on effector functions. *Front. Immunol.* **6**, (2015).

249. Schoch, A. *et al.* Charge-mediated influence of the antibody variable domain on FcRn-dependent pharmacokinetics. *Proc. Natl. Acad. Sci. U. S. A.* **112**, 5997–6002 (2015).

250. Warwicker, J., Charonis, S. & Curtis, R. A. Lysine and arginine content of proteins: Computational analysis suggests a new tool for solubility design. *Mol. Pharm.* **11**, 294–303 (2014).

251. Corcione, A. *et al.* Recapitulation of B cell differentiation in the central nervous system of patients with multiple sclerosis. *Proc. Natl. Acad. Sci. U. S. A.* **101**, 11064–11069 (2004).

252. Harp, C. *et al.* Cerebrospinal fluid B cells from multiple sclerosis patients are subject to normal germinal center selection. *J. Neuroimmunol.* **183**, 189–199 (2007).

253. Beltrán, E. *et al.* Intrathecal somatic hypermutation of IgM in multiple sclerosis and neuroinflammation. *Brain* **137**, 2703–2714 (2014).

254. Henriksson, A., Kam-Hansen, S. & Link, H. IgM, IgA and IgG producing cells in cerebrospinal fluid and peripheral blood in multiple sclerosis. *Clin. Exp. Immunol.* **62**, 176–84 (1985).

255. Pröbstel, A. K. *et al.* Gut microbiota–specific iga+ B cells traffic to the CNS in active multiple sclerosis. *Sci. Immunol.* **5**, (2020).

256. Oruc, Z., Boumédiène, A., Le Bert, M. & Khamlichi, A. A. Replacement of Iγ3 germ-line promoter by Iγ1 inhibits class-switch recombination to IgG3. *Proc. Natl. Acad. Sci. U. S. A.* **104**, 20484–20489 (2007).

257. Hu, Y. *et al.* Regulation of Germline Promoters by the Two Human Ig Heavy Chain 3′ α Enhancers. *J. Immunol.* **164**, 6380–6386 (2000).

258. Giambra, V. *et al.* Allele *1 of HS1.2 Enhancer Associates with Selective IgA Deficiency and IgM Concentration. *J. Immunol.* **183**, 8280–8285 (2009).

259. Jones, B. G. *et al.* Complex sex-biased antibody responses: estrogen receptors bind estrogen response elements centered within immunoglobulin heavy chain gene enhancers. *Int. Immunol.* **31**, 141–156 (2019).

260. O'Connor, K. C. *et al.* Antibodies from inflamed central nervous system tissue recognize myelin oligodendrocyte glycoprotein. *J. Immunol.* **175**, 1974–82 (2005).

261. Ligocki, A. J. *et al.* A distinct class of antibodies may be an indicator of gray matter autoimmunity in early and established relapsing remitting multiple sclerosis patients. *ASN Neuro* **7**, (2015).

262. He, B. *et al.* Rapid isolation and immune profiling of SARS-CoV-2 specific memory B cell in convalescent COVID-19 patients via LIBRA-seq. *Signal Transduct. Target. Ther.* **6**, 1–12 (2021).

263. Ekiert, D. C. *et al.* Antibody recognition of a highly conserved influenza virus epitope. *Science (80-.).* **324**, 246–251 (2009).

264. Gorny, M. K. *et al.* Preferential use of the VH5-51 gene segment by the human immune response to code for antibodies against the V3 domain of HIV-1. *Mol. Immunol.* **46**, 917–926 (2009).

265. Parameswaran, P. *et al.* Convergent antibody signatures in human dengue. *Cell Host Microbe* **13**, 691–700 (2013).

266. Davis, C. W. *et al.* Longitudinal Analysis of the Human B Cell Response to Ebola Virus Infection. *Cell* **177**, 1566-1582.e17 (2019).

267. Lucas, A. H., Moulton, K. D., Tang, V. R. & Reason, D. C. Combinatorial library cloning of human antibodies to Streptococcus pneumoniae capsular polysaccharides: Variable region primary structures and evidence for somatic mutation of Fab fragments specific for capsular serotypes 6B, 14, and 23F. *Infect. Immun.* **69**, 853–864 (2001).

268. Snir, O. *et al.* Stereotyped antibody responses target posttranslationally modified gluten in celiac disease. *JCI Insight* **2**, (2017).

269. Henry Dunand, C. J. & Wilson, P. C. Restricted, canonical, stereotyped and convergent immunoglobulin responses. *Philosophical transactions of the Royal Society of London. Series B, Biological sciences* vol. 370 (2015).

270. Lee, J. H. *et al.* Vaccine genetics of IGHV1-2 VRC01-class broadly neutralizing antibody precursor naïve human B cells. *npj Vaccines* **6**, 1–12 (2021).

271. Mikocziova, I., Greiff, V. & Sollid, L. M. Immunoglobulin germline gene variation and its impact on human disease. *Genes and Immunity* (2021) doi:10.1038/s41435-021-00145-5.

272. Xu, X. H. & McFarlin, D. E. Oligoclonal bands in csf: Twins with ms. *Neurology* **34**, 769–774 (1984).

273. Zeman, A. Z. J. *et al.* A study of oligoclonal band negative multiple sclerosis. *J. Neurol. Neurosurg. Psychiatry* **60**, 27–30 (1996).

274. Huss, A. M. *et al.* Importance of cerebrospinal fluid analysis in the era of McDonald 2010 criteria: a German–Austrian retrospective multicenter study in patients with a clinically isolated syndrome. *J. Neurol.* **263**, 2499–2504 (2016).

275. Schwenkenbecher, P. *et al.* Clinically isolated syndrome according to mcdonald 2010: Intrathecal IgG synthesis still predictive for conversion to multiple sclerosis. *Int. J. Mol. Sci.* **18**, (2017).

276. Rojas, J. I., Tizio, S., Patrucco, L. & Cristiano, E. Oligoclonal bands in multiple sclerosis patients: Worse prognosis? *Neurol. Res.* **34**, 889–892 (2012).

277. Mancuso, R. *et al.* Effects of natalizumab on oligoclonal bands in the cerebrospinal fluid of multiple sclerosis patients: A longitudinal study. *Mult. Scler. J.* **20**, 1900–1903 (2014).

278. Rejdak, K., Stelmasiak, Z. & Grieb, P. Cladribine induces long lasting oligoclonal bands disappearance in relapsing multiple sclerosis patients: 10-year observational study. *Mult. Scler. Relat. Disord.* **27**, 117–120 (2019).

279. Sipe, J. C. *et al.* Cladribine in treatment of chronic progressive multiple sclerosis. *Lancet* **344**, 9–13 (1994).

280. Larsson, D., Åkerfeldt, T., Carlson, K. & Burman, J. Intrathecal immunoglobulins and neurofilament light after autologous haematopoietic stem cell transplantation for multiple sclerosis. *Mult. Scler. J.* **26**, 1351–1359 (2020).

281. Simonsen, C. S. *et al.* The diagnostic value of IgG index versus oligoclonal bands in cerebrospinal fluid of patients with multiple sclerosis. *Mult. Scler. J. - Exp. Transl. Clin.* **6**, (2020).

282. Altinier, S. *et al.* Free light chains in cerebrospinal fluid of multiple sclerosis patients negative for IgG oligoclonal bands. *Clin. Chim. Acta* **496**, 117–120 (2019).

283. Houen, G. *et al.* Antibodies to Epstein-Barr virus and neurotropic viruses in multiple sclerosis and optic neuritis. *J. Neuroimmunol.* **346**, (2020).

284. Absinta, M. *et al.* A lymphocyte–microglia–astrocyte axis in chronic active multiple sclerosis. *Nature* **597**, 709–714 (2021).

285. Pollok, K. *et al.* The chronically inflamed central nervous system provides niches for long-lived plasma cells. *Acta Neuropathol. Commun.* **5**, 88 (2017).

286. Thangarajh, M., Masterman, T., Hillert, J., Moerk, S. & Jonsson, R. A proliferation-inducing ligand (APRIL) is expressed by astrocytes and is increased in multiple sclerosis. *Scand. J. Immunol.* **65**, 92–98 (2007).

287. Rentzos, M. *et al.* IL-15 is elevated in serum and cerebrospinal fluid of patients with multiple sclerosis. *J. Neurol. Sci.* **241**, 25–29 (2006).

288. Watkins, L. M. *et al.* Complement is activated in progressive multiple sclerosis cortical grey matter lesions. *J. Neuroinflammation* **13**, 1–13 (2016).

289. Stork, L. *et al.* Antibody signatures in patients with histopathologically defined multiple sclerosis patterns. *Acta Neuropathol.* **139**, 547–564 (2020).

290. Sladkova, V., Mares, J., Hlustik, P., Langova, J. & Kanovsky, P. Intrathecal synthesis in particular types of multiple sclerosis. *Biomed. Pap.* **158**, 124–126 (2014).

291. Villar, L. M. *et al.* Intrathecal synthesis of oligoclonal IgM against myelin lipids predicts an aggressive disease course in MS. *J. Clin. Invest.* **115**, 187–194 (2005).

292. Blauth, K., Owens, G. P. & Bennett, J. L. The ins and outs of B cells in multiple sclerosis. *Frontiers in Immunology* vol. 6 565 (2015).

293. Nissimov, N. *et al.* B cells reappear less mature and more activated after their anti-CD20-mediated depletion in multiple sclerosis. *Proc. Natl. Acad. Sci. U. S. A.* **117**, 25690–25699 (2020).

294. Edwards, K. R. *et al.* A pharmacokinetic and biomarker study of delayed-release dimethyl fumarate in subjects with secondary progressive multiple sclerosis: evaluation of cerebrospinal fluid penetration and the effects on exploratory biomarkers. *Mult. Scler. Relat. Disord.* **51**, (2021).

295. Litjens, N. H. R. *et al.* In vitro pharmacokinetics of anti-psoriatic fumaric acid esters. *BMC Pharmacol.* **4**, 1–7 (2004).

296. Sheikh, S. I. *et al.* Tolerability and pharmacokinetics of delayed-release dimethyl fumarate administered with and without aspirin in healthy volunteers. *Clin. Ther.* **35**, 1582-1594.e9 (2013).

297. Kappos, L. *et al.* Atacicept in multiple sclerosis (ATAMS): A randomised, placebo-controlled, double-blind, phase 2 trial. *Lancet Neurol.* **13**, 353–363 (2014).

298. Tak, P. P. *et al.* Atacicept in patients with rheumatoid arthritis: Results of a multicenter, phase Ib, double-blind, placebo-controlled, dose-escalating, single- and repeated-dose study. *Arthritis Rheum.* **58**,

61–72 (2008).

299. Silk, M. & Nantz, E. Efficacy and Safety of Tabalumab in Patients with Relapsing-Remitting Multiple Sclerosis: A Randomized, Double-Blind, Placebo-Controlled Study (P3.397). *Neurology* **90**, P3.397 (2018).

300. Baker, D., Pryce, G., James, L. K., Schmierer, K. & Giovannoni, G. Failed B cell survival factor trials support the importance of memory B cells in multiple sclerosis. *European Journal of Neurology* vol. 27 221–228 (2020).

301. Pers, J. O. *et al.* B-cell depletion and repopulation in autoimmune diseases. *Clinical Reviews in Allergy and Immunology* vol. 34 50–55 (2008).

I

 DOI: 10.1002/eji.202149576 Eur. J. Immunol. 2022. 52: 550–565

Clinical

European Journal of Immunology HIGHLIGHTS

FRONTLINE | Research Article

Stereotyped B-cell responses are linked to IgG constant region polymorphisms in multiple sclerosis

Ida Lindeman[#1,2,3], *Justyna Polak*[#2,3], *Shuo-Wang Qiao*[1,2,3], *Trygve Holmøy*[4,5], *Rune A. Høglund*[4,5], *Frode Vartdal*[2,3], *Pål Berg-Hansen*[6], *Ludvig M. Sollid*[1,2,3] and *Andreas Lossius*[3,4,7]

[1] Department of Immunology, Oslo University Hospital, Oslo, Norway
[2] Department of Immunology, Institute of Clinical Medicine, University of Oslo, Oslo, Norway
[3] K.G. Jebsen Coeliac Disease Research Centre, University of Oslo, Oslo, Norway
[4] Department of Neurology, Akershus University Hospital, Lørenskog, Norway
[5] Department of Neurology, Institute of Clinical Medicine, University of Oslo, Oslo, Norway
[6] Department of Neurology, Oslo University Hospital, Oslo, Norway
[7] Department of Molecular Medicine, Institute of Basic Medical Sciences, University of Oslo, Oslo, Norway

Clonally related B cells infiltrate the brain, meninges, and cerebrospinal fluid of MS patients, but the mechanisms driving the B-cell response and shaping the immunoglobulin repertoires remain unclear. Here, we used single-cell full-length RNA-seq and BCR reconstruction to simultaneously assess the phenotypes, isotypes, constant region polymorphisms, and the paired heavy- and light-chain repertoires in intrathecal B cells. We detected extensive clonal connections between the memory B cell and antibody-secreting cell (ASC) compartments and observed clonally related cells of different isotypes including IgM/IgG1, IgG1/IgA1, IgG1/IgG2, and IgM/IgA1. There was a strong dominance of the G1m1 allotype constant region polymorphisms in ASCs, but not in memory B cells. Tightly linked to the G1m1 allotype, we found a preferential pairing of the immunoglobulin heavy-chain variable *(IGHV)*4 gene family with the κ variable *(IGKV)*1 gene family. The *IGHV*4-39 gene was most used and showed the highest frequency of pairing with *IGKV*1-5 and *IGKV*1*(D)*-33. These results link IgG constant region polymorphisms to stereotyped B-cell responses in MS and indicate that the intrathecal B-cell response in these patients could be directed against structurally similar epitopes.

Keywords: B cells · Cerebrospinal fluid · Immunoglobulins · Multiple sclerosis · Single-cell RNA sequencing

Additional supporting information may be found online in the Supporting Information section at the end of the article.

Introduction

More than half a century ago, Kabat and colleagues discovered that MS patients have increased levels of IgG in their CSF [1]. Using more sensitive techniques, such as agarose electrophoresis and isoelectric focusing, intrathecally synthesized IgG can be detected as oligoclonal bands (OCBs) in more than 90% of patients [2]. OCBs of other isotypes, such as IgM and IgA, can also be found to a variable extent and might be of prognostic value [3, 4]. A proportion of the secreted IgG proteome in the CSF matches IgG transcripts from B-lineage cells in the brain parenchyma, meninges, and the CSF of MS patients, suggesting

Correspondence: Dr. Andreas Lossius
e-mail: andreas.lossius@medisin.uio.no

[#]Ida Lindeman and Justyna Polak contributed equally to this work.

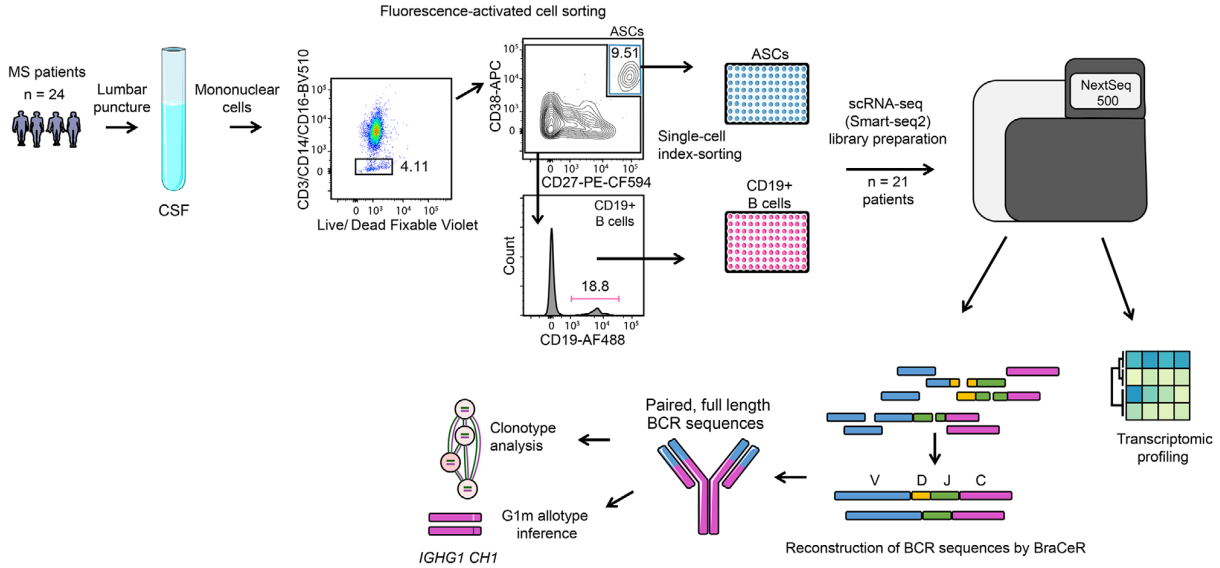

Figure 1. Schematics of single B-cell sorting, sequencing library preparation, and data analysis. Fresh CSF samples were stained and analyzed by flow cytometry. Debris and doublets were excluded (not shown). After excluding $CD3^+$, $CD14^+$, and $CD16^+$ cells in a dump channel, $CD38^{++}CD27^{++}$ single antibody-secreting cells (ASCs) were sorted into 96-well plates containing lysis buffer. For every other plate, we inverted the latter gate and collected single $CD38^{-/dim}$ $CD27^{-/dim}$ $CD19^+$ B cells. From the lysed cells, single-cell RNA-sequencing (scRNA-seq) libraries were prepared following a modified Smart-Seq2 protocol and sequenced on an Illumina NextSeq500 platform. B-cell receptor (BCR) sequences were reconstructed using BraCeR. Some of the elements in the figure were modified from Servier Medical Art, licensed under a Creative Common Attribution 3.0 Generic License. http://smart.servier.com.

that CSF IgG is secreted by B-lineage cells within these compartments [5,6]. Accordingly, studies have demonstrated an intrathecal enrichment of antibody-secreting cells (ASCs) that are clonally related [7–11], have undergone somatic hypermutation [7,9-13], and have B-cell receptors (BCRs) displaying a biased usage of variable heavy-chain (V_H) genes toward the *IGHV4* family [9,10,14]. These studies have provided important biological insights, but they were based on cloning and sequencing of V_H genes from a limited number of single cells or bulk sequencing that does not permit pairing of V_H and variable light-chain (V_L) genes. Analysis of paired V_H:V_L sequences from a sufficient number of single B-lineage cells is key to establish the degree of clonal expansion, determine the mutational load, accurately trace clonal evolution based on somatic mutations within both immunoglobulin chains, and to detect convergent B-cell responses with V_H:V_L pairing preferences.

The constant region of IgG1 comprises the G1m allotypes that are polymorphic markers encoded by the *IGHG1* gene. We have recently demonstrated that MS patients heterozygous for the *IGHG1* alleles expressing the G1m1 and G1m3 allotypes of IgG1 display a selective intrathecal enrichment of ASCs expressing the G1m1 allotype [15]. This was unexpected, as maturing B cells in the bone marrow undergo random allelic exclusion of the immunoglobulin genes. Thus, the immunoglobulin alleles are expected to be evenly distributed in the B-cell pool of heterozygous carriers, which was the case in the blood of MS patients, and in the CSF of patients with *Lyme neuroborreliosis* [15] and *varicella zoster* virus encephalitis [16].

To dissect the mechanisms shaping the intrathecal immunoglobulin repertoires in MS, we performed an in-depth study of B-lineage cells in MS patients using a full-length single-cell RNA-sequencing (scRNA-seq) protocol [17]. We combined this with BraCeR [18], a bioinformatic pipeline that provides accurate reconstruction of paired BCR sequences, clonality inference, and lineage tracing of single B cells. This approach has recently proven useful in the study of autoimmune plasma cells in celiac disease [19]. In the present study, it allowed us to simultaneously assess the detailed phenotypes, isotypes, allotypes, and for the first time, trace the clonal evolution of CSF B cells based on somatic mutations within full-length paired immunoglobulin V_H:V_L sequences.

Results

Full-length RNA-seq of single B-lineage cells in the CSF of MS patients

We performed flow cytometry index-sorting and scRNA-seq of B-lineage cells collected from MS patients during diagnostic lumbar puncture (Fig. 1, Table 1 and Supporting information Table S1). ASCs were sorted first, and other B-cell phenotypes were included on every other 96-well plate if the number of cells was sufficient (Supporting information Fig. S1). After quality control, we analyzed the transcriptomic profiles of 1621 ASCs from 21 MS patients and another 544 B-lineage cells from ten of the patients

Table 1. Patient characteristics

ID	Sex	Age	Diagnosis	Initial presenting symptom	Disease duration (months)	Relapses	Months since last relapse	CSF cell count[a]	OCB[b]	Albumin ratio	IgG index	Allotype[c]	IGHG1 Alleles[d]
MS1	M	27	RR-MS	Optic neuritis	15	1	15	16	+	5.1	0.93	G1m1	*02/(*10?)[e]
MS2	M	36	SP-MS	Motor symptoms (PTM)	120	3	12	36	+	12	1.7	G1m1/G1m3	*02/*03
MS3	F	26	RR-MS	Motor symptoms (PTM)	36	1	36	4	+	3.8	1.1	G1m3	*03
MS4	M	20	RR-MS	Sensory symptoms (PTM)	48	1	48	19	+	6.2	0.81	G1m3	*03
MS5	F	46	RR-MS	Vertigo	24	3	3	19	+	3.1	0.72	G1m3	*03
MS6	F	49	RR-MS	Vertigo	12	1	12	4	+	3.8	0.69	G1m1/G1m3	*02/*03
MS7	F	37	RR-MS	Optic neuritis	0	1	0	5	+	7.5	0.67	G1m1/G1m3	*02/*03
MS8	F	31	RR-MS	Motor symptoms	1	1	1	33	+	3.2	2.1	G1m1/G1m3	*02/*03
MS9	F	24	RR-MS	Motor symptoms	3	1	3	4	+	4.0	0.69	G1m3	*03
MS10	M	52	RR-MS	Motor symptoms (PTM)	7	1	7	6	+	5.0	1.1	G1m1/G1m3	*02[f]
MS11	F	44	RR-MS	Optic neuritis	0	1	0	18	+	6.4	1.1	G1m3	*03
MS12	F	39	RR-MS	Sensory symptoms	72	2	12	4	+	3.8	0.59	G1m3	*03
MS13	F	38	RR-MS	Sensory symptoms	24	2	6	10	+	3.8	1.6	G1m1/G1m3	*02/(*03 or *08)[f]
MS14	M	21	RR-MS	Sensory symptoms (PTM)	1	1	1	21	+	6.4	0.95	G1m1/G1m3	*07/*03
MS15	M	36	RR-MS	Sensory symptoms	7	1	7	6	+	7.2	0.54	G1m3	*03
MS16	F	37	RR-MS	Optic neuritis	132	1	132	8	+	6.2	1.7	G1m1	*02[e]
MS17	M	25	RR-MS	Sensory symptoms (PTM)	0	1	0	6	+	7.5	0.58	G1m1/G1m3	*02[f]
MS18	F	44	RR-MS	Sensory symptoms	9	2	2	4	+	5.6	0.56	G1m3	*03
MS19	F	48	RR-MS	Sensory symptoms	72	2	0	17	+	4.3	1.3	G1m1/G1m3	*07/*03
MS20	M	35	RR-MS	Motor symptoms	12	2	0	5	+	3.3	0.75	G1m1/G1m3	*02/*03
MS21	F	39	RR-MS	Optic neuritis	48	2	13	9	+	2.8	1.5	G1m1/G1m3	*02[f]

[a] Mononuclear cells count per microliter of CSF.
[b] Positive (+) for more than two CSF restricted oligoclonal bands on isoelectric focusing.
[c] Determined in serum.
[d] Inferred computationally by quantifying the transcription of each allele in IgG1-expressing cells.
[e] Too few cells to determine if patient is homozygous for IGHG1*02 or also carries another allele coding for G1m1.
[f] G1m3-encoding allele could not be determined computationally or is uncertain due to too few cells and/or strong skewing toward G1m1 usage.
F, female; M, male; PTM, partial transverse myelitis; RR-MS, relapsing-remitting multiple sclerosis; SP-MS, secondary progressive multiple sclerosis.

Table 2. Features used to phenotype B-lineage cells

		Marker	
B-cell population	Phenotype	Surface	BCR (transcriptome)
Antibody secreting cells (ASCs)		$CD27^{++}$, $CD38^{++}$	> 10% Ig reads
Naïve		$CD27^{-}$, $CD19^{+}$	IgD and/or IgM; mutation rate <0.01[a]; mutations <5[b]
Memory	Non-switched $CD27^{+}$	$CD27^{+}$, $CD19^{+}$	IgD and/or IgM
	Non-switched $CD27^{-/dim}$	$CD27^{-/dim}$, $CD19^{+}$	IgD and/or IgM
	Switched $CD27^{+}$	$CD27^{+}$, $CD19^{+}$	IgG or IgA
	Switched $CD27^{-/dim}$	$CD27^{-/dim}$, $CD19^{+}$	IgG or IgA

[a] IMGT V-segment mutation number divided by the length of the reconstructed V-segment (average of values for heavy and light chain or only one chain if not both reconstructed).
[b] Calculated as a sum of all mutations in the V-segment of heavy and light chain.

(Supporting information Tables S2 and 3). All B-lineage cells were phenotyped according to the surface expression of CD19, CD27, and CD38 assessed by flow cytometry, in addition to isotypes, the proportion of immunoglobulin transcripts, and the somatic mutation load (Table 2). Based on this, we defined populations of ASCs, naïve and memory B cells. Confirming previous studies [20, 21], we found that $CD27^{+}$ memory B cells dominated among sorted $CD19^{+}$ B cells, while naïve cells constituted only a minor part (Fig. 2A). We further separated memory B cells into non-switched $CD27^{-/dim}$, non-switched $CD27^{+}$, switched $CD27^{-/dim}$, and switched $CD27^{+}$ memory B cells. The transcriptomes of these populations were visualized using Uniform Manifold Approximation and Projection (UMAP), identifying distinct clusters of ASCs, naïve B cells, and memory B cells (Fig. 2B and Supporting information Fig. S2A and B).

Next, we analyzed the expression of genes in the main B-lineage populations (Fig. 2C and D). As expected, the ASCs expressed typical plasmablast/plasma cell genes such as *XBP1*, *IRF4*, *PRDM1* (BLIMP-1), and a proportion (45%) expressed *SDC1* (CD138). *MS4A1* (CD20) was highly expressed by almost all memory and naïve B cells, whereas only a minor proportion of ASCs expressed this gene. We detected ubiquitous expression of human leukocyte antigen (HLA) class II genes, although the ASCs displayed a lower expression of these genes than the other B-lineage populations (Fig. 2C). All populations expressed cathepsins, which are required for antigen processing. Further, we detected expression of the gene encoding the costimulatory molecule CD40 in a proportion of all cell populations, and minor proportions expressed *CD80* and *CD86*. Corroborating and extending recent findings by others [21], we found that memory and naïve populations expressed high levels of *CXCR4*, in addition to restricted expression of *CXCR3*, *CXCR5, CCR6, CCR7*, and *IL10RA* among others, while ASCs expressed genes such as *TNFRSF17, IFNAR2*, and *IL21R* and also *CXCR3* and *CXCR4* (Fig. 2C and D). Expression of the activation-induced cytidine deaminase gene *(AICDA)* gene was detected in a small proportion of cells in all populations.

ASCs in the CSF constitute a continuity from immature plasmablasts to more differentiated phenotypes

The phenotype of ASCs in the CSF of MS patients has not been unequivocally established [15,20,22]. We found that approximately 22% of the ASCs expressed the proliferation marker *MKI67* (Ki-67), suggesting they were plasmablasts rather than end-differentiated plasma cells (Fig. 2E and Supporting information Fig. S2C). Notably, the ASCs clustered based on inferred cell-cycle phase when visualized by UMAP (Fig. 2E), and *MKI67* was as anticipated, expressed in cells assigned to the G2M or S phases. This held true also when excluding *MKI67* from the list of genes that is used to infer cell-cycle phase (Supporting information Fig. S2C). When visualized by UMAP, ASCs assigned to the nonproliferative G1/0 phase (66.9%) displayed a seemingly gradual transition between a major population of ASCs with high expression of *SDC1* (CD138) and a smaller population expressing *MS4A1* (CD20) (Fig. 2D). The percentage of ASCs in the different cell-cycle phases was, however, not significantly different from the other B-cell lineages (Fig. 2E, right panel). Taken together, these data suggest that ASCs in the CSF of MS patients are proliferating plasmablasts within different stages of differentiation. However, a proportion of the ASCs in the inferred G1/0 phase may represent true end-differentiated nondividing plasma cells.

IgG, IgA, and IgM/IgD B-lineage cells show distinct transcriptional profiles and mutational load

Full-length recombined BCR sequences, stretching into the constant region, allowed us to define the isotype of sorted B-lineage cells. As expected from earlier studies [15, 23], IgG1 was by far the most prevalent isotype among ASCs, while both IgM and IgG1 isotypes were often used in the memory subset (Fig. 2F). We observed a gradual transition between naïve, nonclass-switched

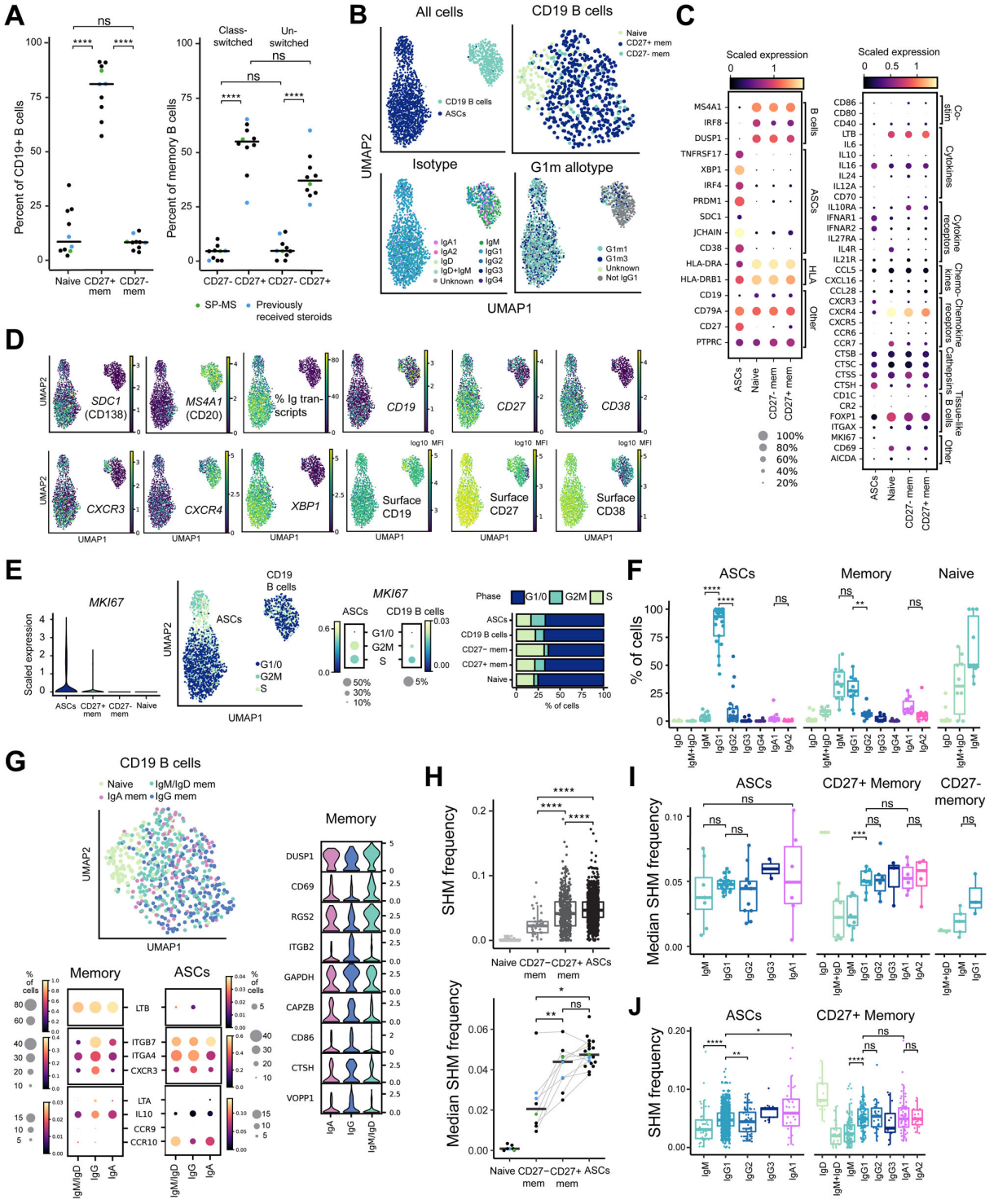

Figure 2. Transcriptional and mutational profiling of B-lineage cells from the cerebrospinal fluid of multiple sclerosis patients. (A) Frequencies of sorted CD19$^+$ B cells being classified as naïve or memory B-cell subsets (Table 2). (B) UMAP projection of all B-lineage cells (upper left; n = 21, 2165 cells), only the CD19$^+$ B cells (upper right; n = 10, 544 cells), and all B-lineage cells colored according to isotype (lower left) and IgG1 (G1m) allotype (lower right). (C) Heatmap showing expression of genes of particular interest in all B-lineage cells in (B). ASC: antibody-secreting cell, HLA: human leukocyte antigen. (D) UMAP projections colored by genes of interest or median fluorescence intensity (MFI) of the cell surface markers CD19, CD27, and CD38 (bottom row) obtained during index sorting. (E) *MKI67* expression and inferred cell-cycle phase in each B-lineage population. (F) Isotype distribution based on reconstructed B-cell receptor (BCR) sequences. Each data point represents a patient with more than one cell for a given cell

and class-switched memory B cells when visualized by UMAP (Fig. 2G). Genes that were found to be significantly higher expressed in memory B cells of the IgM/IgD compared to IgG and IgA isotypes included *DUSP1*, *CD69*, and *RGS2* (encoding regulator of G-protein signaling 2). *CTSH* (encoding cathepsin H) and *CD86* were significantly higher expressed in IgG memory B cells, suggesting an increased importance of antigen presentation in these cells. IgG memory B cells also had the highest expression of *CXCR3*, which is shown to be important for recruitment of B-lineage cells in inflamed tissues [24]. In contrast to a recent report [25], we did not detect a distinct regulatory phenotype of IgA-expressing B-lineage cells in the CSF, and we did not find evidence to support that IgA-expressing B-lineage cells express higher levels of gut-homing markers than their IgM/IgD and IgG counterparts (Fig. 2G).

Next, we investigated the mutational load of each reconstructed BCR sequence. The numbers of somatic mutations varied between populations (Fig. 2H) and isotype (sub)classes (Fig. 2I and J). In line with previous reports [26, 27], $CD27^{-/dim}$ memory B cells displayed significantly fewer mutations than their $CD27^{+}$ counterparts. However, this was not statistically significant on an individual level when excluding MS2, MS19, and MS20 from the analysis (Supporting information Table S4). Among ASCs, we observed the highest number of mutations in class-switched cells. In the memory B-cell population, IgD-only cells showed the highest mutational load, followed by class-switched memory cells (Fig. 2I and J).

B-lineage cells in the CSF of MS patients undergo intrathecal maturation

Next, we analyzed clonal relationships between B-lineage cells using BraCeR. BraCeR, for paired heavy and light chains, assigns clonal relationships between cells, which are then depicted as clonal networks, and additionally, lineage trees for individual clones, consisting of cells with different mutational patterns (Fig. 3). In all 21 patients, clonally related cells were detected, with a median of 61.6% [39.7–83.1%] of all ASCs belonging to a clone (Fig. 3A and B, and Supporting information Table S5). For the first time, we traced the clonal evolution of B-lineage cells based on somatic mutations in the paired full-length variable heavy- and light-chain genes. We reconstructed lineage trees in 17 patients (Fig. 3C, Supporting information Fig. S3A and Table S5). Interestingly, we commonly observed highly mutated clones consisting solely of cells with identical mutational patterns (Supporting information Table S5). The four patients with no reconstructed lineage trees were in the lower range of sorted ASCs and displayed clonally expanded ASCs with the exact same mutational patterns.

Our approach, where both heavy and light chains are involved in determining clonal relations combined with transcriptomic profiling of cells, made it possible to trace linkage between memory B cells and ASCs. Strikingly, we observed clonal sharing between memory B and ASCs in seven out of ten patients from whom both cell populations were sorted (Fig. 3D and E, and Supporting information Fig. S3B). The majority of memory cells belonging to clones containing ASCs shared identical V-regions with at least one ASC, while we also observed the acquisition of mutations. In one patient, we found clonally expanded memory B cells with no detected members of the clones among the ASCs (Fig. 3F). The lack of connections between memory B cells and ASC in three patients could possibly be attributed to low cell numbers (Fig. 3E). We also explored the clonal evolution of the ASCs in relation to their cell-cycle stage and found extensive clonal connections between cells in different stages (Supporting information Fig. S4A–D).

The most commonly found expanded sequences other than IgG1 were of the IgG2 isotype subclass (Table 3, Supporting information Fig. S4E). In eight patients, we also found expanded IgA1 and/or IgM ASCs. Additionally, we detected expanded IgG3 ASCs in two patients and expanded IgG4 ASCs in one patient. Interestingly, we found examples of clones comprising B-lineage cells of different isotypes, including IgM and IgG1, IgG1 and IgA1, IgG1 and IgG2, and IgM and IgA1 (Fig. 3D and G). This could suggest that class-switch recombination has taken place intrathecally and that at least a proportion of the IgG, IgM, and IgA B-lineage cells share a common origin and target the same antigens.

ASCs show a more biased usage of the G1m1 allotype than memory B cells

BraCeR infers the CH1 region of the *IGHC* alleles of reconstructed heavy chains, allowing for detection of isotypes and distinction between the G1m1 and G1m3 allotypes on a cellular level. Due to random allelic exclusion of immunoglobulin genes, there is a 50/50 distribution of the *IGHC* alleles among B-lineage cells in

type. (G) Differentially expressed genes (DEGs) between B-lineage cells of different isotypes. The UMAP of $CD19^{+}$ B cells (upper left) is identical to (B), but colors refer to naïve cells and the isotype of memory cells. For gene expression analysis of memory B cells, naïve B cells were removed from the scaled scRNA-seq expression data for $CD19^{+}$ B cells, and the cells were grouped according to isotype (198 IgM/IgD, 172 IgG, 86 IgA cells). Gene expression analysis was performed separately for the ASCs (55 IgM/IgD, 1529 IgG, 34 IgA cells). Statistically significant DEGs for the memory B cells (Wilcoxon rank-sum test adjusted for multiple testing) with a log fold change greater than 1 are displayed in a violin plot (right). (H) Somatic hypermutation (SHM) frequency in the heavy- and light-chain variable region of B-lineage cells by phenotype. Left panel shows all BCR sequences (Wilcoxon rank-sum test); right panel shows median frequency for each patient (Wilcoxon signed-rank test, excluding unpaired data points). Grey lines connect data points from the same patient for memory B cells and ASCs. (I), (J) SHM frequency in the heavy- and light-chain variable region of B-lineage cells by phenotype and isotype. Median frequency for each patient (I) or frequency in all BCR sequences (J; Wilcoxon rank-sum test) are shown. (A-J) Data shown are analyses of ASCs from 21 MS patients and other B-cell phenotypes from ten of the patients. *p*-values throughout Figure 2 are given with the following significance levels: $^{*}p < 0.05$; $^{**}p < 0.01$; $^{***}p < 0.001$; $^{****}p < 0.0001$; ns: $p > 0.05$.

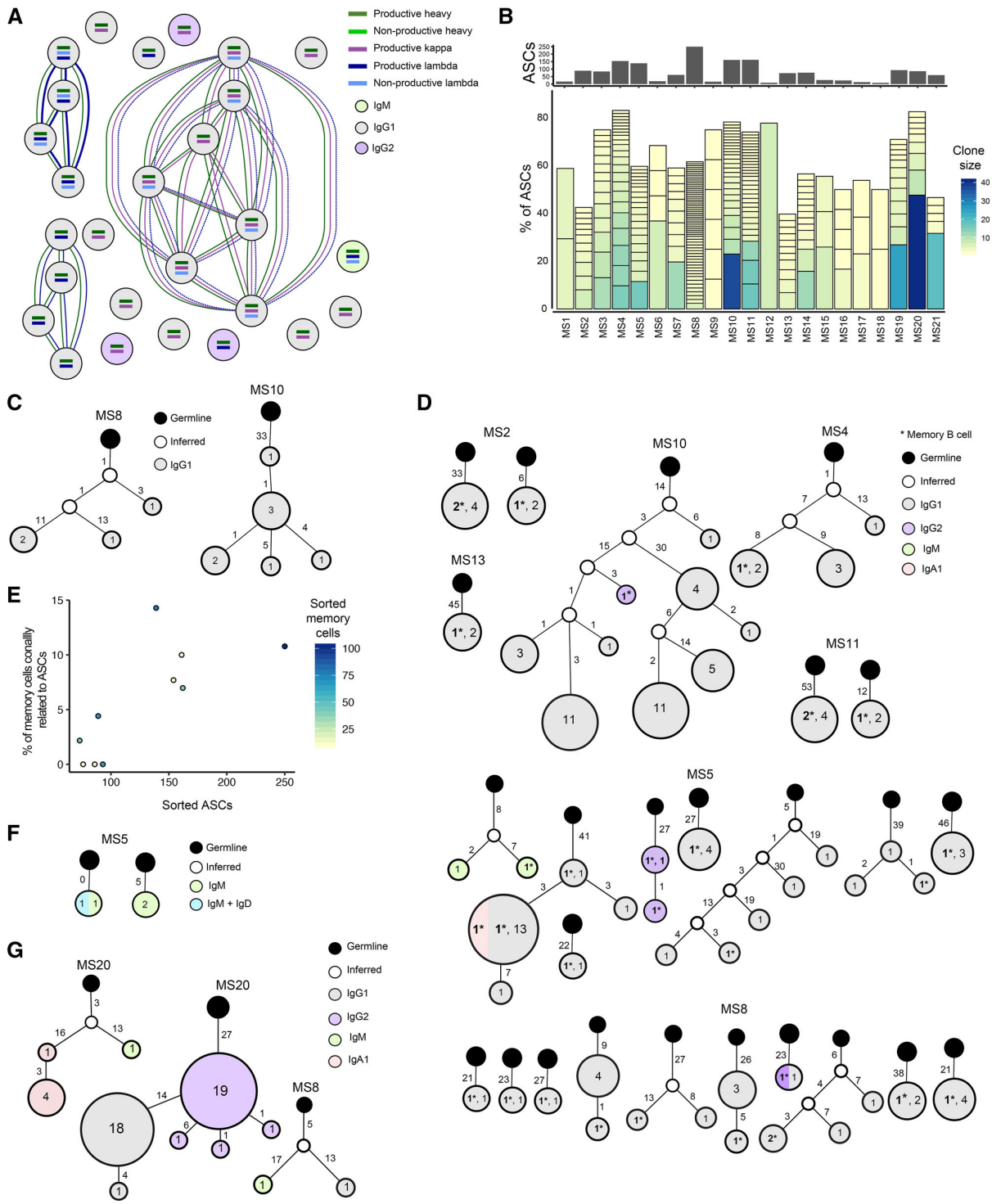

Figure 3. B-lineage cells in the CSF are clonally related, undergo somatic hypermutation, isotype switching, and intrathecal maturation. (A) Example of clonal relationships between antibody secreting cells (ASCs) of patient MS15 inferred by BraCeR. (B) Sizes of clonal groups found for ASCs in each patient. The colors indicate number of cells belonging to each clone group, size of boxes is proportionate to the size of clones. Only clonally expanded cells are shown. The grey columns on the top depict the total number of ASCs included in the analysis for each patient. (C) Representative ASC lineage trees generated by BraCeR for two clones, with inferred germinal sequences at the root. The number of mutations between each node is shown next to the branch. The size of each node is proportionate to the number of cells containing a given unique BCR sequence. The number

Table 3. Clonal expansion of other isotypes than IgG1

ID	IgA1	IgM	IgG2	IgG3	IgG4
MS2	-	-	1 (2)	-	-
MS3	-	1(2)	1 (11)	-	-
MS4	-	2(3)	1 (4)	-	-
MS5	-	2(3-5)	1 (2)	1 (6)	-
	-	2(2)	1 (2)	-	-
MS6	-	-	2 (2–7)	-	-
MS8	1(2)	-	-	-	-
MS9	1(2)	-	1 (2)	-	-
MS10	2 (2)	-	-	-	-
MS11	1 (2)	1(3)	2 (2–3)	1(3)	-
MS14	-	-	2 (7-12)	-	1(2)
MS20	1(5[a])	1(2)	3 (2–22[b])	-	-

Numbers of clonotypes for each patient with numbers in brackets indicating sizes of clonal expansion.
All cells are expanded ASCs except the shaded, which are expanded memory B cells.
[a] Clone additionally contains one IgM ASC.
[b] Part of a large expanded clone containing 22 IgG2 and 19 IgG1 ASCs.

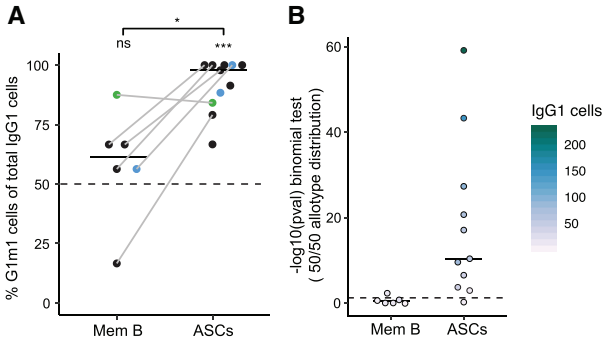

Figure 4. The intrathecal ASC population is skewed toward the G1m1 allotype in G1m1/G1m3 heterozygous MS patients. (A) G1m1 allotype distribution in IgG1 memory B cells (n = 6) and antibody-secreting cells (ASCs; n = 11) of G1m1/G1m3 heterozygous patients. Each dot represents the percentage of IgG1 cells that are of the G1m1 allotype for each patient and horizontal solid lines depict median for all patients. Lines connect ASCs and memory B cells from the same patients. The patient with SP-MS is indicated in green, while the two patients previously treated with corticosteroids are indicated in blue. Frequencies of G1m1 cells were compared within each population (one-sided binomial test) and between paired memory and ASCs populations (paired *t*-test), where four patients were excluded due to absence of a memory cell population (no $CD38^{dim/-}CD27^{dim/-}CD19^{+}$ cells sorted) and one patient due to only one IgG1 memory B cell being present for this patient. The horizontal dashed line at 50% represents the expected distribution of G1m1 cells due to random allelic exclusion. The indicated p-value significance levels are: $^{*}p < 0.05$; $^{***}p < 0.001$; ns > 0.05. (B) *p*-values resulting from two-sided binomial tests for each population within each patient. Solid horizontal lines indicate median values. The horizontal dashed line represents statistical significance ($p = 0.05$). (A–B) Data shown are analyses of ASCs from 11 G1m1/G1m3 heterozygous MS patients and memory B cells from six of the patients.

the blood of heterozygous individuals [15]. We have previously shown, based on flow cytometry, that G1m1-expressing ASCs are preferentially enriched in the CSF of MS patients [15]. To address this on a transcriptomic level, we limited the analysis to G1m1/G1m3 heterozygous patients and calculated the proportion of G1m1-expressing cells among IgG1 ASCs and memory B cells (Fig. 4A and B, Supporting information Table S6). In agreement with our previous study, the results showed a predominance of G1m1 ASCs (Fig. 4A; median 97.8% [66.7–100%]). On an individual level, a statistically significant skewing toward the G1m1 allotype in the ASC population was seen in 10 of 11 of the G1m1/G1m3 heterozygous patients (Fig. 4B). The G1m1 bias was significantly higher in ASCs than memory B cells (Fig. 4A).

ASCs expressing G1m1 show preferential pairing of V_H and V_L genes

Previous studies have shown that the *IGHV4* gene segments are dominating the CNS and CSF heavy-chain repertoires [14,28]. We stratified the heavy-chain repertoires of ASCs according to G1m allotype and found that a preferential use of *IGHV4* gene segments is associated with the G1m1 allotype, but not with the G1m3 allotype (Fig. 5A and Supporting information Fig. S5A and B). In the G1m1-expressing memory B-cell population, on the other hand, we did not detect a similar bias of *IGHV4* gene segments usage (Supporting information Fig. S5B). To confirm the association between *IGHV4* gene segments and G1m1 in a completely independent patient cohort, we reanalyzed *IGHV* sequencing data from bulk CSF B-lineage cells of 12 MS patients previously published by us [10,29]. We used the total *IGHV* pool, driving bias toward ASCs-derived sequences (Supporting information Fig. S6A) [30], but analyzing unique sequences yielded similar results (Supporting information Fig. S6B). Next, we investigated the repertoire of the light chains in single IgG1 ASCs. The results showed that a strong preference for the κ light chain was connected to the G1m1 allotype of the paired heavy chain, but not the G1m3 allotype (Fig. 5B and Supporting information Fig. S7A). No significant κ light chain bias was seen for G1m1-expressing memory B cells, but this could possibly be attributed to few data points and large variation (Supporting information Fig. S7A). We also investigated the use of light-chain constant region genes and alleles (Supporting information Fig. S7B and C). In agreement with the expected high allele frequency of the Km3 allotype in Caucasians [31], we detected use of the Km3-encoding *IGKC*01* allele in all patients with κ-expressing cells. Two patients were

inside each node represents number of cells with the unique sequence. (D) Clones comprising both memory B cells and ASCs, visualized as lineage trees as in (C). (E) Relationship between number of sequenced memory B cells, ASCs, and percent of memory B cells found to be clonally linked to ASCs. Each dot represents one patient. (F) Lineages trees of the only two expanded memory B-cell clones that were exclusively limited to the $CD19^{+}$ B-cell compartment. (G) Examples of multiple isotypes found within B-lineage clones, visualized as lineage trees. (A-G) Data shown are analyses of ASCs from 21 MS patients and memory B cells from ten of the patients.

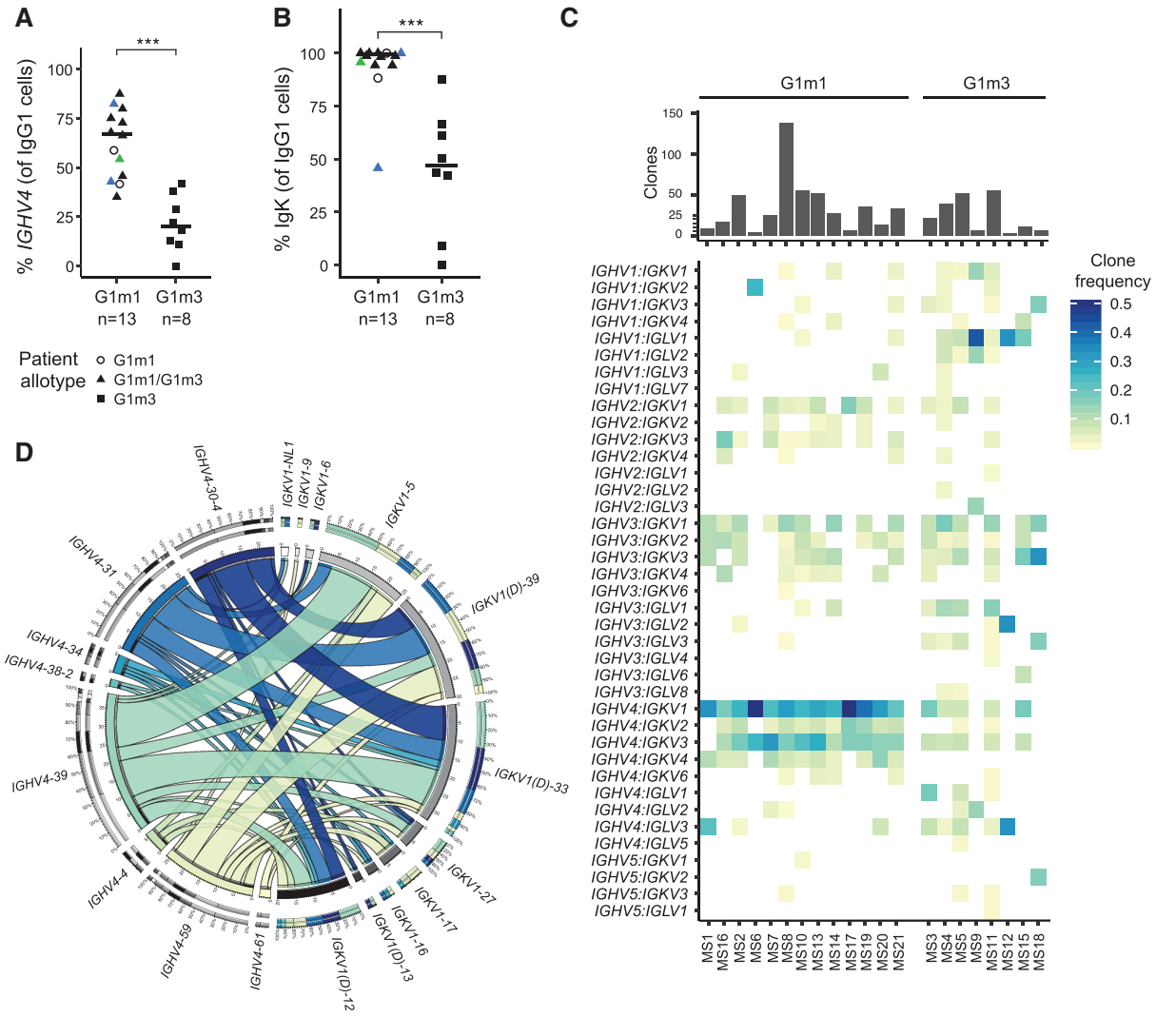

Figure 5. The G1m1 allotype is associated with a stereotyped BCR repertoire. Analysis was performed on the V_H and V_L sequences of IgG1 antibody-secreting cells (ASCs). G1m1 cells from G1m1 homozygous and G1m1/G1m3 heterozygous patients are considered G1m1, whereas only sequences from G1m3 homozygous individuals are denoted as G1m3. G1m3 cells from heterozygous patients were excluded from the analysis due to low cell numbers. Cell numbers for each patient are specified in Supporting information Table S6. A Wilcoxon rank-sum test was used in A and B, with *p*-value significance levels $^{*}p < 0.05$; $^{***}p < 0.001$; ns: $p > 0.05$. (A) Percentage of G1m1 and G1m3 cells using *IGHV4* gene segments. Each dot represents a patient and is shaped according to patient G1m1/G1m3 carrier status; horizontal line represents median value. The patient with SP-MS is indicated in green, while the two patients previously treated with corticosteroids are indicated in blue. (B) κ light chain usage of G1m1 and G1m3 ASCs. Each dot represents a patient; horizontal lines represent median values. (C) Heatmap showing V_H:V_L gene segment pairing frequencies for G1m1 and G1m3 ASCs, where clonally expanded cells are treated as one cell. (D) Circos plot visualizing the *IGHV4*:*IGKV1* gene segment pairings for G1m1 ASCs, where each clone group is treated as one sequence. Pairing is depicted as lines connecting *IGHV4* and *IGKV1* genes inside the circle, where thickness corresponds to pairing frequencies. Sequences from all G1m1 carriers (n = 13, in total 151 unique clones) were pooled together. (A-D) Data shown are analyses of ASCs from 21 MS patients.

heterozygous for *IGKC*01* and the Km1,2-encoding *IGKC*04* alleles, and exhibited no preferential usage of either alleles (Supporting information Fig. S7C). No serological allotypes are known for the λ light chain, which instead exhibits variation through a variable number of different *IGLC* genes. We observed no strong preference of any specific *IGLC* genes in G1m1 and G1m3 cells (Supporting information Fig. S7C).

The analysis of single B-lineage cells allowed us to gain insight into the V_H:V_L pairings, which is key to understanding antigen-driven B-cell responses and may sometimes show specific signatory combinations [32,33]. To exclude the influence of clonal expansion on the pairing frequencies, only one sequence per clonotype was considered. In ASCs expressing G1m1, we observed a preferential pairing of *IGHV4* with *IGKV1*, and to a lesser degree,

IGKV3 gene segments (Fig. 5C). The same pairing preference was not observed for G1m3-expressing ASCs. This pattern was also evident when taking clonal expansion into account (Supporting information Fig. S8A), but it was not clear in the memory B-cell population (Supporting information Fig. S8B). Finally, we explored the pairing frequencies of genes within the *IGHV4* and *IGKV1* gene families in G1m1-expressing ASCs. The *IGHV4-39* gene was mostly used and showed the highest frequency of pairing with *IGKV1-5* (frequency of 9.9%) and *IGKV1(D)-33* (8.4%) (Fig. 5D).

Discussion

In the present study, we analyzed the paired full-length rearranged immunoglobulin heavy- and light-chain gene usage and transcriptome of intrathecal B-lineage cells in MS. We achieved this by combining full-length transcriptomic profiling of single cells along with analysis using BraCeR. The results reveal a common pattern across patients with a preferential V_H:V_L pairing tightly linked to the G1m1 allotype in ASCs. Confirming our previous findings on a transcriptional level [15], the G1m1-expressing ASCs were enriched in the CSF of G1m1/G1m3 heterozygous patients. Our approach further allowed us to demonstrate (i) clonally expanded IgG1, IgG2, IgG3, IgG4, IgA1, and IgM B-lineage cells and clonal connections between them, (ii) accurate lineage trees based on mutations in both heavy- and light-chain genes of clonally expanded ASCs, and (iii) the presence of expanded memory B cells and extensive clonal connections between the memory B-cell and ASC compartments.

Previous studies have demonstrated that immunoglobulin heavy-chain sequences from the brain, CSF, and cervical lymph nodes of MS patients are clonally expanded and have undergone somatic hypermutation, which is indicative of an antigen-driven immune response [7,9,10,12, 14,21,34-36]. *IGHV4* gene segments have been portrayed as dominant in the CSF and brain of patients with MS and clinically isolated syndrome [14,28,37], and have also been shown to acquire specific mutations and displaying increased specificity toward neuroantigens [38,39]. At a closer look, however, it seems that a *IGHV4* bias is only present in a proportion of patients, although this has not been made a matter of contention by previous studies [9,10]. The present results offer a potential explanation, which is possible to verify in previously published data if the G1m1 carrier status of the patients is determined. Indeed, reanalyzing data from our own group that were generated using bulk sequencing of CSF B cells and a multiplex PCR technique confirmed the association between the G1m1 carrier status and a biased usage of *IGHV4* gene segments [10,29]. Curiously, the present data also show a connection between G1m1 expression and κ light-chain usage. While κ light-chain usage was highly dominant among ASCs of G1m1-carriers, several G1m3 homozygous patients showed a predominance of λ light chains in the ASC population. Thus, the G1m1 carrier status could have implications for the diagnostic sensitivity of free light-chain levels in the CSF, which is increasingly being recognized as a valuable diagnostic test in MS [40] and might correlate with the frequency of ASCs expressing the light chain [41].

Preferential pairing of *IGHV4* and *IGKV1* in the BCR of ASCs expressing G1m1 bears a resemblance to stereotyped B-cell responses observed in other diseases, including celiac disease [42], HIV infection [43], and influenza infection [44], that are driven by particular antigenic epitopes [45]. The target antigens of the intrathecal humoral immune response in MS, however, have not been unequivocally defined. Some early studies reported reactivity against myelin-associated antigens [46,47] and EBV [48], but none of these findings have been reproduced in independent studies [8,49]. More recent studies have shown that some antibodies expressed by CSF B cells recognize neuronal nuclei and/or astrocytes [50] and lead to demyelination in spinal cord explant cultures [51]. Finally, a study reported that a proportion of CSF IgG might target cellular debris [52]. Nevertheless, independent of the nature of the antigen, the stereotyped B-cell response with a preferential V_H:V_L pairing demonstrated here argues that these B-lineage cells target a set of epitopes that may be shared between patients.

We have previously demonstrated that the G1m1 allotype dominates the intrathecal humoral immune response in G1m1/G1m3 heterozygous MS patients, but not in controls with neuroborreliosis [15]. The present study confirms the observation in MS patients using gene expression analysis of single CSF ASCs and extends the findings demonstrating that the G1m1 bias is not present to the same degree in intrathecal memory B cells. The mechanisms driving such a biased maturation are currently not known, but one important clue comes from the findings of a connection between the G1m1 allotype and particular V_H and V_L gene segments, suggesting that the ASCs target certain antigenic epitopes. Linkage disequilibrium between constant region alleles expressing G1m1 and certain *IGHV* alleles on chromosome 14 and/or conformational changes in the variable antigen-binding region induced by the G1m allotypes in the constant region are potential explanations to how an antigen-driven B-cell response could show such a preference. In support of the latter idea, it has been shown that the constant region of immunoglobulins may affect the affinity and specificity of the variable region [53]. The biased usage of *IGKV* gene segments located on chromosome 2, on the other hand, could be the result of interactions with the expressed heavy chain and the antigen. It is conceivable that the distinct BCR repertoire we observe in patients carrying the G1m1 allotype may have consequences for disease risk and phenotype. Accordingly, it is known that genetic markers in linkage disequilibrium with the G1m1-encoding alleles are associated with higher IgG index [54] and lower IgM index [55], and possibly with MS risk [55]. The current study is underpowered to address these questions, and further studies investigating the association with the disease risk and phenotype are warranted.

Previous studies have detected clonal connections between B-lineage cells in the periphery and the CNS in MS [9-11,25,34]. Interestingly, a recent study demonstrates that meningeal B-cells in mice derive locally from the calvaria bone marrow, and that the meningeal compartments provide a developmental niche for

CNS B cells [56]. Although this has not been investigated during neuroinflammation in humans, it introduces the possibility that intrathecal B cells in MS could originate within or immediately adjacent to the CNS. In line with this idea, B-cell follicles have been demonstrated in the meninges of patients with long-standing disease [57] and could also be present already at an earlier stage [58]. Expression of the activation-induced cytidine deaminase gene *(AICDA)*, which encodes the DNA-editing deaminase involved in somatic hypermutation and class-switch recombination, has previously been detected in intrathecal B-lineage cells [13]. In the present study, we were able to confirm this observation in a small proportion of the single cells investigated. More importantly, we observed extensive connections between the intrathecal memory and ASC compartments and found evidence of isotype switching from IgM to IgG1, from IgG1 to IgA1, and from IgG1 to IgG2.

Our observations of a relatively high mutational rate in IgM ASCs in the CSF of MS patients are in line with a previous study that demonstrated a very high level of somatic mutations in IgM chains in CSF compared to blood [13]. We also detected expanded and extensively mutated IgA ASCs, which confirms early studies detecting IgA-producing cells in the CSF [59,60]. A recent study found that a proportion of IgA-producing cells in the CSF recognize gut microbiota, and the authors proposed that such cells could represent a population of regulatory cells [25]. In the present study, however, we did not detect any distinct regulatory phenotype of IgA-expressing B-lineage cells in the CSF. We also observed a few instances of clonal connections between IgA1 and IgG1/IgM isotypes, arguing against disparate origins. However, it is possible that different populations of IgA plasma cells in MS may play divergent roles in the disease process.

This is the first study to provide a detailed clonal evolution of B-lineage cells in the CSF of MS patients based on somatic mutations in paired heavy- and light-chain sequences. In contrast to previous studies utilizing different variants of bulk amplification and sequencing of heavy-chain transcripts [9–11], we found evidence of a more focused humoral immune response characterized by smaller lineage trees with fewer offspring per ancestor node. This may seem surprising, as one might have expected larger lineage trees due to the fact that we were able to detect mutations also within the light chains. A likely explanation is that high-throughput bulk sequencing introduces PCR and sequencing errors, which are inherently impossible to discern from somatic mutations [61]. Accordingly, studies using bulk sequencing of heavy-chain transcripts are losing important information of somatic mutations in the light-chain genes, while at the same time, inevitably interpreting PCR and sequencing errors as somatic mutations in heavy-chain genes.

There are limitations to our study that need to be recognized. The number of B-lineage cells in the CSF of MS patients is generally scarce, and it is important to keep in mind that the number of cells in a collected sample only represents a small part of a larger population of B-lineage cells with a plethora of different phenotypes within the CNS. Underscoring this fact, we recently demonstrated that the clonal overlap of CSF B cells at two different time points is much lower than the overlap of the secreted CSF IgG proteome [29]. Moreover, the lack of a control group of patients with other inflammatory neurological diseases does not allow us to conclude that the transcriptomic profile of CSF B cells is unique for MS. The strong dominance of the G1m1 allotype constant region polymorphisms in ASCs, on the other hand, recapitulates our previous findings on a protein level [15]. In this previous study, the G1m1 allotype bias was not present in the CSF of patients with *Lyme neuroborreliosis*, indicating that it is not a general consequence of neuroinflammation.

Our study represents one of the most detailed investigations of B-lineage cells in the CSF of MS patients to date. For the first time, we demonstrate a strong connection between a G1m allotype and the heavy- and light-chain variable gene repertoires. We anticipate that such interactions can point to biological effects of the G1m allotypes that might be of importance in humoral immune responses in MS.

Materials and methods

Patients and sample collection

Twenty-four subjects with symptoms and brain MRI scans strongly suggestive of MS were recruited during diagnostic work-up at the Departments of Neurology at Akershus University Hospital and Oslo University Hospital. All the patients were of Caucasian ethnicity. Three patients were excluded due to too low frequency of ASCs and/or absence of OCBs (Supporting information Table S1). Based on MRI scans, clinical symptoms, and CSF findings, 20 included patients met the criteria of relapsing-remitting MS according to the 2017 McDonald revisions [62], and one patient had developed a secondary-progressive disease (Table 1). MS19 and MS20 had been previously treated with intravenous infusions of methylprednisolone at 1 gram per day for 3 days within 2 weeks of inclusion. None of the other patients had received corticosteroids or any other type of immunomodulatory treatment. The study was approved by the Committee for Research Ethics at the South-Eastern Norwegian Health Authority (2009/23, S-04143a). All patients signed a written informed consent.

CSF and serum were collected during diagnostic lumbar puncture. The first 7 mL of CSF was collected for diagnostic purposes, and 2 × 9 mL CSF was subsequently collected in 15 mL Falcon tubes. Collected CSF was centrifuged (1600 rpm, 10 min, room temperature [RT]) and cell pellets were resuspended in approximately 100 μL of supernatant. Cell count and the presence of red blood cells was checked in a Bürker counting chamber, and none of the CSF samples contained enough cells to indicate contamination of lymphocytes from blood. Serum was left at RT for at least 30 min after collection, centrifuged (2800 rpm, 10 min, RT) and stored at −80°C. It was subsequently thawed and used to determine the expression of the G1m allotypes of each subject by ELISA according to a previously published protocol [15].

Single-cell sorting by flow cytometry

For flow cytometry cell sorting, we adhered to the guidelines for the use of flow cytometry and cell sorting in immunological studies [63]. The CSF cell suspension was transferred to a V-bottom plate, centrifuged (1600 rpm, 4 min, 4°C) and the supernatant was removed. Cells were resuspended in 40 μL of Live/Dead Fixable Violet (Molecular Probes L34963) according to the manufacturer's instructions and incubated at RT for 15 min in the dark. A total of 10 μL of 30% BSA was added, followed by a mixture of the following anti-human antibodies from BD Biosciences: CD3-BV510 (HIT3a), CD14-BV510 (MφP9), CD16-BV510 (3G8), CD19-AF488 (HIB19), CD27-PE-CF594 (M-T271), CD38-APC (HIT2), IgD-APC-H7 (IA6-2). Cell suspensions were incubated for 30 min on ice, centrifuged (1600 rpm, 4 min, 4°C), and washed once with flow buffer (PBS, 0.5% BSA, 2 mM EDTA). Cells were resuspended in 200 μL of flow buffer and taken for single-cell index sorting on a FACS ARIA III cell sorter equipped with 408, 488, 561, and 633 nm lasers (BD Biosciences) at the flow cytometry core facility at the Oslo University Hospital. Single ASCs and B cells were sorted from the same tube into separate plates (Fig. 1). The ASCs were sorted first, and other B-cell phenotypes were included on every other 96-well plate, if the number of cells was sufficient. We performed index sorting into 96-well plates (BioRad) containing 2 μL lysis buffer per well (1:20 RNase inhibitor [Clontech] in 0.2% v/v Triton X-100 [Sigma]).

Generation of scRNA-seq libraries

Plates containing sorted single cells were spun down (2500 rpm, 5 min, 4°C) and stored at −80°C or immediately processed for cDNA synthesis. cDNA synthesis was done following the Smart-Seq2 protocol [17] with minor modifications as described below. For reverse transcription, SmartScribe RT (Clontech) and corresponding buffer was used. Further, a modified TSO primer with biotinylation was introduced: Bio-AAGCAGTGGTATCAACGCAGAGTACrGrG+G. In the cDNA amplification step, ASCs underwent 21 cycles of amplification and $CD19^+$ B cells were amplified with 22 cycles. Amplified cDNA was purified with 20 μL Ampure XP (Agencourt) beads per well. Tagmentation was done using in-house made Tn5 transposase [64] dually indexed with Nextera (XT) N7xx and S5xx index primers (125 nM). Purified libraries, consisting of up to 384 cells each, were sequenced on the Illumina NextSeq500 platform at the Norwegian Sequencing Centre using 75 bp paired-end read high-output sequencing runs, resulting in approximately 1 million reads per cell.

Processing of raw sequencing data

Low-quality sequences and adapter sequences were trimmed off the raw scRNA-seq reads with Cutadapt version 1.18 [65] and Trim Galore version 0.6.1 in paired-end mode. We then quantified transcript expression using Salmon version 0.11.3 [66], building the salmon index using cDNA sequences from GRCh38.94 and a k-mer length of 25. Quantified transcripts were subsequently collapsed to gene level, and corrected for transcript length using tximport version 1.8.0 [67]. Quality control was performed in R version 3.5.3 using the scater package [68], and was based on the following measures: Number of detected genes and reads, percent mitochondrial genes, reads mapping to the reference, percent immunoglobulin genes, and successful reconstruction of at least one productively rearranged heavy-chain BCR sequence by BraCeR [18]. Library-specific threshold values are given in Supporting information Table S2.

B-cell receptor analysis

Raw reads were provided as input to BraCeR [18] in *assemble* mode to reconstruct full-length paired heavy- and light-BCR chains for each cell. We ran BraCeR assembly with--*threshold 5000* for ASCs and--*threshold 500* for B cells to filter out reconstructed BCRs likely arising from well-to-well contamination or PCR errors in indices. BraCeR yielded the full-length recombined V-region of heavy and light chains in most cells, and additionally sufficient coverage of the constant region to determine isotypes and G1m1 or G1m3 allotypes based on perfect, full-length alignment to the CH1 region of the *IGHG1* alleles.

BraCeR was subsequently used in *summarise* mode to identify clonal relationships between cells and construct lineage trees based on paired heavy and light chains. We identified clonally related B-lineage cells separately for each patient with the following parameters: *--include_multiplets --infer_lineage*. Likely cell multiplets were then manually removed as previously described [69]. All heavy- and light-chain rearrangements used in the subsequent analyses were productive.

Information regarding variable (V), diversity (D), and joining (J) gene segment usage, light chain, isotype, clonality, etc. was extracted from the summary files generated by BraCeR and used for more extensive BCR repertoire analysis using Change-O and Alakazam version 0.3.0 [70]. The number of V-segment somatic mutations was identified for the most highly expressed heavy and light chain in each cell using IMGT/HighV-QUEST [71] and normalized by the length of the V-segment of each reconstructed sequence. To remove ambiguous gene assignment of duplicated V genes, those gene segments were collapsed into newly created subgroups, for example, *IGKV1-33* and *IGKV1D-33* were collapsed into *IGKV1(D)-33*. A Circos plot, visualizing the *IGHV4:IGKV1* gene pairing frequencies, was generated using the Circos Table Viewer [72].

IGHG1 allele inference

While the G1m allotypes expressed by each patient were determined serologically, we also computationally inferred the specific *IGHG1* alleles carried by each individual using Salmon [66] and

a custom script. In short, reads from IgG1 cells were mapped to all *IGHG1* reference allele sequences obtained from IMGT, and the *IGHG1* allele with highest mapping rate to the CH1, CH2, and CH3 parts of *IGHG1* was determined as the *IGHG1* allele for each cell. Allele assignments for each cell for each patient were manually inspected, and patient-specific alleles were determined based on the most frequent allele assignments.

Gene expression analysis and phenotyping of B-lineage cells

Subsets of B-lineage cells were initially determined according to the surface expression of CD27 and CD38 measured by flow cytometry, isotype inferred by BraCeR, and somatic mutation load (Table 2). Immunoglobulin genes are frequently expressed in B-lineage cells and were discarded from the gene expression analysis before normalization to avoid masking of non-immunoglobulin-related transcriptional differences. Genes with more than three reads detected in more than five cells were retained. The gene expression matrix was subset according to cells of interest, and subsequently normalized by total reads and logarithmized as $X = \ln(X + 1)$ with scanpy version 1.4.4 [73]. We then identified highly variable genes using the highly_variable_genes function of scanpy (*min_mean = 0.1*, *max_mean = 10*, *min_disp = 0.25*). To remove batch effects and reduce patient-to-patient variation, we regressed out number of detected genes and reads, percent mitochondrial genes, and patient-specific variation, while retaining variation explained by cell type, using NaiveDE (https://github.com/Teichlab/NaiveDE) and the highly variable genes. Last, the expression matrix was scaled using sklearn (scikit-learn v0.21.3) [74]. We then used scanpy to run Principal Component Analysis of the scaled expression matrices, and visualized the populations using UMAP for dimension reduction [75]. The first 25 principal components were used for visualization of all the cells together, while only the first seven principal components were used for visualization of only the $CD19^+$ B cells. Cell cycle phase of each cell was inferred using the score_genes_cell_cycle function of scanpy using the provided regev_lab_cell_cycle_genes.txt file for specifying genes associated with the S and G2M phases.

Statistics

Statistical analysis and plots were made using R version 3.5.3 and ggpubr version 0.2.4. Somatic mutation frequencies were compared between all sequences of different isotypes or B-lineage populations using a Wilcoxon rank-sum test, while median somatic mutation frequencies for each patient were compared across B-lineage populations with a Wilcoxon signed-rank test. Frequencies of G1m1 cells were compared within ASCs and memory B cells using a binomial test. Paired *t*-test was used to analyze differences in G1m1 usage between ASCs and memory B cells and between G1m1 and G1m3 cells in G1m1/G1m3 heterozygous patients. Wilcoxon rank-sum test was used to test differences in Igκ usage for IgG1 ASCs expressing G1m1 or G1m3 and proportion of cells using *IGHV* family genes depending on the expressed G1m allotype. All tests were two-sided with a significance level of 0.05 unless otherwise stated in the figure legends. To ensure that the patient with SP-MS (MS2) and the two patients who had been previously treated with corticosteroids (MS19 and MS20) did not introduce any bias, all statistical analyses were performed with and without these three patients (Supporting information Table S4).

Acknowledgments: We would like to express our gratitude to patients who participated in this study. We thank Łukasz Wyrożemski for invaluable assistance in performing experiments. The study was funded by grants from the Norwegian Women's Public Health Association, the Norwegian Research Council (Project No. 314376), the University of Oslo World-leading research program on human immunology (WL-IMMUNOLOGY), and by Stiftelsen KG Jebsen (Project No. SKGJ-MED-017). In addition, A.L. is the recipient of Per B. Larsen's grant 2018, Odd Fellow's research Grant 2019, and the Norwegian Neurological Association research prize in multiple sclerosis 2019 provided by Sanofi Genzyme.

Conflict of interest: AL and JP are recipients of unrestricted research grants provided by Sanofi Genzyme and Novartis, respectively.

Author contributions: AL, JP, LMS, FV, and TH conceived the study and designed the experiments. AL, RH, TH, and PBH recruited patients and provided patient data. AL, IL, JP, SWQ, and FV conducted experiments. IL, JP and AL conducted data analysis. AL, IL, and JP drafted the manuscript. All authors contributed to revising the manuscript.

Peer review: The peer review history for this article is available at https://publons.com/publon/10.1002/eji.202149576.

Data availability statement: The raw scRNA-seq fastq files, reconstructed BCR sequences and accompanying metadata have been deposited at the European Genome-Phenome Archive under accession number EGAS00001005745, with controlled access.

References

1 **Kabat, E. A., Glusman, M. and Knaub, V.**, Quantitative estimation of the albumin and gamma globulin in normal and pathologic cerebrospinal fluid by immunochemical methods. *Am. J. Med.* 1948. **4**: 653–662.

2 **Stangel, M., Fredrikson, S., Meinl, E., Petzold, A., Stuve, O. and Tumani, H.**, The utility of cerebrospinal fluid analysis in patients with multiple sclerosis. *Nat. Rev. Neurol.* 2013. **9**: 267–276.

3 **Link, H. and Laurenzi, M. A.**, Immunoglobulin class and light chain type of oligoclonal bands in CSF in multiple sclerosis determined by agarose gel electrophoresis and immunofixation. *Ann. Neurol.* 1979. **6**: 107–110.

4 **Pfuhl, C., Grittner, U., Giess, R. M., Scheel, M., Behrens, J. R., Rasche, L., Pache, F. C. et al.,** Intrathecal IgM production is a strong risk factor for early conversion to multiple sclerosis. *Neurology* 2019. **93**: e1439–e1451.

5 **Obermeier, B., Mentele, R., Malotka, J., Kellermann, J., Kumpfel, T., Wekerle, H., Lottspeich, F. et al.,** Matching of oligoclonal immunoglobulin transcriptomes and proteomes of cerebrospinal fluid in multiple sclerosis. *Nat. Med.* 2008. **14**: 688–693.

6 **Obermeier, B., Lovato, L., Mentele, R., Bruck, W., Forne, I., Imhof, A., Lottspeich, F. et al.,** Related B cell clones that populate the CSF and CNS of patients with multiple sclerosis produce CSF immunoglobulin. *J. Neuroimmunol.* 2011. **233**: 245–248.

7 **Qin, Y., Duquette, P., Zhang, Y., Talbot, P., Poole, R. and Antel, J.**, Clonal expansion and somatic hypermutation of V(H) genes of B cells from cerebrospinal fluid in multiple sclerosis. *J. Clin. Invest.* 1998. **102**: 1045–1050.

8 **Owens, G. P., Bennett, J. L., Lassmann, H., O'Connor, K. C., Ritchie, A. M., Shearer, A., Lam, C. et al.,** Antibodies produced by clonally expanded plasma cells in multiple sclerosis cerebrospinal fluid. *Ann. Neurol.* 2009. **65**: 639–649.

9 **von Budingen, H. C., Kuo, T. C., Sirota, M., van Belle, C. J., Apeltsin, L., Glanville, J., Cree, B. A. et al.,** B cell exchange across the blood-brain barrier in multiple sclerosis. *J. Clin. Invest.* 2012. **122**: 4533–4543.

10 **Johansen, J. N., Vartdal, F., Desmarais, C., Tutturen, A. E., de Souza, G. A., Lossius, A. and Holmoy, T.,** Intrathecal BCR transcriptome in multiple sclerosis versus other neuroinflammation: equally diverse and compartmentalized, but more mutated, biased and overlapping with the proteome. *Clin. Immunol.* 2015. **160**: 211–225.

11 **Eggers, E. L., Michel, B. A., Wu, H., Wang, S. Z., Bevan, C. J., Abounasr, A., Pierson, N. S. et al.,** Clonal relationships of CSF B cells in treatment-naive multiple sclerosis patients. *JCI Insight* 2017. **2**: e92724.

12 **Colombo, M., Dono, M., Gazzola, P., Roncella, S., Valetto, A., Chiorazzi, N., Mancardi, G. L. et al.,** Accumulation of clonally related B lymphocytes in the cerebrospinal fluid of multiple sclerosis patients. *J. Immunol.* 2000. **164**: 2782–2789.

13 **Beltran, E., Obermeier, B., Moser, M., Coret, F., Simo-Castello, M., Bosca, I., Perez-Miralles, F. et al.,** Intrathecal somatic hypermutation of IgM in multiple sclerosis and neuroinflammation. *Brain* 2014. **137**: 2703–2714.

14 **Owens, G. P., Winges, K. M., Ritchie, A. M., Edwards, S., Burgoon, M. P., Lehnhoff, L., Nielsen, K. et al.,** VH4 gene segments dominate the intrathecal humoral immune response in multiple sclerosis. *J. Immunol.* 2007. **179**: 6343–6351.

15 **Lossius, A., Tomescu-Baciu, A., Holmoy, T., Vedeler, C. A., Rosjo, E., Lorentzen, A. R., Casetta, I. et al.,** Selective intrathecal enrichment of G1m1-positive B cells in multiple sclerosis. *Ann. Clin. Transl. Neurol.* 2017. **4**: 756–761.

16 **Tomescu-Baciu, A., Vartdal, F., Holmoy, T., Vedeler, C. A. and Lossius, A.**, G1m1 predominance of intrathecal virus-specific antibodies in multiple sclerosis. *Ann. Clin. Transl. Neurol.* 2018. **5**: 1303–1309.

17 **Picelli, S., Faridani, O. R., Bjorklund, A. K., Winberg, G., Sagasser, S. and Sandberg, R.**, Full-length RNA-seq from single cells using Smart-seq2. *Nat. Protoc.* 2014. **9**: 171–181.

18 **Lindeman, I., Emerton, G., Mamanova, L., Snir, O., Polanski, K., Qiao, S. W., Sollid, L. M. et al.,** BraCeR: B-cell-receptor reconstruction and clonality inference from single-cell RNA-seq. *Nat. Methods* 2018. **15**: 563–565.

19 **Lindeman, I., Zhou, C., Eggesbo, L. M., Miao, Z., Polak, J., Lundin, K. E. A., Jahnsen, J. et al.,** Longevity, clonal relationship, and transcriptional program of celiac disease-specific plasma cells. *J. Exp. Med.* 2021. 218.

20 **Cepok, S., Rosche, B., Grummel, V., Vogel, F., Zhou, D., Sayn, J., Sommer, N. et al.,** Short-lived plasma blasts are the main B cell effector subset during the course of multiple sclerosis. *Brain* 2005. **128**: 1667–1676.

21 **Ramesh, A., Schubert, R. D., Greenfield, A. L., Dandekar, R., Loudermilk, R., Sabatino, J. J., Jr., Koelzer, M. T. et al.,** A pathogenic and clonally expanded B cell transcriptome in active multiple sclerosis. *Proc. Natl. Acad. Sci. U. S. A.* 2020. **117**: 22932–22943.

22 **Corcione, A., Casazza, S., Ferretti, E., Giunti, D., Zappia, E., Pistorio, A., Gambini, C. et al.,** Recapitulation of B cell differentiation in the central nervous system of patients with multiple sclerosis. *Proc. Natl. Acad. Sci. U. S. A.* 2004. **101**: 11064–11069.

23 **Vartdal, F. and Vandvik, B.**, Multiple sclerosis: subclasses of intrathecally synthesized IgG and measles and varicella zoster virus IgG antibodies. *Clin. Exp. Immunol.* 1983. **54**: 641–647.

24 **Marques, C. P., Kapil, P., Hinton, D. R., Hindinger, C., Nutt, S. L., Ransohoff, R. M., Phares, T. W. et al.,** CXCR3-dependent plasma blast migration to the central nervous system during viral encephalomyelitis. *J. Virol.* 2011. **85**: 6136–6147.

25 **Probstel, A. K., Zhou, X., Baumann, R., Wischnewski, S., Kutza, M., Rojas, O. L., Sellrie, K. et al.,** Gut microbiota-specific IgA(+) B cells traffic to the CNS in active multiple sclerosis. *Sci. Immunol.* 2020. **5**: eabc7191.

26 **Fecteau, J. F., Cote, G. and Neron, S.**, A new memory CD27-IgG+ B cell population in peripheral blood expressing VH genes with low frequency of somatic mutation. *J. Immunol.* 2006. **177**: 3728–3736.

27 **Berkowska, M. A., Driessen, G. J., Bikos, V., Grosserichter-Wagener, C., Stamatopoulos, K., Cerutti, A., He, B. et al.,** Human memory B cells originate from three distinct germinal center-dependent and -independent maturation pathways. *Blood* 2011. **118**: 2150–2158.

28 **Owens, G. P., Kraus, H., Burgoon, M. P., Smith-Jensen, T., Devlin, M. E. and Gilden, D. H.**, Restricted use of VH4 germline segments in an acute multiple sclerosis brain. *Ann. Neurol.* 1998. **43**: 236–243.

29 **Tomescu-Baciu, A., Johansen, J. N., Holmoy, T., Greiff, V., Stensland, M., de Souza, G. A., Vartdal, F. et al.,** Persistence of intrathecal oligoclonal B cells and IgG in multiple sclerosis. *J. Neuroimmunol.* 2019. **333**: 576966.

30 **Chen-Bettecken, U., Wecker, E. and Schimpl, A.**, Transcriptional control of μ- and κ-Gene expression in resting and bacterial lipopolysaccharide-activated normal B cells. *Immunobiology* 1987. **174**: 162–176.

31 **Lefranc, M. P. and Lefranc, G.**, Human Gm, Km, and Am allotypes and their molecular characterization: a remarkable demonstration of polymorphism. *Methods Mol. Biol.* 2012. **882**: 635–680.

32 **DeKosky, B. J., Lungu, O. I., Park, D., Johnson, E. L., Charab, W., Chrysostomou, C., Kuroda, D. et al.,** Large-scale sequence and structural comparisons of human naive and antigen-experienced antibody repertoires. *Proc. Natl. Acad. Sci. U. S. A.* 2016. **113**: E2636–2645.

33 **Roy, B., Neumann, R. S., Snir, O., Iversen, R., Sandve, G. K., Lundin, K. E. A. and Sollid, L. M.**, High-throughput single-cell analysis of B cell receptor usage among autoantigen-specific plasma cells in celiac disease. *J. Immunol.* 2017. **199**: 782–791.

34 **Stern, J. N., Yaari, G., Vander Heiden, J. A., Church, G., Donahue, W. F., Hintzen, R. Q., Huttner, A. J. et al.,** B cells populating the multiple sclerosis brain mature in the draining cervical lymph nodes. *Sci. Transl. Med.* 2014. **6**: 248ra107.

35 **Owens, G. P., Ritchie, A. M., Burgoon, M. P., Williamson, R. A., Corboy, J. R. and Gilden, D. H.**, Single-cell repertoire analysis demonstrates that clonal expansion is a prominent feature of the B cell response in multiple sclerosis cerebrospinal fluid. *J. Immunol.* 2003. **171**: 2725–2733.

36 **Qin, Y., Duquette, P., Zhang, Y., Olek, M., Da, R. R., Richardson, J., Antel, J. P. et al.,** Intrathecal B-cell clonal expansion, an early sign of humoral immunity, in the cerebrospinal fluid of patients with clinically isolated

syndrome suggestive of multiple sclerosis. *Lab. Invest.* 2003. **83**: 1081–1088.

37 **Bennett, J. L., Haubold, K., Ritchie, A. M., Edwards, S. J., Burgoon, M., Shearer, A. J., Gilden, D. H. et al.,** CSF IgG heavy-chain bias in patients at the time of a clinically isolated syndrome. *J. Neuroimmunol.* 2008. **199**: 126–132.

38 **Cameron, E. M., Spencer, S., Lazarini, J., Harp, C. T., Ward, E. S., Burgoon, M., Owens, G. P. et al.,** Potential of a unique antibody gene signature to predict conversion to clinically definite multiple sclerosis. *J. Neuroimmunol.* 2009. **213**: 123–130.

39 **Rivas, J. R., Ireland, S. J., Chkheidze, R., Rounds, W. H., Lim, J., Johnson, J., Ramirez, D. M. et al.,** Peripheral VH4+ plasmablasts demonstrate autoreactive B cell expansion toward brain antigens in early multiple sclerosis patients. *Acta Neuropathol.* 2017. **133**: 43–60.

40 **Leurs, C. E., Twaalfhoven, H., Lissenberg-Witte, B. I., van Pesch, V., Dujmovic, I., Drulovic, J., Castellazzi, M. et al.,** Kappa free light chains is a valid tool in the diagnostics of MS: A large multicenter study. *Mult. Scler.* 2020. **26**: 912–923.

41 **Rathbone, E., Durant, L., Kinsella, J., Parker, A. R., Hassan-Smith, G., Douglas, M. R. and Curnow, S. J.,** Cerebrospinal fluid immunoglobulin light chain ratios predict disease progression in multiple sclerosis. *J. Neurol. Neurosurg. Psychiatry* 2018. **89**: 1044–1049.

42 **Di Niro, R., Mesin, L., Zheng, N. Y., Stamnaes, J., Morrissey, M., Lee, J. H., Huang, M. et al.,** High abundance of plasma cells secreting transglutaminase 2-specific IgA autoantibodies with limited somatic hypermutation in celiac disease intestinal lesions. *Nat. Med.* 2012. **18**: 441–445.

43 **Gorny, M. K., Wang, X. H., Williams, C., Volsky, B., Revesz, K., Witover, B., Burda, S. et al.,** Preferential use of the VH5-51 gene segment by the human immune response to code for antibodies against the V3 domain of HIV-1. *Mol. Immunol.* 2009. **46**: 917–926.

44 **Ekiert, D. C., Bhabha, G., Elsliger, M. A., Friesen, R. H., Jongeneelen, M., Throsby, M., Goudsmit, J. et al.,** Antibody recognition of a highly conserved influenza virus epitope. *Science* 2009. **324**: 246–251.

45 **Henry Dunand, C. J. and Wilson, P. C.,** Restricted, canonical, stereotyped and convergent immunoglobulin responses. *Philos. Trans. R. Soc. Lond. B Biol. Sci.* 2015. 370.

46 **O'Connor, K. C., Appel, H., Bregoli, L., Call, M. E., Catz, I., Chan, J. A., Moore, N. H. et al.,** Antibodies from inflamed central nervous system tissue recognize myelin oligodendrocyte glycoprotein. *J. Immunol.* 2005. **175**: 1974–1982.

47 **Kanter, J. L., Narayana, S., Ho, P. P., Catz, I., Warren, K. G., Sobel, R. A., Steinman, L. et al.,** Lipid microarrays identify key mediators of autoimmune brain inflammation. *Nat. Med.* 2006. **12**: 138–143.

48 **Cepok, S., Zhou, D., Srivastava, R., Nessler, S., Stei, S., Bussow, K., Sommer, N. et al.,** Identification of Epstein-Barr virus proteins as putative targets of the immune response in multiple sclerosis. *J. Clin. Invest.* 2005. **115**: 1352–1360.

49 **Otto, C., Oltmann, A., Stein, A., Frenzel, K., Schroeter, J., Habbel, P., Gartner, B. et al.,** Intrathecal EBV antibodies are part of the polyspecific immune response in multiple sclerosis. *Neurology* 2011. **76**: 1316–1321.

50 **Ligocki, A. J., Rivas, J. R., Rounds, W. H., Guzman, A. A., Li, M., Spadaro, M., Lahey, L. et al.,** A distinct class of antibodies may be an indicator of gray matter autoimmunity in early and established relapsing remitting multiple sclerosis patients. *ASN Neuro.* 2015. **7**: 1759091415609613.

51 **Blauth, K., Soltys, J., Matschulat, A., Reiter, C. R., Ritchie, A., Baird, N. L., Bennett, J. L. et al.,** Antibodies produced by clonally expanded plasma cells in multiple sclerosis cerebrospinal fluid cause demyelination of spinal cord explants. *Acta Neuropathol.* 2015. **130**: 765–781.

52 **Brandle, S. M., Obermeier, B., Senel, M., Bruder, J., Mentele, R., Khademi, M., Olsson, T. et al.,** Distinct oligoclonal band antibodies in multiple sclerosis recognize ubiquitous self-proteins. *Proc. Natl. Acad. Sci. U. S. A.* 2016. **113**: 7864–7869.

53 **Torres, M. and Casadevall, A.,** The immunoglobulin constant region contributes to affinity and specificity. *Trends Immunol.* 2008. **29**: 91–97.

54 **Buck, D., Albrecht, E., Aslam, M., Goris, A., Hauenstein, N., Jochim, A.,** International Multiple Sclerosis Genetics Consortium, **et al.,** Genetic variants in the immunoglobulin heavy chain locus are associated with the IgG index in multiple sclerosis. *Ann. Neurol.* 2013. **73**: 86–94.

55 **Delgado-Garcia, M., Matesanz, F., Alcina, A., Fedetz, M., Garcia-Sanchez, M. I., Ruiz-Pena, J. L., Fernandez, O. et al.,** A new risk variant for multiple sclerosis at the immunoglobulin heavy chain locus associates with intrathecal IgG, IgM index and oligoclonal bands. *Mult. Scler.* 2015. **21**: 1104–1111.

56 **Brioschi, S., Wang, W. L., Peng, V., Wang, M., Shchukina, I., Greenberg, Z. J., Bando, J. K. et al.,** Heterogeneity of meningeal B cells reveals a lymphopoietic niche at the CNS borders. *Science* 2021. **373**: eabf9277.

57 **Serafini, B., Rosicarelli, B., Magliozzi, R., Stigliano, E. and Aloisi, F.,** Detection of ectopic B-cell follicles with germinal centers in the meninges of patients with secondary progressive multiple sclerosis. *Brain Pathol.* 2004. **14**: 164–174.

58 **Absinta, M., Vuolo, L., Rao, A., Nair, G., Sati, P., Cortese, I. C., Ohayon, J. et al.,** Gadolinium-based MRI characterization of leptomeningeal inflammation in multiple sclerosis. *Neurology* 2015. **85**: 18–28.

59 **Esiri, M.,** Immunoglobulin-containing cells in multiple-sclerosis plaques. *Lancet* 1977. **310**: 478–480.

60 **Henriksson, A., Kam-Hansen, S. and Link, H.,** IgM, IgA and IgG producing cells in cerebrospinal fluid and peripheral blood in multiple sclerosis. *Clin. Exp. Immunol.* 1985. **62**: 176–184.

61 **Robasky, K., Lewis, N. E. and Church, G. M.,** The role of replicates for error mitigation in next-generation sequencing. *Nat. Rev. Genet.* 2014. **15**: 56–62.

62 **Thompson, A. J., Banwell, B. L., Barkhof, F., Carroll, W. M., Coetzee, T., Comi, G., Correale, J.** et al., Diagnosis of multiple sclerosis: 2017 revisions of the McDonald criteria. *Lancet Neurol.* 2018. **17**: 162–173.

63 **Cossarizza, A., Chang, H. D., Radbruch, A., Acs, A., Adam, D., Adam-Klages, S., Agace, W. W.** et al., Guidelines for the use of flow cytometry and cell sorting in immunological studies (second edition). *Eur. J. Immunol.* 2019. **49**: 1457–1973.

64 **Picelli, S., Bjorklund, A. K., Reinius, B., Sagasser, S., Winberg, G. and Sandberg, R.,** Tn5 transposase and tagmentation procedures for massively scaled sequencing projects. *Genome Res.* 2014. **24**: 2033–2040.

65 **Martin, M.,** Cutadapt removes adapter sequences from high-throughput sequencing reads. *EMBnet J.* 2011. **17**: 10–12.

66 **Patro, R., Duggal, G., Love, M. I., Irizarry, R. A. and Kingsford, C.,** Salmon provides fast and bias-aware quantification of transcript expression. *Nat. Methods* 2017. **14**: 417–419.

67 **Soneson, C., Love, M. I. and Robinson, M. D.,** Differential analyses for RNA-seq: transcript-level estimates improve gene-level inferences. *F1000Res* 2015. **4**: 1521.

68 **McCarthy, D. J., Campbell, K. R., Lun, A. T. and Wills, Q. F.,** Scater: pre-processing, quality control, normalization and visualization of single-cell RNA-seq data in R. *Bioinformatics* 2017. **33**: 1179–1186.

69 **Lindeman, I. and Stubbington, M. J. T.**, Antigen Receptor Sequence reconstruction and clonality inference from scRNA-Seq data. *Methods Mol. Biol.* 2019. **1935**: 223–249.

70 **Gupta, N. T., Vander Heiden, J. A., Uduman, M., Gadala-Maria, D., Yaari, G. and Kleinstein, S. H.**, Change-O: a toolkit for analyzing large-scale B cell immunoglobulin repertoire sequencing data. *Bioinformatics* 2015. **31**: 3356–3358.

71 **Brochet, X., Lefranc, M. P. and Giudicelli, V.**, IMGT/V-QUEST: the highly customized and integrated system for IG and TR standardized V-J and V-D-J sequence analysis. *Nucleic. Acids. Res.* 2008. **36**: W503–W508.

72 **Krzywinski, M., Schein, J., Birol, I., Connors, J., Gascoyne, R., Horsman, D., Jones, S. J.** et al., Circos: an information aesthetic for comparative genomics. *Genome Res.* 2009. **19**: 1639–1645.

73 **Wolf, F. A., Angerer, P. and Theis, F. J.**, SCANPY: large-scale single-cell gene expression data analysis. *Genome Biol.* 2018. **19**: 15.

74 **Pedregosa, F., Varoquaux, G., Gramfort, A., Michel, V., Thirion, B., Grisel, O., Blondel, M.** et al., Scikit-learn: machine learning in Python. *J. Mach. Learn Res.* 2011. **12**: 2825–2830.

75 **McInnes, L., Healy, J. and Melville, J.**, UMAP: Uniform Manifold Approximation and Projection for Dimension Reduction. *arXiv:1802.03426v3 [preprint]* 2018.

Abbreviations: **ASC:** antibody-secreting cells · **BCR:** B-cell receptor · **OCBs:** oligoclonal bands · **RT:** room temperature · **scRNA-seq:** single-cell RNA-sequencing · **UMAP:** Uniform Manifold Approximation and Projection

Full correspondence: Dr. Andreas Lossius, Department of Molecular Medicine, Institute of Basic Medical Sciences, University of Oslo, PO Box 1110 Blindern, 0317 Oslo, Norway.
e-mail: andreas.lossius@medisin.uio.no

Received: 12/8/2021
Revised: 19/11/2021
Accepted: 10/1/2022
Accepted article online: 29/1/2022

Stereotyped B-cell responses are linked to IgG constant region polymorphisms in multiple sclerosis (Lindeman *et al.*)

Supporting information

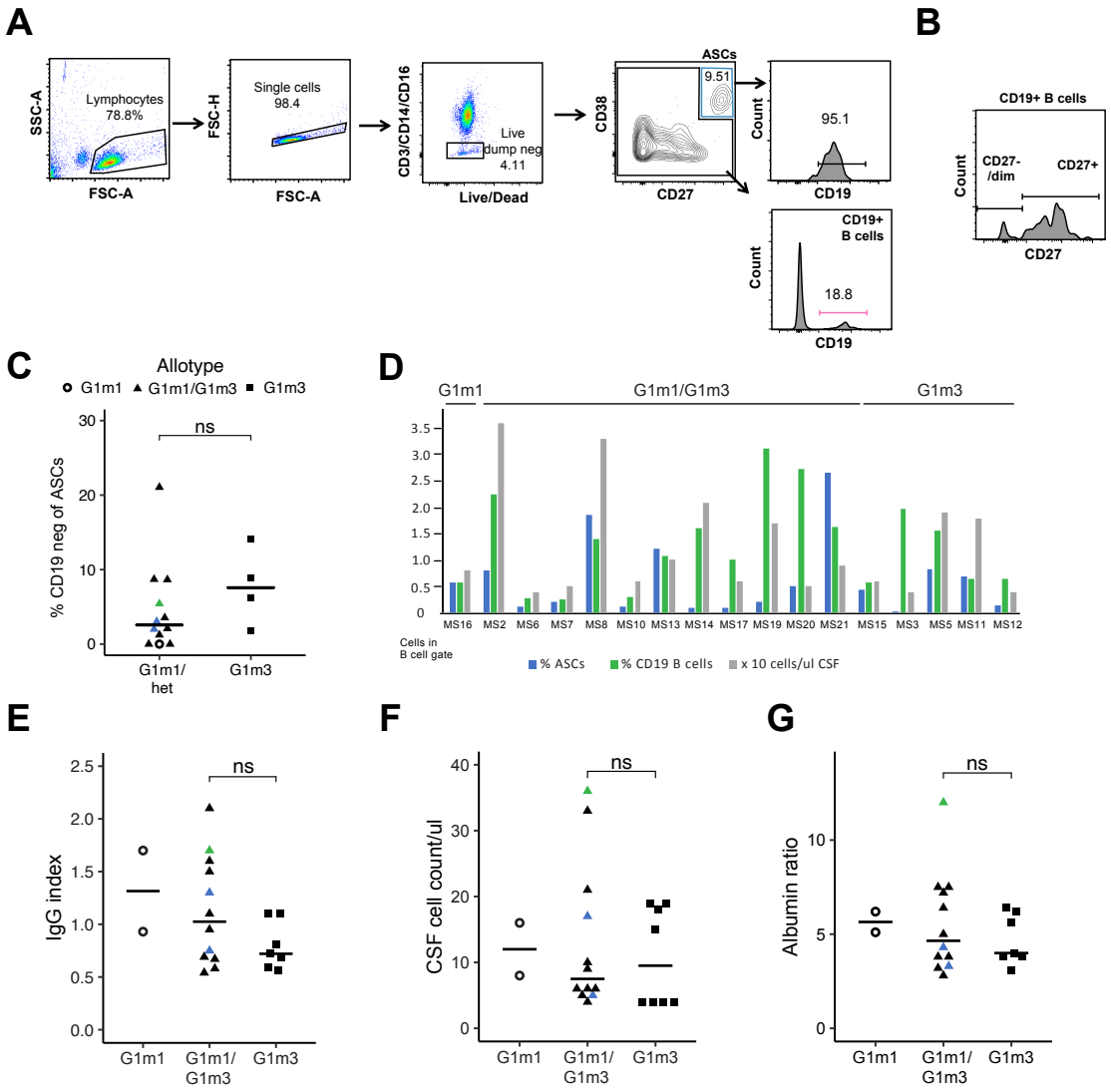

Supplementary Figure 1. Analysis of intrathecal B-lineage cells and related parameters. (A) Representative flow cytometry gating strategy for one patient showing sorting and analysis gates. (B) Representative flow cytometry gating strategy for one patient showing gating of index-sorted CD19^{+} B cells into CD27^{+} and CD27$^{-/dim}$ populations. (C) Percent of ASCs being CD19 negative according to flow cytometry analysis. Data for all patients with a substantial number of recorded events are summarized (n=17). The patient with SP-MS is indicated in green, while the two patients previously treated with corticosteroids are indicated in blue. Differences between patient groups were tested using an unpaired t-test. (D) Percent ASCs and CD19^{+} B cells according to flow cytometry analysis for all patients with a substantial number of recorded events (n=17). CSF cell count is displayed in gray. (E), (F), (G) IgG index (E), CSF cell count (F) and albumin ratio (G) for included patients, stratified by patient allotype. Differences between G1m1/G1m3 heterozygotes and G1m3 homozygotes were tested using unpaired t-tests. Ns = p>0.05.

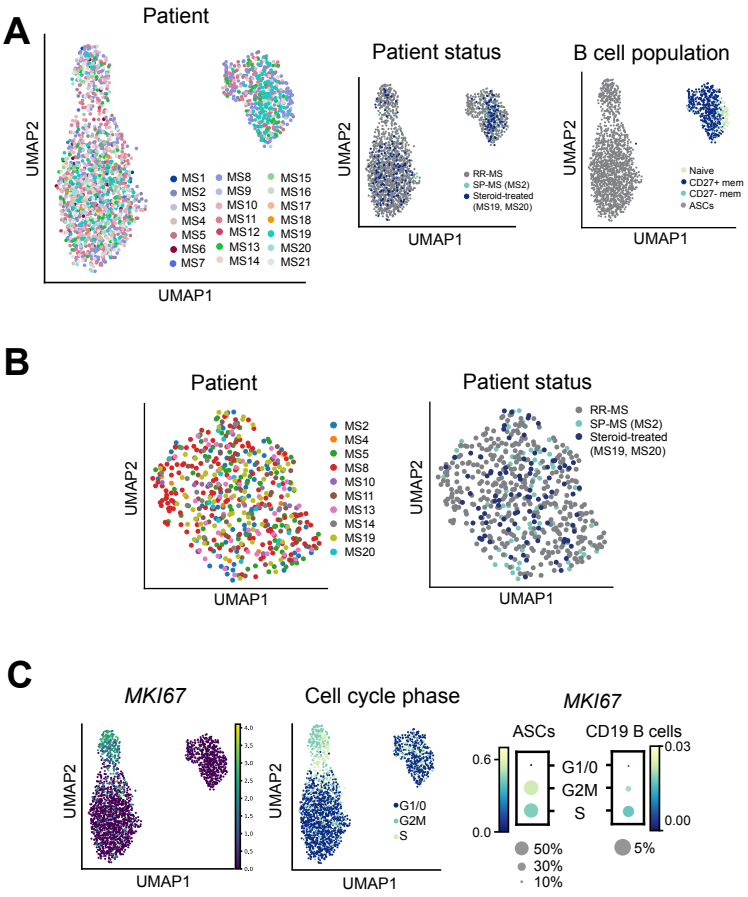

Supplementary Figure 2. The transcriptional profile of B-lineage cells from the CSF of 21 MS patients were visualized using UMAP as in Figure 2B. (A) UMAP projection of all B-lineage cells (2165 cells) from all 21 patients, colored by patient, patient status and B-cell population. (B) UMAP projection of all CD19^{+} B-lineage cells (544 cells) from all 10 patients for which this cell population was sorted, colored by patient and patient status. (C) UMAP projections as in (A), colored by *MKI67* expression (left) and inferred cell cycle (right) without using *MKI67* in the list of proliferation-associated genes. Dot plots show expression of *MKI67* in ASCs and CD19^{+} B cells according to the cell cycle phases shown in the UMAP plot.

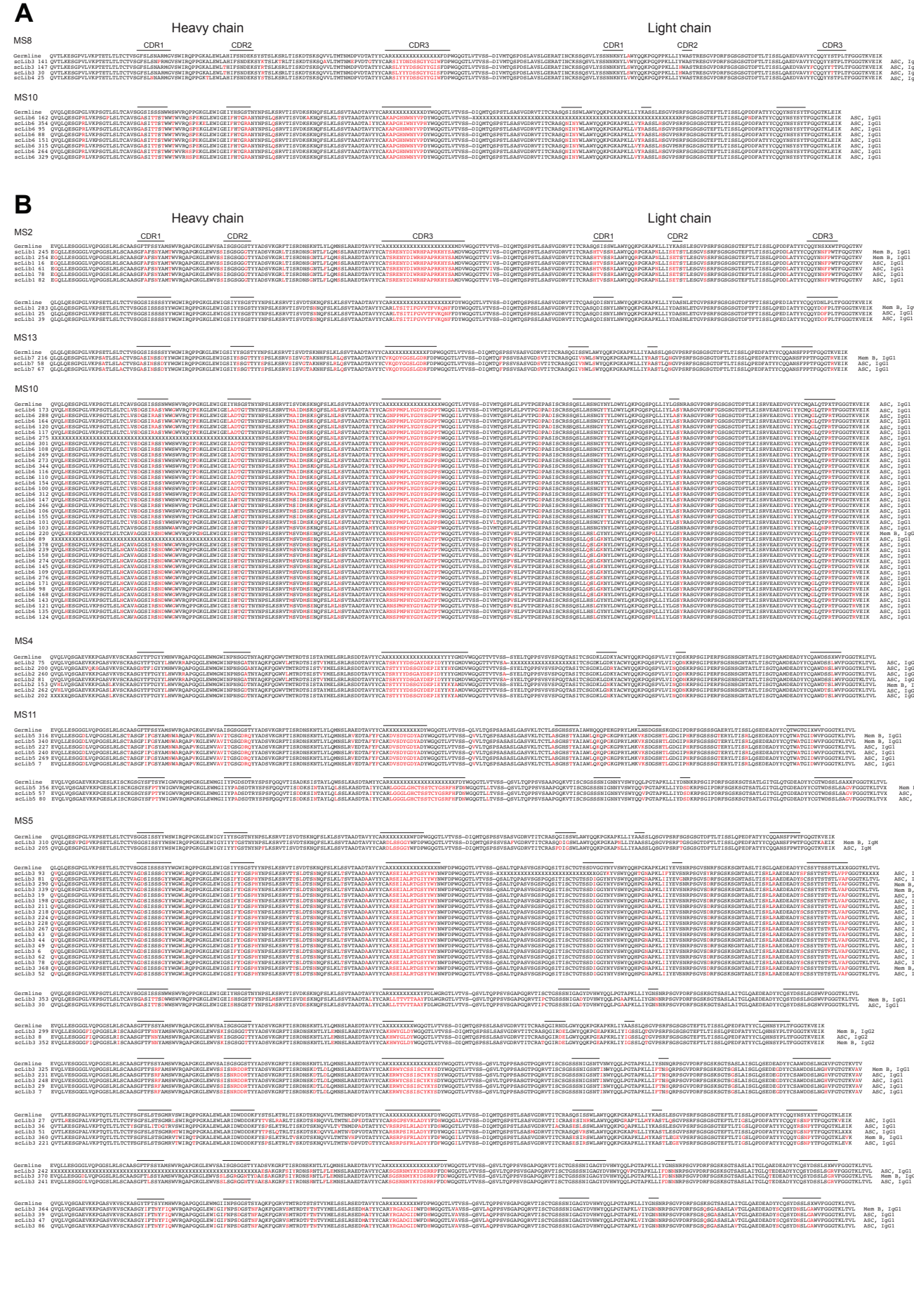
A
Heavy chain
Light chain
MS8
CDR1
CDR2
CDR3
CDR1
CDR2
CDR3
MS10
B
Heavy chain
Light chain
MS2
CDR1
CDR2
CDR3
CDR1
CDR2
CDR3
MS13
MS10
MS4
MS11
MS5

B cont.

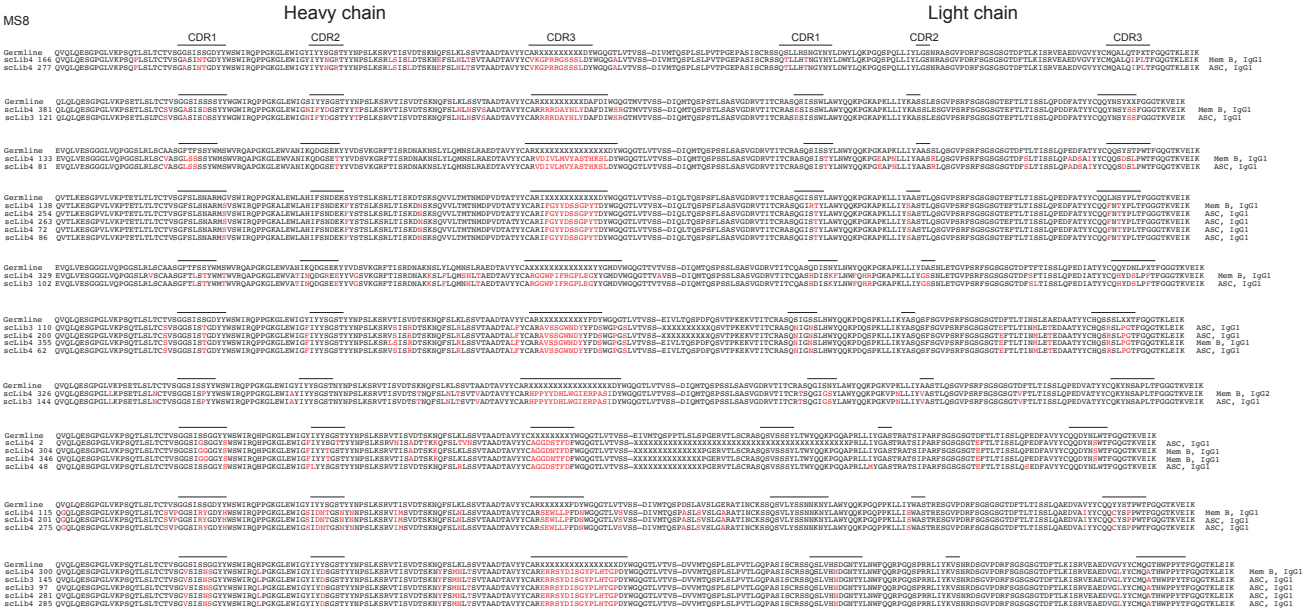

Supplementary Figure 3. Alignment of paired heavy- and light-chain amino acid sequences depicted as lineage trees in the main Figure 3C and D. The amino acid sequences were deduced from nucleotide sequences obtained from Smart-Seq2 and analysis with BraCeR. Germline-encoded amino acids are shown in black letters. Amino acids that were introduced by somatic mutations or comprise the NDN nucleotides (added nucleotides flanking the D gene segment) of the CDR3 are shown in red letters. (A) Alignment of paired heavy- and light-chains of the representative lineage trees in Figure 3C. (B) Alignment of paired heavy- and light-chains of clones comprising both memory B cells and antibody-secreting cells (ASCs) depicted as lineage trees in Figure 3D.

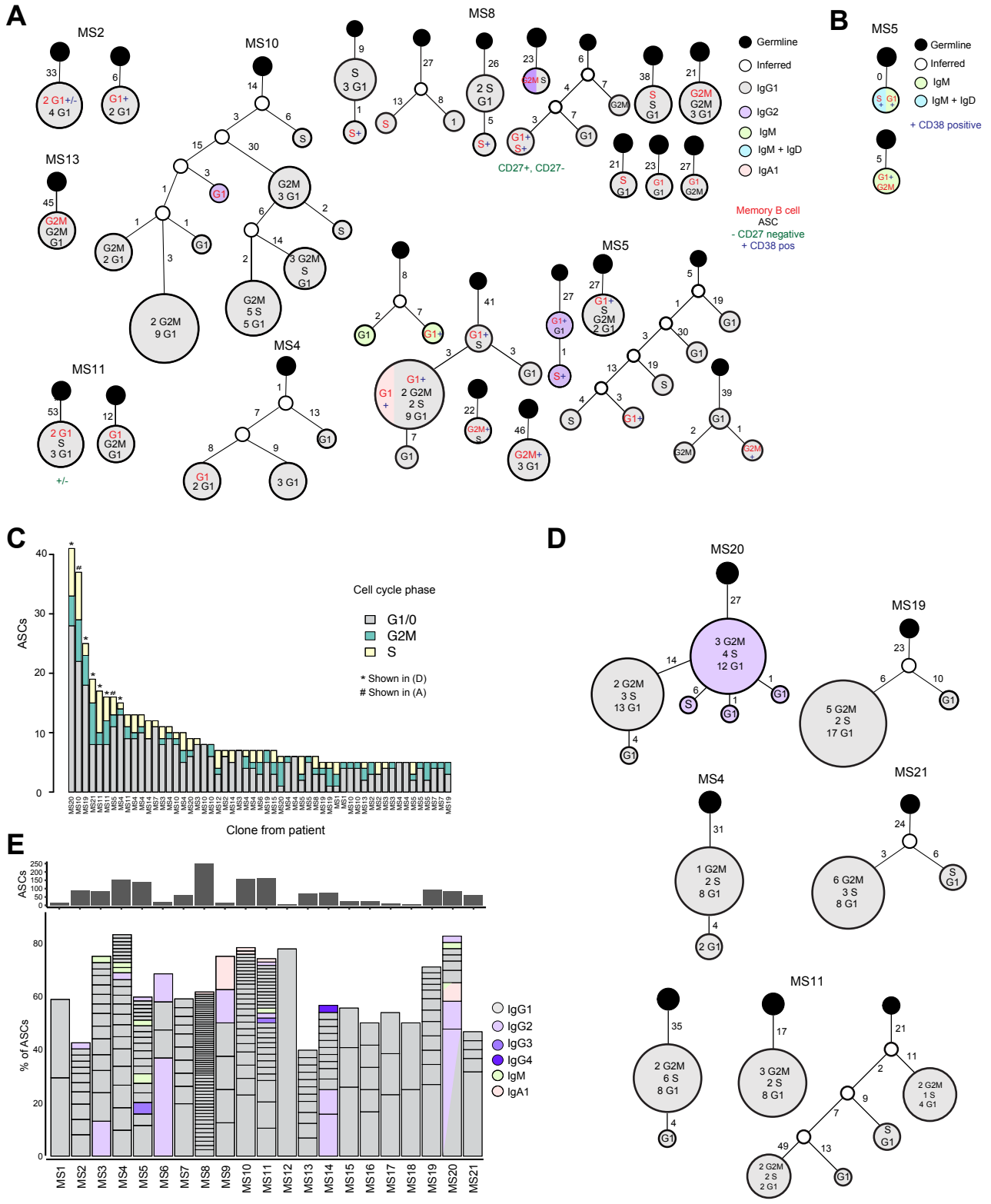

Supplementary Figure 4. Clonal connections across cell cycle stages and isotypes. (A) Lineage trees consisting of ASCs and memory B cells with annotated cell cycle stage and CD38 and CD27 cell surface expression. (B) Lineage trees restricted to memory B cells with annotated cell cycle stage and surface expression of CD38 and CD27. (C) Cell cycle stage of largest expanded clone groups. (D) Lineage trees for largest expanded clone groups. (E) Isotype of clone groups determined by BraCeR.

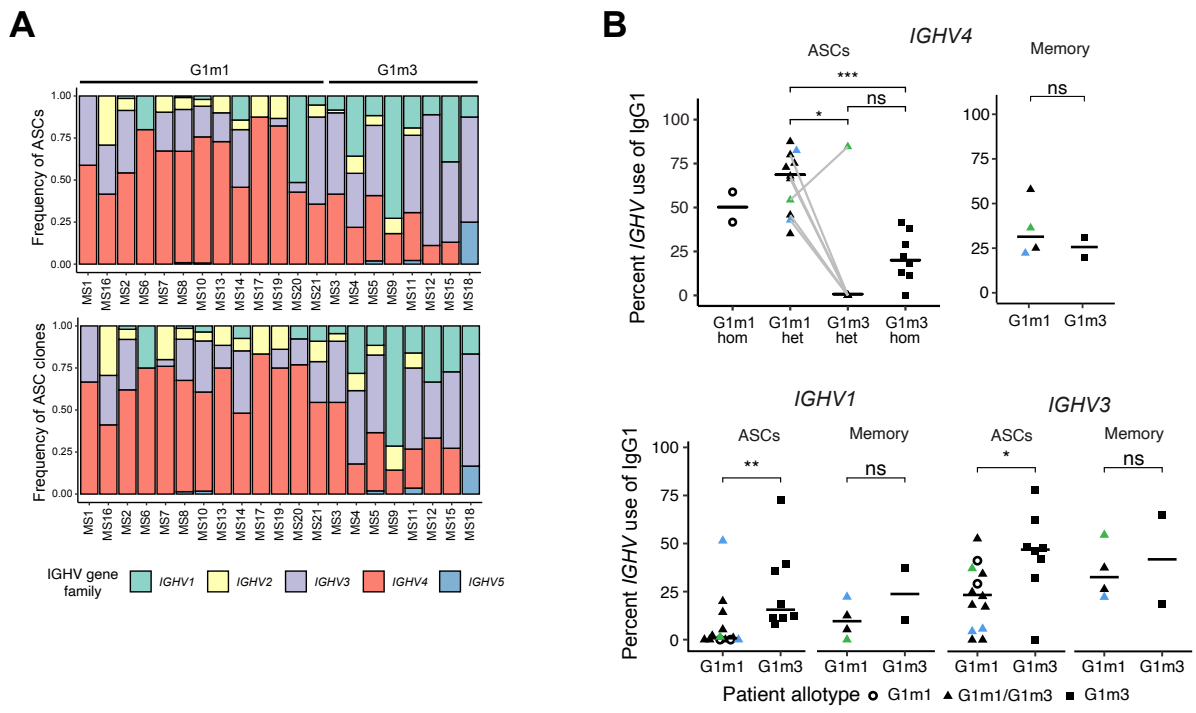

Supplementary Figure 5. *IGHV* gene usage in B-lineage cells from the cerebrospinal fluid. (A) *IGHV* gene family usage in ASCs in each patient, grouped by G1m1 carrier status. (B) *IGHV4* gene family usage in ASCs for G1m1 cells coming from homozygous or heterozygous patients and G1m3 cells from homozygous or heterozygous patients (upper left) and for memory B cells (upper right). Lower panel shows *IGHV1* and *IGHV3* gene family usage in G1m1 and G1m3 ASCs and memory B cells. Each dot represents a patient; horizontal line is median for all patients in the given group. Lines connect G1m1 and G1m3 ASCs from the same patient. Two of the heterozygous patients had no ASCs expressing G1m3. The patient with SP-MS is indicated in green, while the two patients previously treated with corticosteroids are indicated in blue. Statistical differences were tested using paired t-test (G1m1 versus G1m3 cells from heterozygotes) and Wilcoxon rank-sum test for unpaired data (G1m1 cells from heterozygous patients versus G1m3 cells from homozygous) with p-value significance levels *: $p<0.05$; **: $p<0.01$; ***: $p<0.001$; ns: $p>0.05$.

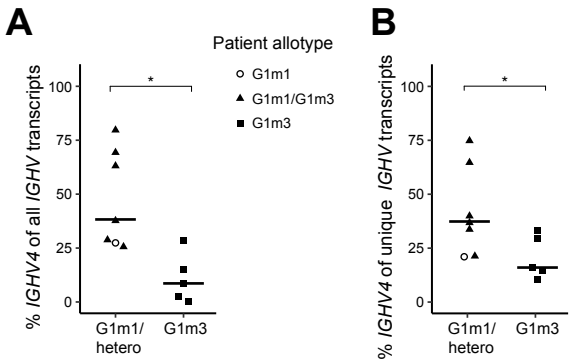

Supplementary Figure 6. A reanalysis of previously published bulk RNA-seq data of *IGHV* genes from unsorted IgG B cells [1, 2] according to the presence (n=7) or absence (n=5) of the G1m1 allotype determined by serotyping. The sequences were analyzed using the total *IGHV* transcript pool (A) and unique *IGHV* transcripts (B). The differences between the groups were compared using Wilcoxon rank-sum test with p-value significance levels *: $p<0.05$.

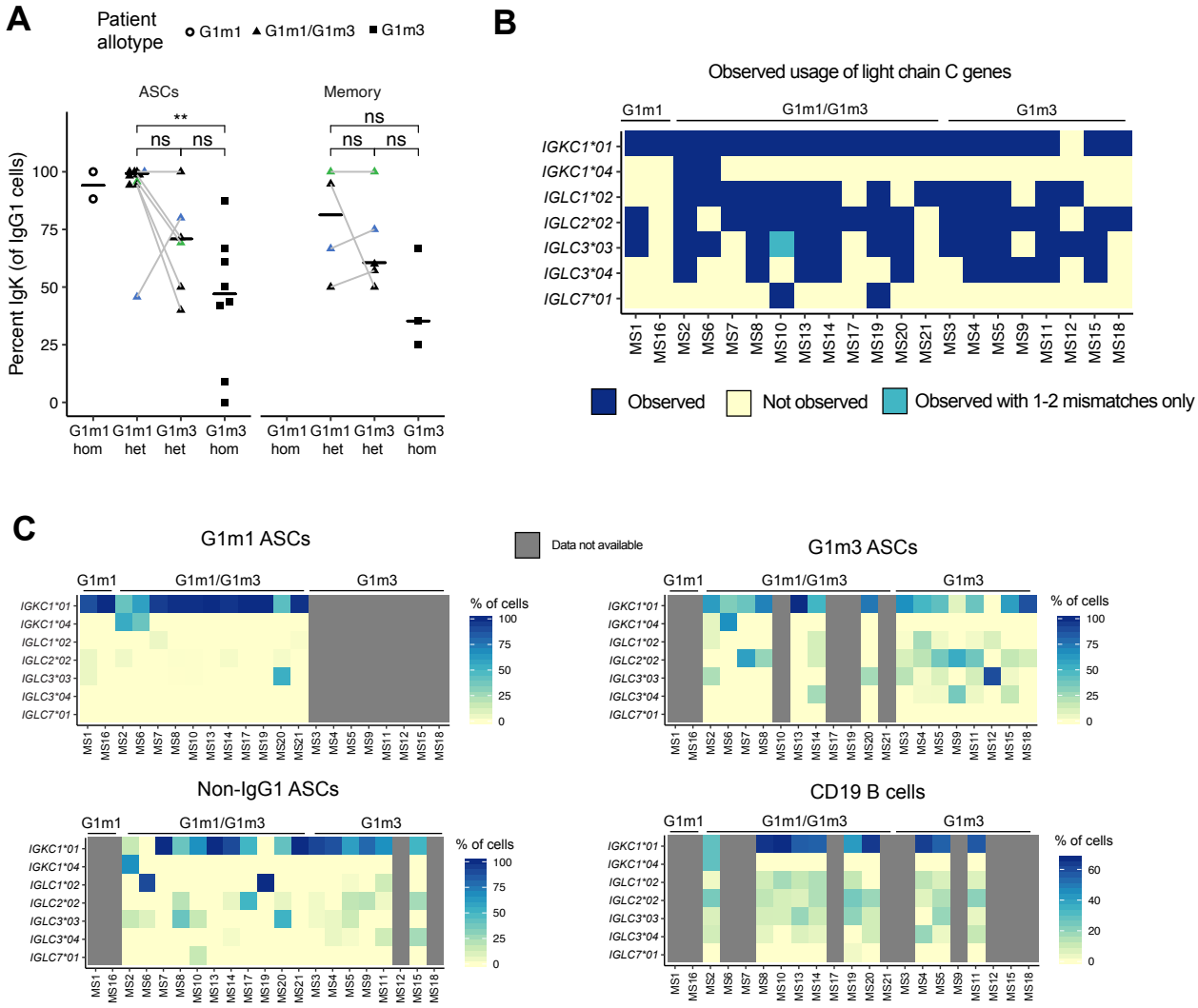

Supplementary Figure 7. Light chain constant gene usage in B-lineage cells from the cerebrospinal fluid. (A) Frequency of ASCs and memory B cells using κ light chain for each patient, grouped by patient allotype. Each dot represents a patient; cell populations from the same patients are connected by a line. The patient with SP-MS is indicated in green, while the two patients previously treated with corticosteroids are indicated in blue. Statistical differences between G1m1 and G1m3 cells from heterozygotes were tested using a paired t-test. Differences between G1m1 cells from heterozygous patients and G1m3 cells from homozygous patients were compared by Wilcoxon rank-sum test. The indicated p-value significance levels are: **: $p<0.01$; ns>0.05. Data points based on fewer than two cells were excluded from the analysis. (B) Observed usage (presence or absence in at least one B-lineage cell) of specific Ig light chain constant region genes and alleles in each patient. Constant region reconstructed by BraCeR was compared to germline reference sequences to determine perfect, full-length matches to each allele. (C) Frequency of usage of specific Ig light chain constant region genes and alleles in each patient, stratified by allotype, isotype and cell population.

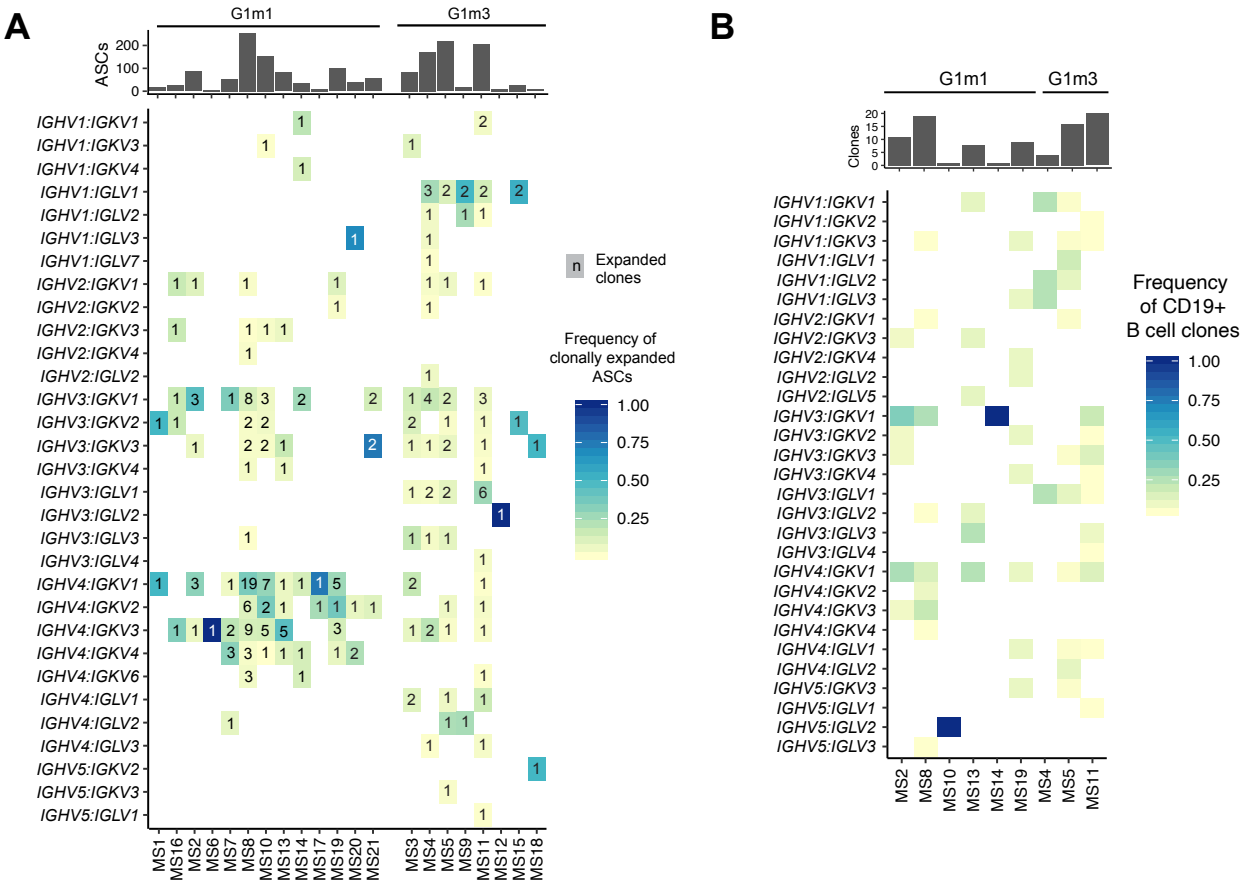

Supplementary Figure 8. The V_H:V_L pairing in expanded ASCs and memory B cells. (A) Heatmap showing V_H:V_L gene segment pairing frequencies for clonally expanded G1m1 and G1m3 ASCs only. The numbers within each square indicate the number of clone groups using each gene combination, while the color represents frequency of total number of clonally expanded ASCs. (B) Heatmap showing V_H:V_L gene segment pairing frequencies for G1m1 and G1m3 memory B cells. Cells belonging to a clone group are treated as one cell.

Supplementary Table 1. Excluded patients.

ID	Sex	Age	Diagnosis	Disease duration (months)	Relapses	Months since last relapse	CSF cell count[A]	OCB[B]	Albumin ratio	IgG index	Allotype[C]	Reason for exclusion
MS22	F	42	RR-MS	12	1	12	4	+	6.6	0.64	G1m3	Few sorted cells (8 ASCs)
MS23	M	27	RR-MS	2	1	2	4	-	9.0	0.53	G1m1/G1m3	No OCBs; few sorted cells (2 ASCs)
MS24	F	38	Clinically isolated syndrome	168	1	168	4	-	6.6	0.58	G1m1	No OCBs; few sorted cells (2 ASCs)

F-female; M-male; RR-MS – relapsing-remitting multiple sclerosis; ND – not determined.
[A]mononuclear cells count per microliter of CSF
[B]positive (+) or negative (-) for more than 2 CSF restricted oligoclonal bands on isoelectric focusing
[C]determined in serum

Supplementary Table 2. Library-specific threshold values for quality control (QC) of scRNA-seq data.

Library	Subjects	Cell type	Min. reads	Max. reads	Min. genes	Max. genes	% mapped reads	% Ig reads	% mt reads	BCR	Total cells	QC pass
scLib1	MS1	ASC	$1x10^5$	$2.5x10^6$	1000	5800	>40	>10	<8	Productive IgH	29	17
	MS2	B						<10			93	71
		ASC						>10			96	89
	MS3	ASC						>10			96	84
scLib2	MS4	B	$1x10^5$	$1.2x10^6$	1200	5100	>40	<10	<8	Productive IgH	96	17
		ASC						>10			192	154
	MS7	ASC									77	61
	MS9	ASC									19	16
scLib3	MS5	B	$1x10^5$	$1.8x10^6$	1000	6100	>40	<10	<8	Productive IgH	90	81
		ASC						>10			167	139
	MS6	ASC									22	19
	MS8	ASC									96	79
scLib4	MS8	B	$1.5x10^5$	$1.9x10^6$	1000	6200	>40	<10	<8	Productive IgH	192	159
		ASC						>10			192	171
scLib5	MS11	B	$1.5x10^5$	$1.1x10^6$	1000	6000	>40	<10	<8	Productive IgH	80	45
		ASC						>10			192	162
scLib6	MS10	B	$1.5x10^5$	$2x10^6$	1000	5800	>40	<10	<8	Productive IgH	70	12
		ASC						>10			208	161
scLib7	MS12	ASC	$1.5x10^5$	$2.7x10^6$	1000	6000	>40	>10	<8	Productive IgH	14	9
	MS13	B						<10			96	47
		ASC						>10			103	73
	MS14	B						<10			44	22
		ASC						>10			96	76
scLib8	MS16	ASC	$1.5x10^5$	$2.7x10^6$	800	6000	>40	>10	<8	Productive IgH	34	24
	MS20	ASC						>10			96	86
		B						<10			96	16
scLib9	MS15	ASC	$1.5x10^5$	$2.7x10^6$	1000	6000	>40	>10	<8	Productive IgH	31	27
	MS17	ASC									18	13
	MS18	ASC									8	8
	MS19	ASC									96	93
		B						<10			112	74
	MS21	ASC						>10			88	60
Total											**3052**	**2165**

IgH = immunoglobulin heavy chain, mt = mitochondrial.

Supplementary Table 3. Number of analyzed cells from CSF B-cell populations.

	B-cell subsets						
			Memory				
Subject ID	Antibody secreting cells	Naïve	Non-switched $CD27^{-/dim}$	Non-switched $CD27^{+}$	Switched $CD27^{-/dim}$	Switched $CD27^{+}$	Unclassified
MS1	17	-	-	-	-	-	-
MS2	89	3	3	24	3	38	-
MS3	84	-	-	-	-	-	-
MS4	154	4	1	5	0	7	-
MS5	139	4	2	33	1	41	-
MS6	19	-	-	-	-	-	-
MS7	61	-	-	-	-	-	-
MS8	250	55	6	49	7	40	2
MS9	16	-	-	-	-	-	-
MS10	161	2	-	3	1	6	-
MS11	162	2	-	14	2	27	-
MS12	9	-	-	-	-	-	-
MS13	73	1	2	18	2	24	-
MS14	76	5	2	5	-	9	1
MS15	27	-	-	-	-	-	-
MS16	24	-	-	-	-	-	-
MS17	13	-	-	-	-	-	-
MS18	8	-	-	-	-	-	-
MS19	93	8	3	17	3	43	-
MS20	86	1	2	9	0	4	
MS21	60	-	-	-	-	-	-
Total	**1621**	**85**	**21**	**177**	**19**	**239**	**3**

Supplementary Table 4. Results from statistical tests performed with and without MS2, MS19 and MS20.

Figure	Subpanel	Populations	p-value all patients	p-value without MS2, MS19 and MS20	Statistical test
2A		Naive vs CD27+ mem	0.000011	0.00058	Unpaired wilcoxon
2A		Naive vs CD27- mem	0.71	0.41	Unpaired wilcoxon
2A		CD27+ mem vs CD27- mem	0.000011	0.00058	Unpaired wilcoxon
2A		Sw vs un-sw CD27+	0.13	0.039	Paired t-test
2A		Sw CD27+ vs sw CD27-	0.0000012	0.000028	Paired t-test
2A		Sw CD27+ vs un-sw CD27-	0.0000042	0.00011	Paired t-test
2A		Sw CD27- vs un-sw CD27-	0.43	0.78	Paired t-test
2F	ASCs	IgM vs IgG1	1.1E-14	3.7E-13	Paired t-test
2F	ASCs	IgG1 vs IgG2	9.6E-10	5.6E-09	Paired t-test
2F	ASCs	IgA1 vs IgA2	0.077	0.13	Paired t-test
2F	Memory	IgM vs IgG1	0.39	0.67	Paired t-test
2F	Memory	IgG1 vs IgG2	0.0037	0.014	Paired t-test
2F	Memory	IgA1 vs IgA2	0.10	0.40	Paired t-test
2H	Top	CD27- mem vs CD27+ mem	0.0000088	0.0011	Unpaired wilcoxon
2H	Top	CD27+ mem vs ASCs	0.0000068	0.00000030	Unpaired wilcoxon
2H	Top	CD27- mem vs ASCs	2.4E-12	0.000000037	Unpaired wilcoxon
2H	Bottom	CD27- mem vs CD27+ mem	0.0078	0.062	Paired wilcoxon
2H	Bottom	CD27+ mem vs ASCs	0.084	0.22	Paired wilcoxon
2H	Bottom	CD27- mem vs ASCs	0.016	0.13	Paired wilcoxon
2I	ASCs	IgM vs IgG1	0.11	0.021	Unpaired wilcoxon
2I	ASCs	IgG1 vs IgG2	0.24	0.23	Unpaired wilcoxon
2I	ASCs	IgG1 vs IgA1	1	0.54	Unpaired wilcoxon
2I	CD27+	IgM vs IgG1	0.00058	0.0087	Unpaired wilcoxon
2I	CD27+	IgG1 vs IgG2	0.75	0.76	Unpaired wilcoxon
2I	CD27+	IgG1 vs IgA1	0.75	0.35	Unpaired wilcoxon
2I	CD27+	IgA1 vs IgA2	0.91	0.53	Unpaired wilcoxon
2I	CD27-	IgM vs IgG1	0.14	0.20	Unpaired wilcoxon
2J	ASCs	IgM vs IgG1	9.0E-07	1.2E-07	Unpaired wilcoxon
2J	ASCs	IgG1 vs IgG2	0.0046	0.11	Unpaired wilcoxon
2J	ASCs	IgG1 vs IgA1	0.031	0.0012	Unpaired wilcoxon
2J	CD27+	IgM vs IgG1	4.6E-16	9.4E-14	Unpaired wilcoxon
2J	CD27+	IgG1 vs IgG2	0.69	0.91	Unpaired wilcoxon
2J	CD27+	IgG1 vs IgA1	0.86	0.49	Unpaired wilcoxon
2J	CD27+	IgA1 vs IgA2	0.99	0.68	Unpaired wilcoxon
4A		Mem B	0.11	0.25	One-sided binomial
4A		ASCs	0.00050	0.0040	One-sided binomial
4A		Mem B vs ASCs	0.011	0.0093	Paired t-test
5A		G1m1 vs G1m3	0.00021	0.00016	Unpaired wilcoxon
5B		G1m1 vs G1m3	0.00054	0.00042	Unpaired wilcoxon
S1C		G1m1/het vs G1m3	0.35	0.45	Unpaired t-test
S1E		G1m1/G1m3 vs G1m3	0.072	0.18	Unpaired t-test
S1F		G1m1/G1m3 vs G1m3	0.52	0.85	Unpaired t-test
S1G		G1m1/G1m3 vs G1m3	0.36	0.52	Unpaired t-test
S5B	Upper left	G1m1 het vs G1m3 het	0.038	0.0028	Paired t-test
S5B	Upper left	G1m3 het vs G1m3 hom	0.081	0.017	Unpaired wilcoxon
S5B	Upper left	G1m1 het vs G1m3 hom	0.00032	0.0019	Unpaired wilcoxon
S5B	Upper right	G1m1 vs G1m3	0.53	0.67	Unpaired wilcoxon
S5B	Lower left	ASCs (G1m1 vs G1m3)	0.0093	0.0062	Unpaired wilcoxon
S5B	Lower left	Memory (G1m1 vs G1m3)	0.53	0.67	Unpaired wilcoxon
S5B	Lower right	ASCs (G1m1 vs G1m3)	0.022	0.036	Unpaired wilcoxon
S5B	Lower right	Memory (G1m1 vs G1m3)	1	1	Unpaired wilcoxon
S7A	ASCs	G1m1 het vs G1m3 het	0.20	0.077	Paired t-test
S7A	ASCs	G1m3 het vs G1m3 hom	0.18	0.46	Unpaired wilcoxon
S7A	ASCs	G1m1 het vs G1m3 hom	0.0032	0.0027	Unpaired wilcoxon
S7A	Memory	G1m1 het vs G1m3 het	0.60	0.60	Paired t-test
S7A	Memory	G1m3 het vs G1m3 hom	0.5	1	Unpaired wilcoxon
S7A	Memory	G1m1 het vs G1m3 hom	0.46	1	Unpaired wilcoxon

Supplementary Table 5. Clonal expansion of antibody-secreting cells

				Lineage tracing				
Patient ID	% clonal cells	Size of clonotypes	Expanded clonotypes	Lineage trees	Unique sequences per tree	Clonotype size	SHM (range) within tree	Isotype
MS1	58.8	5	2	0	-	-	-	-
MS2	42.5	2-7	12	1	2	5	44-50	IgG1
MS3	75.0	2-11	14	5	3	9	35-49	IgG1
					2	3	27-31	IgG1
					3	5	23-25	IgG1
					2	11	47-50	IgG2
					2	4	19-22	IgG1
MS4	83.1	2-15	23	3	3	6	14-17	IgG1
					2	2	23-26	IgG1
					2	13	31-35	IgG1
MS5	59.7	2-16	20	7	4	16	44-51	IgG1
					3	5	12-22	IgM
					3	3	47-58	IgG1
					4	4	24-37	IgG1
					3	6	56-59	IgG1
					2	2	39-41	IgG1
					4	6	42-46	IgG3
MS6	68.4	2-7	4	2	2	2	50-53	IgG1
					2	2	36-41	IgG2
MS7	65.6	2-12	10	4	2	2	32-33	IgG1
					2	3	68-75	IgG1
					3	5	29-33	IgG1
					2	5	36-40	IgG1
MS8	61.6	2-6	61	28	2	2	32-34	IgG1
					2	2	21-32	IgG1
					2	2	25-45	IgG1
					2	3	22-23	IgG1
					2	2	31-32	IgG1
					3	4	4-15	IgG1
					2	1	27-34	IgG1
					2	2	26-31	IgG1
					2	2	29-30	IgG1
					2	2	23-24	IgG1
					2	2	18	IgG1
					2	3	20-24	IgG1
					2	2	17-18	IgG1
					2	2	24-27	IgG1
					2	2	29-32	IgG1
					2	2	36-37	IgG1
					2	2	18-22	IgG1,IgM
					3	3	34-41	IgG1
					2	2	26-28	IgG1
					2	2	27-28	IgG1
					2	2	15-21	IgG1
					2	2	39-42	IgG1
					2	2	14-20	IgG1
					2	3	28-29	IgG1
					2	2	11-19	IgG1
					2	4	22-27	IgG1
					2	2	16-20	IgG1
					2	2	19	IgG1
MS9	75.0	2	6	2	2	2	52	IgA1

					2	2	21-29	IgG1
MS10	78.3	2-37	26	16	8	37	20-67	IgG1
					3	4	19-28	IgG1
					3	4	26-38	IgG1
					2	2	33-65	IgA1
					5	5	15-21	IgG1
					2	2	20-27	IgG1
					2	2	74-94	IgA1
					5	8	33-39	IgG1
					2	2	14-15	IgG1
					3	3	19-21	IgG1
					2	2	23-28	IgG1
					2	8	26-29	IgG1
					2	10	33-34	IgG1
					2	3	19-21	IgG1
					2	2	26-31	IgG1
					2	2	40-46	IgG1
MS11	74.1	2-17	31	11	2	2	28-32	IgG1
					4	16	32-79	IgG1
					2	4	38-45	IgG1
					2	2	46-49	IgG1
					2	2	27-28	IgG1
					2	2	32	IgG1
					2	3	22-32	IgG1
					2	3	22-27	IgG1
					2	17	35-39	IgG1
					2	2	59-60	IgA1
					2	2	18-19	IgG1
MS12	77.8	7	1	0	-	-	-	-
MS13	39.7	2-5	11	3	2	5	11-27	IgG1
					2	4	23-24	IgG1
					2	3	42-46	IgG1
MS14	56.6	2-12	13	3	2	2	36-44	IgG1
					2	2	41-51	IgG1
					2	12	19-24	IgG2
MS15	55.6	4-7	3	2	2	4	30-31	IgG1
					4	7	25-30	IgG1
MS16	50.0	2-4	5	0	-	-	-	-
MS17	53.8	2-3	3	1	2	2	18	IgG1
MS18	50.0	2	2	0	-	-	-	-
MS19	71.0	2-25	12	5	2	5	21-25	IgG1
					2	25	29-33	IgG1
					3	4	39-48	IgG1
					2	6	29-32	IgG1
					2	4	33	IgG1
MS20	82.6	2-41	9	3	6	41	27-45	IgG1,IgG2
					3	6	16-19	IgA1,IgM
					2	4	27-33	IgG1
MS21	46.7	2-19	5	2	2	2	31-35	IgG1
					2	19	27-30	IgG1

Percent clonal cells refers to the ASCs population. Number of cells detected in the smallest and largest expanded clone groups are specified as size of clonotypes. Lineage trees were created for clones comprising cells with different mutation patterns. SHM was calculated as number of mutations in heavy and light chain compared to inferred IMGT germline sequences.

Supplementary Table 6. Number of analyzed G1m1 and G1m3 cells for each patient.

	Antibody-secreting cells		Memory B cells		Patient allotype
Subject ID	G1m1	G1m3	G1m1	G1m3	
MS1	17	0	-	-	G1m1
MS2	69	13	14	2	G1m1/G1m3
MS3	0	60	-	-	G1m3
MS4	0	137	0	4	G1m3
MS5	0	106	0	17	G1m3
MS6	6	3	-	-	G1m1/G1m3
MS7	53	5	-	-	G1m1/G1m3
MS8	225	5	16	8	G1m1/G1m3
MS9	0	11	-	-	G1m3
MS10	145	0	2	1	G1m1/G1m3
MS11	0	140	0	21	G1m3
MS12	0	9	-	-	G1m3
MS13	70	0	9	7	G1m1/G1m3
MS14	34	9	1	5	G1m1/G1m3
MS15	0	23	-	-	G1m3
MS16	24	0	-	-	G1m1
MS17	11	0	-	-	G1m1/G1m3
MS18	0	8	-	-	G1m3
MS19	92	0	9	7	G1m1/G1m3
MS20	38	5	0	1	G1m1/G1m3
MS21	58	0	-	-	G1m1/G1m3
Total	**842**	**534**	**51**	**73**	

Supplementary references

1 **Johansen, J. N., Vartdal, F., Desmarais, C., Tutturen, A. E., de Souza, G. A., Lossius, A. and Holmoy, T.,** Intrathecal BCR transcriptome in multiple sclerosis versus other neuroinflammation: Equally diverse and compartmentalized, but more mutated, biased and overlapping with the proteome. *Clin. Immunol.* 2015. **160**: 211-225.

2 **Tomescu-Baciu, A., Johansen, J. N., Holmoy, T., Greiff, V., Stensland, M., de Souza, G. A., Vartdal, F. et al,** Persistence of intrathecal oligoclonal B cells and IgG in multiple sclerosis. *J. Neuroimmunol.* 2019. **333**: 576966.

II

frontiers | Frontiers in Cellular Neuroscience

TYPE Brief Research Report
PUBLISHED 08 June 2023
DOI 10.3389/fncel.2023.1189709

OPEN ACCESS

EDITED BY
Olga Rojas,
University Health Network (UHN), Canada

REVIEWED BY
Pentti Tienari,
University of Helsinki, Finland
Fernanda Marques,
University of Minho, Portugal

*CORRESPONDENCE
Andreas Lossius
✉ andreas.lossius@medisin.uio.no

RECEIVED 19 March 2023
ACCEPTED 19 May 2023
PUBLISHED 08 June 2023

CITATION
Polak J, Wagnerberger JH, Torsetnes SB, Lindeman I, Høglund RAA, Vartdal F, Sollid LM and Lossius A (2023) Single-cell transcriptomics combined with proteomics of intrathecal IgG reveal transcriptional heterogeneity of oligoclonal IgG-secreting cells in multiple sclerosis.
Front. Cell. Neurosci. 17:1189709.
doi: 10.3389/fncel.2023.1189709

Single-cell transcriptomics combined with proteomics of intrathecal IgG reveal transcriptional heterogeneity of oligoclonal IgG-secreting cells in multiple sclerosis

Justyna Polak[1,2,3], Johanna H. Wagnerberger[3], Silje Bøen Torsetnes[4], Ida Lindeman[1,2], Rune A. Aa. Høglund[4,5], Frode Vartdal[1,2], Ludvig M. Sollid[1,2,5] and Andreas Lossius[2,3,4]*

[1]Department of Immunology, Oslo University Hospital, University of Oslo, Oslo, Norway, [2]K.G. Jebsen Coeliac Disease Research Centre, University of Oslo, Oslo, Norway, [3]Department of Molecular Medicine, Institute of Basic Medical Sciences, University of Oslo, Oslo, Norway, [4]Department of Neurology, Akershus University Hospital, Lørenskog, Norway, [5]Institute of Clinical Medicine, University of Oslo, Oslo, Norway

The phenotypes of B lineage cells that produce oligoclonal IgG in multiple sclerosis have not been unequivocally determined. Here, we utilized single-cell RNA-seq data of intrathecal B lineage cells in combination with mass spectrometry of intrathecally synthesized IgG to identify its cellular source. We found that the intrathecally produced IgG matched a larger fraction of clonally expanded antibody-secreting cells compared to singletons. The IgG was traced back to two clonally related clusters of antibody-secreting cells, one comprising highly proliferating cells, and the other consisting of more differentiated cells expressing genes associated with immunoglobulin synthesis. These findings suggest some degree of heterogeneity among cells that produce oligoclonal IgG in multiple sclerosis.

KEYWORDS

multiple sclerosis, B cells, plasmablasts, oligoclonal bands (OCB), IgG, cerebrospinal fluid

1. Introduction

Multiple sclerosis (MS) is characterized by a persistent synthesis of IgG within the central nervous system (CNS). Accordingly, deposition of IgG and complement activation products are generally found in all active demyelinating lesions (Breij et al., 2008). In the cerebrospinal fluid (CSF), this locally produced IgG can be detected in more than 90% of the patients as oligoclonal IgG bands (Stangel et al., 2013), which is a diagnostic criterion for the disease (Thompson et al., 2018).

Although the role of oligoclonal IgG in MS is a subject of debate, increasing evidence supports the idea that it may contribute to the disease pathogenesis. Accordingly, the presence of oligoclonal IgG has been linked to higher levels of disease activity and disability,

the conversion from a clinically isolated syndrome to definite MS, greater brain atrophy, and increased disease activity (Caroscio et al., 1986; Avasarala et al., 2001; Joseph et al., 2009; Ferreira et al., 2014; Heussinger et al., 2015; Farina et al., 2017; Seraji-Bozorgzad et al., 2017). Furthermore, a subset of recombinant antibodies constructed from clonally expanded antibody-secreting cells (ASCs) in MS CSF can cause complement-dependent cytotoxicity and demyelination in spinal cord explants and organotypic cerebellar slices (Blauth et al., 2015; Liu et al., 2017). Studies investigating the specificity of intrathecal ASCs have, however, revealed inconsistent results. Some studies have suggested reactivity against myelin-associated antigens (O'Connor et al., 2005; Kanter et al., 2006) and Epstein-Barr virus (Cepok et al., 2005; Lanz et al., 2022), but these findings are not consistent with those of independent studies (Owens et al., 2009; Sargsyan et al., 2010; Otto et al., 2011). Furthermore, one study suggested that some CSF IgG might be directed against intracellular autoantigens released during tissue destruction (Brändle et al., 2016).

The phenotypes of the B lineage cells that constitute the source of the oligoclonal IgG have not been settled, and to what extent these cells are susceptible to current immunomodulating strategies is controversial. Although a proportion of patients have been reported to lose detectable oligoclonal IgG after treatment with cladribine and natalizumab, most patients do seem to have a perpetuating intrathecal IgG synthesis despite highly effective immunomodulatory treatment (Cross et al., 2006; Harrer et al., 2013; Rejdak et al., 2019). This could indicate that the intrathecal IgG in these patients is synthesized by more differentiated long-lived ASCs within CNS survival niches (Eggers et al., 2017). Along the same line, it has been suggested that the development of secondary progressive disease in actively treated patients could be caused by therapy-resistant B lineage cells within such niches and that the presence of oligoclonal IgG might represent a useful endpoint for clinical trials (von Büdingen et al., 2017).

We previously used single-cell full-length RNA-seq and B-cell receptor reconstruction to analyze intrathecal B cells in MS (Lindeman et al., 2022). Here, we revisit the phenotype of the IgG-producing ASCs. To this end, we reanalyze the single-cell RNA-seq data from ten MS patients and combine this with mass spectrometry of intrathecally produced IgG.

2. Method

2.1. Patient inclusion and sample collection

The ten patients included in the study (**Table 1**) are part of a previously published cohort recruited at the Departments of Neurology at Akershus University Hospital and Oslo University Hospital, and details of sample acquisition and preparation are provided elsewhere (Lindeman et al., 2022). From this cohort, we chose patients who had a higher number of sorted and processed cells. MS9 and MS10 had previously been treated for 3 days with methylprednisolone; none of the other patients had received any type of immunomodulatory treatment at inclusion.

2.2. Sample preparation and mass spectrometry

From each patient, we purified IgG from 1 ml of CSF and an equivalent amount of IgG from serum using Protein G Dynabeads (Thermo Fisher Scientific, Waltham, MA, USA). After elution in 20 mM hydrogen chloride, the buffer was exchanged to 50 mM ammonium bicarbonate. After reduction and alkylation (Høglund et al., 2019), 10 μg IgG in 12.5 μl buffer from each sample was transferred to new microcentrifuge tubes and 40 ng of trypsin (Promega, Madison, WI, USA) was added. After 45 min at 57°C in an orbital shaker, another 100 ng of trypsin was added, and the samples were further incubated for 90 min. The liquid chromatography mass-spectrometry analyses were performed in duplicates on a Q Exactive Orbitrap mass spectrometer equipped with an Easy nLC-1000 system (all from Thermo Fisher Scientific, Waltham, MA, USA) as previously described (Høglund et al., 2019).

2.3. Single-cell RNA-sequencing and processing of raw sequence data

The generation of the single-cell RNA-sequencing data set has been described before (Lindeman et al., 2022). In brief, we performed flow cytometry index sorting of CSF B lineage cells into 96-well plates (Bio-Rad, Hercules, CA, USA). Sequencing libraries were generated using an in-house modified Smart-Seq2 protocol and sequenced on an Illumina NextSeq500 platform (Picelli et al., 2014). After demultiplexing, the sequences were trimmed and filtered, and gene expression was quantified with Salmon version 0.11.3 (Patro et al., 2017). Quality control was done in R (R Core Team, 2022)/RStudio (Posit Team, 2022) with the scater package (McCarthy et al., 2017). BraCeR was used to reconstruct the full-length paired heavy- and light-immunoglobulin chains for each cell (Lindeman et al., 2018). Once the paired immunoglobulin sequences have been assigned to each cell, BraCeR groups productive immunoglobulin sequences for each locus in the cell population into clonal clusters using the "bygroup" subcommand of the Change-O toolkit's "DefineClones" function (Gupta et al., 2015). Clonal grouping is based on the identification of common V- and J-gene sets among the sequences, equivalent CDR3 length, and CDR3 nucleotide distances < 0.2 as calculated using a human 5-mer targeting model (Yaari et al., 2013).

2.4. Analysis of mass spectrometry data

Mass spectrometry data was processed using MaxQuant v. 2.1.4.0 with the Andromeda search engine (Cox et al., 2014). Parameters of the search included label-free quantification and iBAQ values. The protein false discovery rate remained at 0.01, and methionine oxidation and acetylation of N-terminal amino acids were set as variable modifications. While running, multiplicates of the same sample match between runs feature was used, with minimum unique peptides set to 1. The library of sequences was constructed separately for each patient based on the amino acid translations of single cell RNA-seq full-length recombined V region of heavy- and light-chain immunoglobulin transcripts

with an extension of 24 nucleotides into the constant region. The MaxQuant output was filtered for intrathecally produced IgG based on heavy/light-chain pairs with $iBAQ_{CSF}$-$iBAQ_{serum}$ > 50 k and $iBAQ_{CSF}/iBAQ_{serum}$ > 1.2, and single heavy chains meeting the same criteria with an additional requirement of at least three unique peptides identified.

2.5. Gene expression analyses and statistics

As outlined in our previous publication (Lindeman et al., 2022), we excluded immunoglobulin genes from the gene expression analysis prior to normalization. To minimize patient-to-patient variability and eliminate batch effects, we regressed out the number of detected genes and reads, percentage of mitochondrial genes, and patient-specific variation, while preserving the variability attributed to cell type. The gene expression analyses were performed in scanpy v.1.9.1 (Wolf et al., 2018), with the aid of scikit-learn v.1.0.2 for scaling the expression matrix (Pedregosa et al., 2011). For visualization, we used UMAP for dimension reduction (McInnes et al., 2018). The pathway enrichment analyses were performed in R/Rstudio using gprofiler2 v.0.2.1 (Kolberg et al., 2020), and visualized in Cytoscape v.3.9.1 (Shannon et al., 2003) using EnrichmentMap v.3.3 (Merico et al., 2010), ClusterMaker2 v.2.3.4 (Morris et al., 2011), and AutoAnnotate v.1.4 (Kucera et al., 2016). Additional figures were made in R/Rstudio with ggplot2 v.2 (Wickham, 2016), ggbreak v.0.1.1 (Xu et al., 2021), and ggpubr v.0.5 (Kassambara, 2023). We used two-sided non-parametric statistical tests with a significance level of 0.05.

3. Result

We analyzed IgG from CSF and serum from ten treatment-naive MS patients (**Table 1**) using mass spectrometry and combined this with single-cell RNA-seq data of sorted B lineage cells from the CSF (Lindeman et al., 2022). To determine the intrathecally synthesized IgG fraction and its cellular source, we performed label-free quantification of IgG in normalized CSF and serum samples matched to paired immunoglobulin heavy- and light-chain transcripts (Cox et al., 2014). We found that a median of 13.5% (range 3.6–32%) of all CSF B lineage cells (collapsed on a clonal level) matched intrathecally produced IgG. Reassuringly, we found that almost all these matches were found among ASCs (**Figure 1A**), whereas the number of hits were low among memory B cells and negligible in the naive B cell pool. The hits within the memory B cell population may be explained by the high degree of clonal relatedness between this population and the ASCs, as we have previously shown (Lindeman et al., 2022). The single-cell analysis data of B lineage cells allowed us to identify clonally expanded populations. A clonally expanded B lineage cell is here defined as a cell that has at least one other B lineage cell from the same patient with identical or related immunoglobulin heavy-chain sequences and identical or related light-chain sequences. The criteria for clonal grouping are outlined in the materials and methods. A singleton, on the other hand, is a cell that is not related in this way to any other sorted B lineage cell. Intrathecally produced IgG matched such clonally expanded populations more frequently than singletons (**Figure 1B**). Taken together, these results show that a proportion of clonally expanded ASCs sampled from the CSF faithfully represent ASCs that are producing oligoclonal IgG.

The ASCs in the RNA-seq dataset are defined based on high surface expression of CD27 and CD38, and a proportion of immunoglobulin reads above 10% of the total transcriptome (Lindeman et al., 2022). We visualized the transcriptomes of the ASCs from the ten patients using UMAP and identified two distinct clusters (**Figure 2A**; **Supplementary Figure 1**). We identified the most differentially expressed genes between the clusters (**Figure 2B**) and performed a gene ontology (GO) enrichment analysis (**Figure 2C**). Whereas ASCs in the first cluster upregulated pathways involved in mitotic division and cytoskeleton organization, the ASCs in the other cluster upregulated pathways concerned with immunoglobulin synthesis and protein production (**Figure 2C**). Accordingly, the proliferation-associated gene *MKI67* was expressed by most cells in cluster 1, but to a much lesser extent in cluster 2 (**Figure 2D**). Further, the proportion of immunoglobulin transcripts per cell was larger in cluster 2

TABLE 1 Patient characteristics.

ID	Sex	Age	Diagnosis	CSF cell count[a]	OCB[b]	Albumin ratio	IgG index
MS1	M	36	SP-MS	36	+	12	1.7
MS2	F	26	RR-MS	4	+	3.8	1.1
MS3	M	20	RR-MS	19	+	6.2	0.81
MS4	F	46	RR-MS	19	+	3.1	0.72
MS5	F	31	RR-MS	33	+	3.2	2.1
MS6	M	52	RR-MS	6	+	5.0	1.1
MS7	F	44	RR-MS	18	+	6.4	1.1
MS8	M	21	RR-MS	21	+	6.4	0.95
MS9	F	48	RR-MS	17	+	4.3	1.3
MS10	M	35	RR-MS	5	+	3.3	0.75

[a]Number of mononuclear cells per microliter of CSF.
[b]More than two CSF-restricted oligoclonal bands on isoelectric focusing.
M, male; F, female; SP-MS, secondary progressive multiple sclerosis; RR-MS, relapsing-remitting multiple sclerosis.

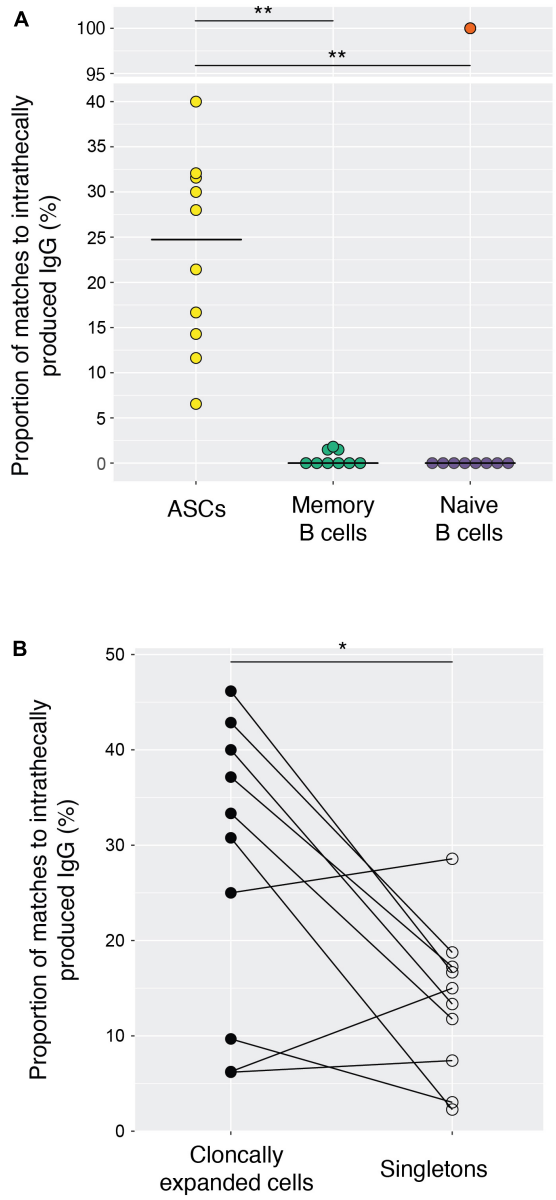

FIGURE 1
Intrathecally produced IgG matches clonally expanded antibody-secreting cells (ASCs) from the cerebrospinal fluid of MS patients. **(A)** The fraction of matches to intrathecal IgG for ASCs (642 cells), memory B cells (150 cells) and naive B cells (84 cells) was calculated for each patient, and each symbol indicates a patient. Clonally related cells were collapsed and treated as a single unit. Naïve and memory B cell populations were present in 9/10 patients. The outlier marked in red represents MS10, in whom we only analyzed a single sorted naïve B cell that also matched intrathecally produced IgG (excluded from statistical analysis). The horizontal lines depict the median values. Two-tailed Wilcoxon signed-rank test, $^{**}p < 0.01$. **(B)** The proportion of clonally expanded ASCs vs. singletons matching intrathecally produced IgG. Each symbol indicates a patient ($n = 10$). Clonally related cells were collapsed and treated as a single unit. Two-tailed Wilcoxon signed-rank test, $^{*}p = 0.0371$.

(Figure 2D), in which the cells also expressed somewhat higher levels of some plasma cell/plasmablast-related genes, including *XBP1* and *CD27* (Figure 2E). We observed strong clonal relatedness between the two clusters (Figure 2F; Supplementary Figure 2), which indicates a common origin and/or that they are in different stages of a maturation pathway. Oligoclonal IgG matched a comparable proportion of ASCs in each cluster (Figure 2G), and the majority of the IgG matched to ASCs that were clonally expanded across the clusters (Figure 2G, lower Venn diagram). Taken together, these data provide evidence of transcriptional heterogeneity of clonally related ASCs producing oligoclonal IgG in MS.

4. Discussion

In the present study, we used single-cell RNA-seq data and combined it with mass spectrometry to trace the oligoclonal IgG-producing cells. The results show that oligoclonal IgG matches with the transcriptome of both heavily proliferating ASCs and more differentiated ASCs that are mainly occupied with immunoglobulin production. The clonal relatedness between these populations with slightly different transcriptional profiles indicates a shared ancestry and/or that they are part of a developmental progression from newly generated plasmablasts to more differentiated phenotypes.

In a previous study, it was demonstrated that intrathecally produced IgG match B cell transcripts from the CSF, suggesting that oligoclonal IgG is secreted by ASCs that are present in the CSF (Obermeier et al., 2008). Nonetheless, several observations indicate that only a proportion of intrathecal ASCs are involved in the production of the main fractions of oligoclonal IgG. First, as demonstrated previously by us and others (Colombo et al., 2003; Greenfield et al., 2019; Tomescu-Baciu et al., 2019), there is a limited clonal overlap in CSF cell samples collected at different time points whereas the pattern of oligoclonal IgG is remarkably stable over time (Walsh and Tourtellotte, 1986; Axelsson et al., 2013; Tomescu-Baciu et al., 2019). This underscores that a finite sample of CSF cells only represents a small proportion of all ASCs in the CNS, and that any random sample will miss relevant oligoclonal IgG-secreting cells and include irrelevant B cell clones. Second, it is well-known that patients with MS have an intrathecal synthesis of IgG against disease-irrelevant pathogens, including measles, rubella and varicella zoster virus, which are not part of the major fractions of oligoclonal IgG (Vartdal et al., 1980; Feki et al., 2018). Therefore, pinpointing the disease-relevant ASCs that are responsible for the production of oligoclonal IgG might be key to dissect the mechanisms driving the intrathecal B cell response in MS.

Our study has several limitations. In order to accurately match oligoclonal IgG to specific subpopulations of B cells and perform a precise characterization and comparison of them, we selected patients from our previously published cohort who had a higher number of sorted and processed B lineage cells. Although this approach provided us with a larger amount of data for analysis, it is important to acknowledge that it might have introduced a selection bias, as it may have preferentially included patients with higher CSF cell numbers and potentially greater disease activity. Therefore, our findings may not be applicable to patients with less active disease. Furthermore, although we observed a lower expression of the proliferation marker *MKI67* in cluster 2, we cannot definitively determine whether these cells are more differentiated plasma cells or if they represent plasmablasts in the G1 phase of the cell cycle –

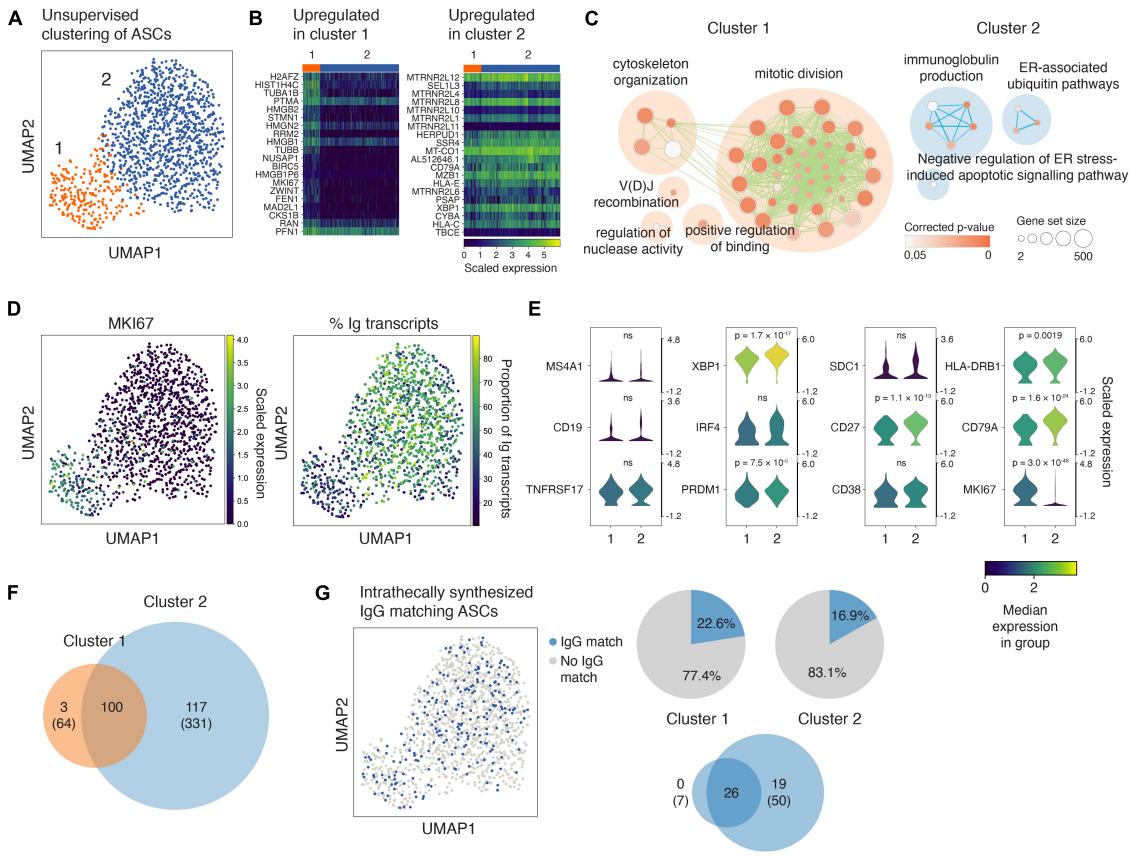

FIGURE 2
Antibody-secreting cells (ASCs) in the cerebrospinal fluid of MS patients cluster in two distinct yet clonally related groups, and intrathecally produced IgG matches cells from both groups. **(A)** UMAP projection and unsupervised clustering of intrathecal ASCs [n = 10 patients (1,283 cells)]. **(B)** Highly differentially expressed genes in each cluster compared to the other cluster. The genes are ranked according to the Mann–Whitney U test. **(C)** Enrichment map depicting Gene Ontology (GO) pathway enrichment analysis of highly differentially expressed genes in each cluster. Each node represents a GO biological process term. Related terms are clustered and labeled using the AutoAnnotate Cytoscape application following published protocols (Reimand et al., 2019). The lines (edges) between the nodes signify that genes are shared between the GO terms. **(D)** The expression of MKI67 and the proportion of immunoglobulin (Ig) transcripts superimposed on the UMAP projection of ASCs. **(E)** Violin plots showing the expression of genes of particular interest for ASCs in the two clusters. The genes in each cluster were compared in Scanpy using Wilcoxon rank-sum test, and the given p-values are adjusted for multiple testing using Bonferroni correction. ns: not significant. **(F)** Venn diagrams depicting the clonal overlap between ASCs in the two UMAP clusters. Given are the numbers of collapsed clonotypes and the number of singletons in brackets. The Venn diagrams are scaled according to the sum of collapsed clonotypes and singletons. Clonal relatedness was based on the identification of common V-and J-gene sets among the sequences, equivalent CDR3 length, and CDR3 nucleotide distances < 0.2 as calculated using a human 5-mer targeting model (Yaari et al., 2013). **(G)** UMAP projection of ASCs colored according to matches with intrathecally produced IgG. The pie charts show the proportion of ASCs matching intrathecally produced IgG in each UMAP cluster, and the Venn diagram shows the clonal overlap of these IgG-matching ASCs in each cluster (clonotypes collapsed and singletons in brackets).

transiently downregulating *MKI67*. Finally, the selected patients had different ages, and one of them had developed secondary progressive disease, indicating a longer disease duration. This heterogeneity may have introduced variability in our study.

Matching mass spectrometry data of IgG to immunoglobulin transcripts can be challenging due to the high degree of sequence homology between the transcripts (Snapkov et al., 2022). Here, we addressed this issue by setting strict criteria for what is considered a hit, requiring peptide hits for both the heavy and light chains of a given IgG molecule, or at least three hits for the heavy chain. However, these strict criteria may lead to a loss of sensitivity, and therefore our study might underestimate the true overlap between the immunoglobulin proteome and transcriptome in the CSF of MS patients. Another potential source of bias in our study is the intrathecal fraction of IgG that originates from serum, as less than 50% of intrathecal IgG in MS represents intrathecally produced oligoclonal IgG (Reiber et al., 1998). To account for this, we utilized label-free quantification of heavy and light chains in serum and CSF, measured by MaxQuant's intensity-based absolute quantification (iBAQ) values, a measure of protein abundance (Schwanhäusser et al., 2011). Of note, all included mass spectrometry hits had an estimated abundance in the CSF of at least twice that in serum.

In conclusion, our study sheds light on the cellular origins of oligoclonal IgG in MS by combining single-cell RNA-seq data with mass spectrometry. Our findings suggest that oligoclonal IgG is produced by both heavily proliferating ASCs and more differentiated ASCs mainly focused on immunoglobulin production, which likely share a common ancestry or developmental progression. Overall, our study

contributes to understanding the intrathecal B cell response in MS and highlights the need for further investigation to pinpoint the disease-relevant ASCs responsible for the production of oligoclonal IgG.

Data availability statement

The datasets presented in this study can be found in online repositories. The names of the repository/repositories and accession number(s) can be found below: https://ega-archive.org, EGAS00001005745 and https://massive.ucsd.edu, MSV000091526.

Ethics statement

The studies involving human participants were reviewed and approved by the Regional Ethical Committee South East, Norway (2009/23). The patients/participants provided their written informed consent to participate in this study.

Author contributions

JP, AL, ST, LS, and FV contributed to the study design. JP, AL, IL, RH, JW, and ST contributed to the collecting and analyzing data. JP, JW, and AL drafted the manuscript. All authors contributed to revising the manuscript and approved the submitted version.

Funding

This study was funded by grants from the Norwegian Women's Public Health Association, the Norwegian Research Council (Project No. 314376), the South-Eastern Norway Regional Health Authority, the University of Oslo World-Leading Research Program on Human Immunology (WL-IMMUNOLOGY), and Stiftelsen K.G. Jebsen (Project No. SKGJ-MED-017). Additionally, JP and AL are the recipients of the Norwegian Neurological Association research prize in multiple sclerosis 2019 and 2020 provided by Sanofi Genzyme and Novartis. AL also received Odd Fellow's Research Grant 2019.

Acknowledgments

We want to express our gratitude to the patients who donated samples for this study.

Conflict of interest

This study received funding from Novartis and Sanofi Genzyme. The funder was not involved in the study design, collection, analysis, interpretation of data, the writing of this article or the decision to submit it for publication.

The authors declare that the research was conducted in the absence of any commercial or financial relationships that could be construed as a potential conflict of interest.

Publisher's note

Supplementary material

The Supplementary Material for this article can be found online at: https://www.frontiersin.org/articles/10.3389/fncel.2023.1189709/full#supplementary-material

References

Avasarala, J. R., Cross, A. H., and Trotter, J. L. (2001). Oligoclonal band number as a marker for prognosis in multiple sclerosis. *Arch. Neurol.* 58, 2044–2045.

Axelsson, M., Mattsson, N., Malmeström, C., Zetterberg, H., and Lycke, J. (2013). The influence of disease duration, clinical course, and immunosuppressive therapy on the synthesis of intrathecal oligoclonal IgG bands in multiple sclerosis. *J. Neuroimmunol.* 264, 100–105. doi: 10.1016/j.jneuroim.2013.09.003

Blauth, K., Soltys, J., Matschulat, A., Reiter, C. R., Ritchie, A., Baird, N. L., et al. (2015). Antibodies produced by clonally expanded plasma cells in multiple sclerosis cerebrospinal fluid cause demyelination of spinal cord explants. *Acta Neuropathol.* 130, 765–781. doi: 10.1007/s00401-015-1500-6

Brändle, S. M., Obermeier, B., Senel, M., Bruder, J., Mentele, R., Khademi, M., et al. (2016). Distinct oligoclonal band antibodies in multiple sclerosis recognize ubiquitous self-proteins. *Proc. Natl. Acad. Sci. U.S.A.* 113, 7864–7869. doi: 10.1073/pnas.1522730113

Breij, E. C. W., Brink, B. P., Veerhuis, R., van den Berg, C., Vloet, R., Yan, R., et al. (2008). Homogeneity of active demyelinating lesions in established multiple sclerosis. *Ann. Neurol.* 63, 16–25.

Caroscio, J. T., Kochwa, S., Sacks, H., Makuku, S., Cohen, J. A., and Yahr, M. D. (1986). Quantitative cerebrospinal fluid IgG measurements as a marker of disease activity in multiple sclerosis. *Arch. Neurol.* 43, 1129–1131. doi: 10.1001/archneur.1986.00520110029009

Cepok, S., Zhou, D., Srivastava, R., Nessler, S., Stei, S., Büssow, K., et al. (2005). Identification of Epstein-barr virus proteins as putative targets of the immune response in multiple sclerosis. *J. Clin. Invest.* 115, 1352–1360. doi: 10.1172/JCI23661

Colombo, M., Dono, M., Gazzola, P., Chiorazzi, N., Mancardi, G., and Ferrarini, M. (2003). Maintenance of B lymphocyte-related clones in the cerebrospinal fluid of multiple sclerosis patients. *Eur. J. Immunol.* 33, 3433–3438. doi: 10.1002/eji.200324144

Cox, J., Hein, M. Y., Luber, C. A., Paron, I., Nagaraj, N., and Mann, M. (2014). Accurate proteome-wide label-free quantification by delayed normalization and maximal peptide ratio extraction, termed MaxLFQ. *Mol. Cell. Proteomics MCP* 13, 2513–2526. doi: 10.1074/mcp.M113.031591

Cross, A. H., Stark, J. L., Lauber, J., Ramsbottom, M. J., and Lyons, J.-A. (2006). Rituximab reduces B cells and T cells in cerebrospinal fluid of multiple sclerosis patients. *J. Neuroimmunol.* 180, 63–70. doi: 10.1016/j.jneuroim.2006.06.029

Eggers, E. L., Michel, B. A., Wu, H., Wang, S.-Z., Bevan, C. J., Abounasr, A., et al. (2017). Clonal relationships of CSF B cells in treatment-naive multiple sclerosis patients. *JCI Insight* 2:e92724. doi: 10.1172/jci.insight.92724

Farina, G., Magliozzi, R., Pitteri, M., Reynolds, R., Rossi, S., Gajofatto, A., et al. (2017). Increased cortical lesion load and intrathecal inflammation is associated with oligoclonal bands in multiple sclerosis patients: A combined CSF and MRI study. *J. Neuroinflammation* 14:40. doi: 10.1186/s12974-017-0812-y

Feki, S., Gargouri, S., Mejdoub, S., Dammak, M., Hachicha, H., Hadiji, O., et al. (2018). The intrathecal polyspecific antiviral immune response (MRZ Reaction): A potential cerebrospinal fluid marker for multiple sclerosis diagnosis. *J. Neuroimmunol.* 321, 66–71. doi: 10.1016/j.jneuroim.2018.05.015

Ferreira, D., Voevodskaya, O., Imrell, K., Stawiarz, L., Spulber, G., Wahlund, L.-O., et al. (2014). Multiple sclerosis patients lacking oligoclonal bands in the cerebrospinal fluid have less global and regional brain atrophy. *J. Neuroimmunol.* 274, 149–154. doi: 10.1016/j.jneuroim.2014.06.010

Greenfield, A. L., Dandekar, R., Ramesh, A., Eggers, E. L., Wu, H., Laurent, S., et al. (2019). Longitudinally persistent cerebrospinal fluid B cells can resist treatment in multiple sclerosis. *JCI Insight* 4:e126599. doi: 10.1172/jci.insight.126599

Gupta, N. T., Heiden, J. A. V., Uduman, M., Gadala-Maria, D., Yaari, G., and Kleinstein, S. H. (2015). Change-O: A toolkit for analyzing large-scale B cell immunoglobulin repertoire sequencing data. *Bioinformatics* 31, 3356–3358. doi: 10.1093/bioinformatics/btv359

Harrer, A., Tumani, H., Niendorf, S., Lauda, F., Geis, C., Weishaupt, A., et al. (2013). Cerebrospinal fluid parameters of B cell-related activity in patients with active disease during natalizumab therapy. *Mult. Scler.* 19, 1209–1212. doi: 10.1177/1352458512463483

Heussinger, N., Kontopantelis, E., Gburek-Augustat, J., Jenke, A., Vollrath, G., Korinthenberg, R., et al. (2015). Oligoclonal bands predict multiple sclerosis in children with optic neuritis. *Ann. Neurol.* 77, 1076–1082.

Høglund, R. A., Torsetnes, S. B., Lossius, A., Bogen, B., Homan, E. J., Bremel, R., et al. (2019). Human cysteine cathepsins degrade immunoglobulin G in vitro in a predictable manner. *Int. J. Mol. Sci.* 20:4843. doi: 10.3390/ijms20194843

Joseph, F. G., Hirst, C. L., Pickersgill, T. P., Ben-Shlomo, Y., Robertson, N. P., and Scolding, N. J. (2009). CSF oligoclonal band status informs prognosis in multiple sclerosis: A case control study of 100 patients. *J. Neurol. Neurosurg. Psychiatry* 80, 292–296. doi: 10.1136/jnnp.2008.150896

Kanter, J. L., Narayana, S., Ho, P. P., Catz, I., Warren, K. G., Sobel, R. A., et al. (2006). Lipid microarrays identify key mediators of autoimmune brain inflammation. *Nat. Med.* 12, 138–143. doi: 10.1038/nm1344

Kassambara, A. (2023). *Ggpubr: 'ggplot2' based publication ready plots*. Available online at: https://CRAN.R-project.org/package=ggpubr (accessed February 1, 2023).

Kolberg, L., Raudvere, U., Kuzmin, I., Vilo, J., and Peterson, H. (2020). gprofiler2–an R package for gene list functional enrichment analysis and namespace conversion toolset g:Profiler. *F1000Res.* 9:709. doi: 10.12688/f1000research.24956.2

Kucera, M., Isserlin, R., Arkhangorodsky, A., and Bader, G. D. (2016). AutoAnnotate: A cytoscape app for summarizing networks with semantic annotations. *F1000Res.* 5:1717. doi: 10.12688/f1000research.9090.1

Lanz, T. V., Brewer, R. C., Ho, P. P., Moon, J.-S., Jude, K. M., Fernandez, D., et al. (2022). Clonally expanded B cells in multiple sclerosis bind EBV EBNA1 and GlialCAM. *Nature* 603, 321–327.

Lindeman, I., Emerton, G., Mamanova, L., Snir, O., Polanski, K., Qiao, S.-W., et al. (2018). BraCeR: B-cell-receptor reconstruction and clonality inference from single-cell RNA-Seq. *Nat. Methods* 15, 563–565. doi: 10.1038/s41592-018-0082-3

Lindeman, I., Polak, J., Qiao, S.-W., Holmøy, T., Høglund, R. A., Vartdal, F., et al. (2022). Stereotyped B-cell responses are linked to IgG constant region polymorphisms in multiple sclerosis. *Eur. J. Immunol.* 52, 550–565. doi: 10.1002/eji.202149576

Liu, Y., Given, K. S., Harlow, D. E., Matschulat, A. M., Macklin, W. B., Bennett, J. L., et al. (2017). Myelin-specific multiple sclerosis antibodies cause complement-dependent oligodendrocyte loss and demyelination. *Acta Neuropathol. Commun.* 5:25. doi: 10.1186/s40478-017-0428-6

McCarthy, D. J., Campbell, K. R., Lun, A. T. L., and Wills, Q. F. (2017). Scater: Pre-processing, quality control, normalization and visualization of single-cell RNA-Seq data in R. *Bioinformatics* 33, 1179–1186. doi: 10.1093/bioinformatics/btw777

McInnes, L., Healy, J., and Melville, J. (2018). UMAP: Uniform manifold approximation and projection for dimension reduction. *arXiv* [preprint]. doi: 10.48550/arXiv.1802.03426

Merico, D., Isserlin, R., Stueker, O., Emili, A., and Bader, G. D. (2010). Enrichment map: A network-based method for gene-set enrichment visualization and interpretation. *PLoS One* 5:e13984. doi: 10.1371/journal.pone.0013984

Morris, J. H., Apeltsin, L., Newman, A. M., Baumbach, J., Wittkop, T., Su, G., et al. (2011). clusterMaker: A multi-algorithm clustering plugin for cytoscape. *BMC Bioinformatics* 12:436. doi: 10.1186/1471-2105-12-436

O'Connor, K. C., Appel, H., Bregoli, L., Call, M. E., Catz, I., Chan, J. A., et al. (2005). Antibodies from inflamed central nervous system tissue recognize myelin oligodendrocyte glycoprotein. *J. Immunol.* 175, 1974–1982. doi: 10.4049/jimmunol.175.3.1974

Obermeier, B., Mentele, R., Malotka, J., Kellermann, J., Kümpfel, T., Wekerle, H., et al. (2008). Matching of oligoclonal immunoglobulin transcriptomes and proteomes of cerebrospinal fluid in multiple sclerosis. *Nat. Med.* 14, 688–693.

Otto, C., Oltmann, A., Stein, A., Frenzel, K., Schroeter, J., Habbel, P., et al. (2011). Intrathecal EBV antibodies are part of the polyspecific immune response in multiple sclerosis. *Neurology* 76, 1316–1321.

Owens, G. P., Bennett, J. L., Lassmann, H., O'Connor, K. C., Ritchie, A. M., Shearer, A., et al. (2009). Antibodies produced by clonally expanded plasma cells in multiple sclerosis cerebrospinal fluid. *Ann. Neurol.* 65, 639–649.

Patro, R., Duggal, G., Love, M. I., Irizarry, R. A., and Kingsford, C. (2017). Salmon provides fast and bias-aware quantification of transcript expression. *Nat. Methods* 14, 417–419. doi: 10.1038/nmeth.4197

Pedregosa, F., Varoquaux, G., Gramfort, A., Michel, V., Thirion, B., Grisel, O., et al. (2011). Scikit-learn: Machine learning in python. *J. Mach. Learn. Res. JMLR* 12, 2825–2830.

Picelli, S., Faridani, O. R., Björklund, A. K., Winberg, G., Sagasser, S., and Sandberg, R. (2014). Full-length RNA-Seq from single cells using smart-seq2. *Nat. Protoc.* 9, 171–181. doi: 10.1038/nprot.2014.006

Posit Team (2022). *RStudio: Integrated development environment for R*. Boston, MA: Posit Software, PBC.

R Core Team (2022). *R: A language and environment for statistical computing*. Vienna: R Foundation for Statistical Computing.

Reiber, H., Ungefehr, S., and Jacobi, C. (1998). The intrathecal, polyspecific and oligoclonal immune response in multiple sclerosis. *Mult. Scler.* 4, 111–117. doi: 10.1177/135245859800400304

Reimand, J., Isserlin, R., Voisin, V., Kucera, M., Tannus-Lopes, C., Rostamianfar, A., et al. (2019). Pathway enrichment analysis and visualization of omics data using g:Profiler, GSEA, Cytoscape and EnrichmentMap. *Nat. Protoc.* 14, 482–517. doi: 10.1038/s41596-018-0103-9

Rejdak, K., Stelmasiak, Z., and Grieb, P. (2019). Cladribine induces long lasting oligoclonal bands disappearance in relapsing multiple sclerosis patients: 10-year observational study. *Mult. Scler. Relat. Disord.* 27, 117–120. doi: 10.1016/j.msard.2018.10.006

Sargsyan, S. A., Shearer, A. J., Ritchie, A. M., Burgoon, M. P., Anderson, S., Hemmer, B., et al. (2010). Absence of epstein-barr virus in the brain and CSF of patients with multiple sclerosis. *Neurology* 74, 1127–1135. doi: 10.1212/WNL.0b013e3181d865a1

Schwanhäusser, B., Busse, D., Li, N., Dittmar, G., Schuchhardt, J., Wolf, J., et al. (2011). Global quantification of mammalian gene expression control. *Nature* 473, 337–342. doi: 10.1038/nature10098

Seraji-Bozorgzad, N., Khan, O., Cree, B. A. C., Bao, F., Caon, C., Zak, I., et al. (2017). Cerebral gray matter atrophy is associated with the CSF IgG index in African American with multiple sclerosis. *J. Neuroimaging* 27, 476–480. doi: 10.1111/jon.12435

Shannon, P., Markiel, A., Ozier, O., Baliga, N. S., Wang, J. T., Ramage, D., et al. (2003). Cytoscape: A software environment for integrated models of biomolecular interaction networks. *Genome Res.* 13, 2498–2504. doi: 10.1101/gr.1239303

Snapkov, I., Chernigovskaya, M., Sinitcyn, P., Lê Quý, K., Nyman, T. A., and Greiff, V. (2022). Progress and challenges in mass spectrometry-based analysis of antibody repertoires. *Trends Biotechnol.* 40, 463–481. doi: 10.1016/j.tibtech.2021.08.006

Stangel, M., Fredrikson, S., Meinl, E., Petzold, A., Stüve, O., and Tumani, H. (2013). The utility of cerebrospinal fluid analysis in patients with multiple sclerosis. *Nat. Rev. Neurol.* 9, 267–276. doi: 10.1038/nrneurol.2013.41

Thompson, A. J., Banwell, B. L., Barkhof, F., Carroll, W. M., Coetzee, T., Comi, G., et al. (2018). Diagnosis of multiple sclerosis: 2017 revisions of the McDonald Criteria. *Lancet Neurol.* 17, 162–173.

Tomescu-Baciu, A., Johansen, J. N., Holmøy, T., Greiff, V., Stensland, M., de Souza, G. A., et al. (2019). Persistence of intrathecal oligoclonal B cells and IgG in multiple sclerosis. *J. Neuroimmunol.* 333:576966. doi: 10.1016/j.jneuroim.2019.576966

Vartdal, F., Vandvik, B., and Norrby, E. (1980). Viral and bacterial antibody responses in multiple sclerosis. *Ann. Neurol.* 8, 248–255.

von Büdingen, H. C., Bischof, A., Eggers, E. L., Wang, S., Bevan, C. J., Cree, B. A., et al. (2017). Onset of secondary progressive MS after long-term rituximab therapy - a case report. *Ann. Clin. Transl. Neurol.* 4, 46–52. doi: 10.1002/acn3.377

Walsh, M. J., and Tourtellotte, W. W. (1986). Temporal invariance and clonal uniformity of brain and cerebrospinal IgG, IgA, and IgM in multiple sclerosis. *J. Exp. Med.* 163, 41–53. doi: 10.1084/jem.163.1.41

Wickham, H. (2016). *ggplot2: Elegant graphics for data analysis*. New York, NY: Springer-Verlag.

Wolf, F. A., Angerer, P., and Theis, F. J. (2018). SCANPY: Large-scale single-cell gene expression data analysis. *Genome Biol.* 19:15. doi: 10.1186/s13059-017-1382-0

Xu, S., Chen, M., Feng, T., Zhan, L., Zhou, L., and Yu, G. (2021). Use Ggbreak to effectively utilize plotting space to deal with large datasets and outliers. *Front. Genet.* 12:774846. doi: 10.3389/fgene.2021.774846

Yaari, G., Heiden, J. A. V., Uduman, M., Gadala-Maria, D., Gupta, N., Stern, J. N. H., et al. (2013). Models of somatic hypermutation targeting and substitution based on synonymous mutations from high-throughput immunoglobulin sequencing data. *Front. Immunol.* 4:358. doi: 10.3389/fimmu.2013.00358

Supplementary Material

Single-cell transcriptomics combined with proteomics of intrathecal IgG reveal transcriptional heterogeneity of oligoclonal IgG-secreting cells in multiple sclerosis

Justyna Polak, Johanna H. Wagnerberger, Silje Bøen Torsetnes, Ida Lindeman, Rune A. Aa. Høglund, Frode Vartdal, Ludvig M. Sollid, Andreas Lossius*

*** Correspondence:** Andreas Lossius: andreas.lossius@medisin.uio.no

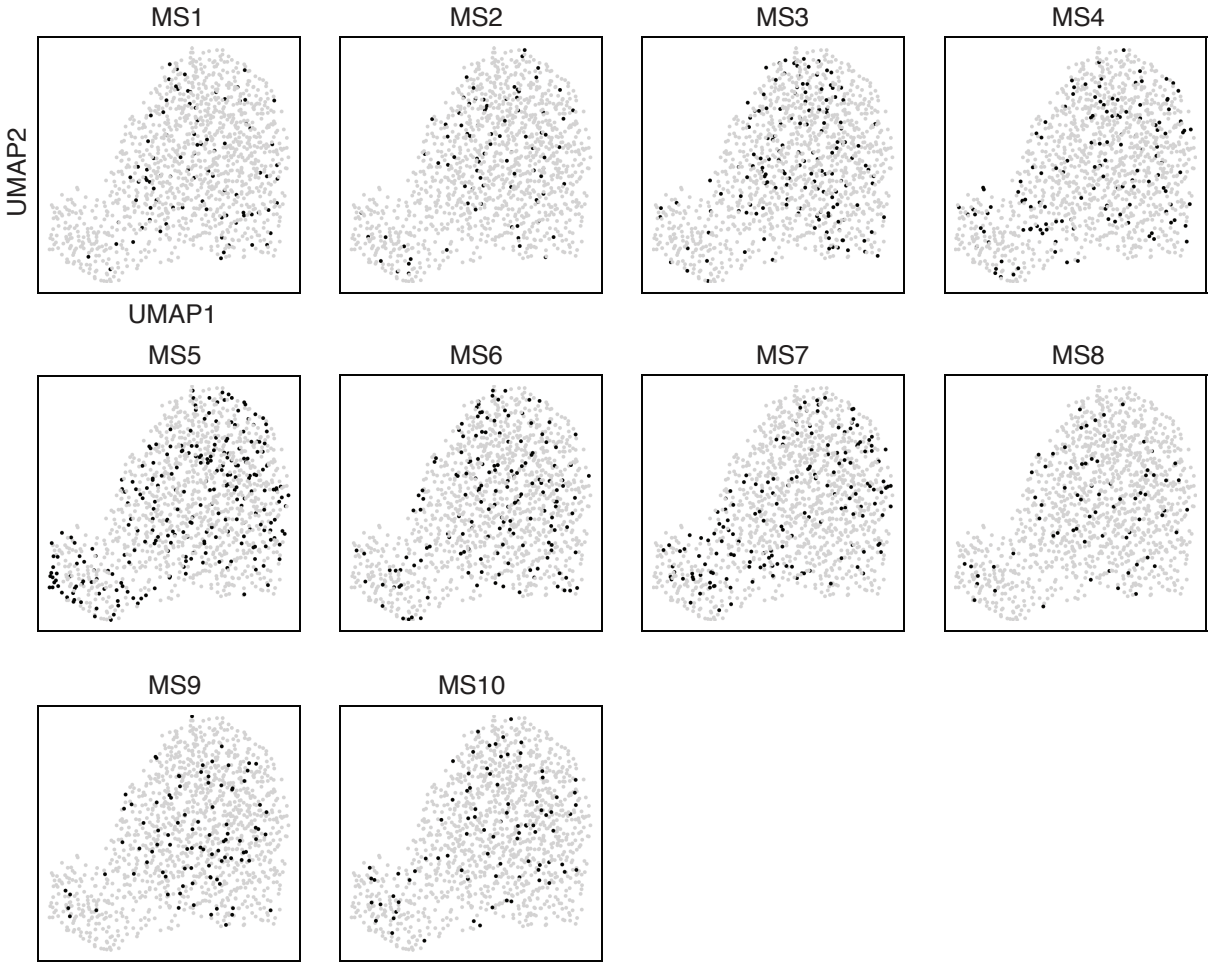

Supplementary Figure 1. UMAP projections of 1283 intrathecal antibody-secreting cells as in Figure 2A, D, and G according to individual patients.

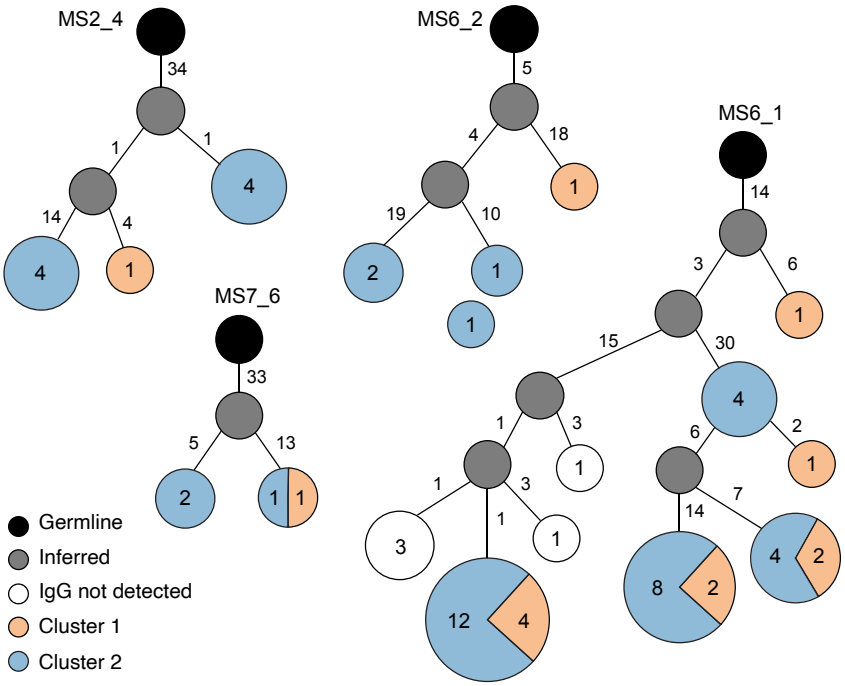

Supplementary Figure 2. Clonal connections across UMAP cluster 1 and 2 as shown in Figure 2A. Representative lineage trees of antibody-secreting cells with clonal members in both UMAP clusters with inferred germinal sequences at the root are shown. The size of the nodes and the number(s) inside the nodes reflects the number of cells with a unique B cell receptor sequence. The number of mutations between the nodes are shown next to each branch.

III

Multiple Sclerosis and Related Disorders 26 (2018) 90–95

Contents lists available at ScienceDirect

Multiple Sclerosis and Related Disorders

journal homepage: www.elsevier.com/locate/msard

B-cell composition in the blood and cerebrospinal fluid of multiple sclerosis patients treated with dimethyl fumarate

Rune A. Høglund[a,b,*], Justyna Polak[b,c], Frode Vartdal[c], Trygve Holmøy[a,b], Andreas Lossius[a,c,*]

[a] Department of Neurology, Akershus University Hospital, Lørenskog, Norway
[b] Institute of Clinical Medicine, University of Oslo, Oslo, Norway
[c] Department of Immunology and Transfusion Medicine, Faculty of Medicine, University of Oslo, Oslo, Norway

ARTICLE INFO

Keywords:
Multiple sclerosis
B cell
Dimethyl fumarate
Memory B cell
Cerebrospinal fluid
Plasmablast

ABSTRACT

Background: B cells may contribute to the immunopathogenesis of multiple sclerosis (MS). Dimethyl fumarate (DMF) has recently been shown to reduce the frequency of memory B cells in blood, but it is not known whether the drug influences the cellular composition in the cerebrospinal fluid (CSF).
Methods: A cross-sectional study examining the cellular composition in blood and cerebrospinal fluid (CSF) from 10 patients treated with DMF and 18 patients receiving other disease modifying drugs or no treatment.
Results: Patients treated with DMF had reduced proportions of memory B cells in blood compared to other MS patients ($p = 0.0007$), and the reduction correlated with treatment duration ($r_s = -0.75$, $p = 0.021$). In the CSF, the absolute number of mononuclear cells were significantly lower in DMF-treated patients compared to the other patients ($p = 0.023$), and there was a disproportionate decrease of plasmablasts ($p = 0.031$).
Conclusion: The results of this exploratory study support a B-cell mediated mechanism of action for DMF in both blood and CSF.

1. Introduction

B cells have an important role in multiple sclerosis (MS), as is evident from several successful clinical trials of B-cell depletion (Hauser et al., 2017; Kappos et al., 2011; Bar-Or et al., 2008). Several potential mechanisms have been proposed, including antigen presentation, cytokine secretion, and antibody production (Lehmann-Horn et al., 2017). In MS, the proportion of immunoglobulin class-switched $CD27^+$ B cells is increased in the cerebrospinal fluid (CSF) compared to the peripheral blood (Eggers et al., 2017), and in particular the frequency of plasmablasts expressing CD38 and CD138 have been shown to be elevated (Cepok et al., 2005; Kowarik et al., 2014). Studies have demonstrated that immunoglobulin class-switched B cells in the CSF are related to B cells in the brain parenchyma (Obermeier et al., 2011), cervical lymph nodes (Stern et al., 2014), and peripheral blood (von Budingen et al., 2012; Johansen et al., 2015), indicating a dynamic exchange between these compartments.

Dimethyl fumarate (DMF) is an oral disease-modifying treatment (DMT) approved for treating relapsing-remitting MS (RRMS). The mechanism of action is not fully clarified (Deeks, 2016), but includes a reduction of peripheral blood $CD19^+CD27^+$ memory B cells (Smith et al., 2017; Longbrake et al., 2017; Li et al., 2017; Lundy et al., 2016). Upon intake, DMF is rapidly metabolized to monomethyl fumarate (MMF), which crosses the blood-brain barrier in animal models and in humans, however only at 15% of plasma concentration (Edwards et al., 2016; Penner et al., 2016).

The penetration of MMF into the CSF, and the exchange of B cells between the periphery, CSF and the central nervous system (CNS), suggest the possibility that DMF may exert a direct or indirect effect on intrathecal B cells. To address this, we examined blood and CSF B-cell subsets from MS patients treated with DMF and patients receiving other or no immunomodulatory treatment. We found that while DMF treatment is associated with a decrease of $CD19^+CD27^+$ memory B cells in the periphery, it is associated with a significant reduction of $CD19^+CD27^+CD38^+$ plasmablasts in CSF.

Abbreviations: CSF, cerebrospinal fluid; DMT, disease modifying therapy; IgG, immunoglobulin G; M/DMF, mono-/dimethyl fumarate; MFI, median fluorescence intensity; MS, multiple sclerosis; RRMS, relapsing remitting MS; TFM, teriflunomide

* Corresponding authors at: Department of Neurology, Akershus University Hospital, PO Box 1000, Lørenskog 1478, Norway.
E-mail addresses: r.a.hoglund@medisin.uio.no (R.A. Høglund), andreas.lossius@rr-research.no (A. Lossius).

https://doi.org/10.1016/j.msard.2018.08.032
Received 26 April 2018; Received in revised form 22 August 2018; Accepted 30 August 2018

Table 1
Demographic and clinical characteristics of patients.

Treatment	DMF	Other	Statistical test
Participants	10	18	–
Age (years)	41 (27–58)	47.5 (25–57)	$p = 0.75$[a]
Sex (M/F)	4/6	5/13	$p = 0.68$[b]
Disease duration (months)	47.5 (10–153)	102 (2–283)	$p = 0.10$[a]
Treatment duration (months)	8 (2–13)	All: 35 (3–152)[c] GA: 79 (18–152) TFM: 12.5 (3–27)	$p = 0.0012$[a]
EDSS score	1.25 (1–3.5)	1.25 (0–5.5)	$p = 0.78$[a]
Number of relapses	1.5 (1–5)	3 (1–6)	$p = 0.11$[a]
Time since last relapse (months)	18.5 (2–118)	5 (1–164)	$p = 0.60$[a]
Albumin ratio[d]	4.4 (3.6–9.24)	4.6 (2.3–6.9)	$p = 0.67$[a]
IgG index[d]	0.7 (0.5–2.1)	1.2 (0.5–1.9)	$p = 0.74$[a]

Numbers given as median (range). DMF: dimethyl fumarate. EDSS: expanded disability status scale. GA: glatiramer acetate. MRI: magnetic resonance imaging. TFM: teriflunomide.
[a] Wilcoxon 2-sample exact test.
[b] Fishers exact test.
[c] untreated patients excluded.
[d] compared between DMF treated and no-treated.

2. Materials and methods

2.1. Patients

MS patients ($n = 28$) were recruited at the Departments of Neurology at Akershus University Hospital and Oslo University Hospital; other data based on the same cohort have been previously published (Lossius et al., 2017). All patients met the 2010 McDonalds criteria for MS (Polman et al., 2011); 1 patient was classified as secondary progressive MS and the remaining as RRMS. All patients had intrathecal synthesis of immunoglobulin G (IgG) at the time of diagnosis, detected as oligoclonal IgG bands by isoelectric focusing. Lumbar puncture was performed either as a part or outside of diagnostic investigations, reflected by the variation in disease duration (Table 1). The study was approved by the Regional Ethical Committee South East (2009/23 S-04143a). All patients gave written informed consent before inclusion.

2.2. Cell subset analysis

For each individual included in this study, blood, serum and CSF samples were collected once, during the same consultation. Blood and CSF mononuclear cells were isolated as described previously, counted using a Neubauer improved hemocytometer, and immediately processed for flow cytometry, which was performed within two hours after sample collection (Johansen et al., 2015; Lossius et al., 2017). For B-cell subset identification we used fluorochrome-conjugated antibodies as described (Lossius et al., 2017), including anti-human CD19, CD27, CD38, CD138, IgG, Ki-67, and HLA-DR, and additionally CD3 and CD14 for dump-channel purposes (BD Biosciences). Paired cell samples from CSF and blood were stained for surface antigens, and after fixation and permeabilization following the manufacturer's instructions (Fixation/Permeabilization Solution Kit, BD Biosciences), the cells were stained for Ki-67. The flow cytometry dataset was reanalyzed for the present study using FlowJo Version 10.2 (FlowJo, LLC). Of note, flow cytometry data from one DMF-treated and one untreated patient were excluded due to technical reasons.

2.3. Quantification of IgG and albumin

For each patient, blood and CSF were collected simultaneously. After centrifugation and removal of cells for immediate flow cytometry analysis, the serum and CSF supernatants were frozen at −80 °C. The supernatants were thawed and analyzed as a single batch within 36 months after the collection and freezing of the first patient sample. The collection and freezing procedures followed the published consensus protocol for the standardization of cerebrospinal fluid collection and biobanking (Teunissen et al., 2009). IgG and albumin in CSF were quantified by nephelometry (BN ProSpec Systems, Siemens). IgG and albumin in serum were determined by turbidimetry and colorimetry, respectively (Vitros 5.1 FS, Ortho Clinical Diagnostics).

2.4. Statistics

Statistical analyses were performed in JMP® pro 12.1 (StataCorp, LLC). Due to non-normality of data, non-parametric 2-sample Wilcoxon exact tests were used to compare groups unless otherwise specified. The significance level was set at 5%, and the tests were two-sided. No correction for multiple testing was performed. Results are presented as median [range]. Figures were made in FlowJo and JMP pro 12.1.

3. Results

3.1. Patients

Ten patients received treatment with DMF at inclusion, whereas 18 received other DMTs or no treatment (7 patients received glatiramer acetate, 4 received teriflunomide, and 7 received no treatment). Clinical and demographic data at the time of CSF and blood (including serum) collection are shown in Table 1. With the exception of treatment durations, which was shorter for the patients treated with DMF than other DMTs, there were no significant differences in clinical characteristics between DMF-treated patients and the other patients . All DMF-treated patients had normal total lymphocyte count before treatment start, with a median value of 1.7×10^9/L [1.2–2.6], and 2 patients developed lymphopenia during DMF treatment ($< 0.9 \times 10^9$/L).

3.2. DMF-treatment is associated with lower numbers of mononuclear cells in the CSF

DMF-treated patients had lower total CSF mononuclear cell counts compared to the other patients (560/mL [80–3000] vs 680/mL [264–6736], $p = 0.023$). Similar results were obtained when comparing DMF-treated patients to those not receiving any treatment (Fig. S1 A). The CSF mononuclear cell count in DMF-treated patients tended to correlate inversely with the treatment duration, but this was not statistically significant (Spearman r_s −0.6, $p = 0.07$).

3.3. DMF reduces the frequency of memory B cells in blood and plasmablasts in the CSF

Previous studies have shown that DMF reduces the number of memory B cells in blood (Smith et al., 2017; Longbrake et al., 2017; Li et al., 2017; Lundy et al., 2016), typically identified as $CD19^+CD27^+$ cells. To identify these cells in blood and CSF, a gating strategy based on available data was devised (Fig. 1). Confirming previous studies, we found that DMF-treatment was associated with a relative reduction in $CD19^+CD27^+CD38^-$ memory B cells in blood (12.8% [2.2–25.2] in DMF-treated vs 26.6% [6.9–46.6] in the other MS patients, $p = 0.0007$, Fig. 2A). Moreover, the reduction correlated strongly with treatment duration ($r_s = -0.75$, $p = 0.021$, Fig. 2B). There were no significant differences between the two groups in the proportions of $CD19^+CD27^+CD38^+$plasmablasts in blood (Fig. 2A). In the CSF, in contrast, there was a selective depletion of $CD19^+CD27^+CD38^+$ plasmablasts among DMF-treated patients (0% [0–13.6] vs 5.4% [0–69.8], $p = 0.031$, Fig. 2A), whereas the relative proportion of $CD19^+CD27^+CD38^-$ memory B cells was similar in both groups

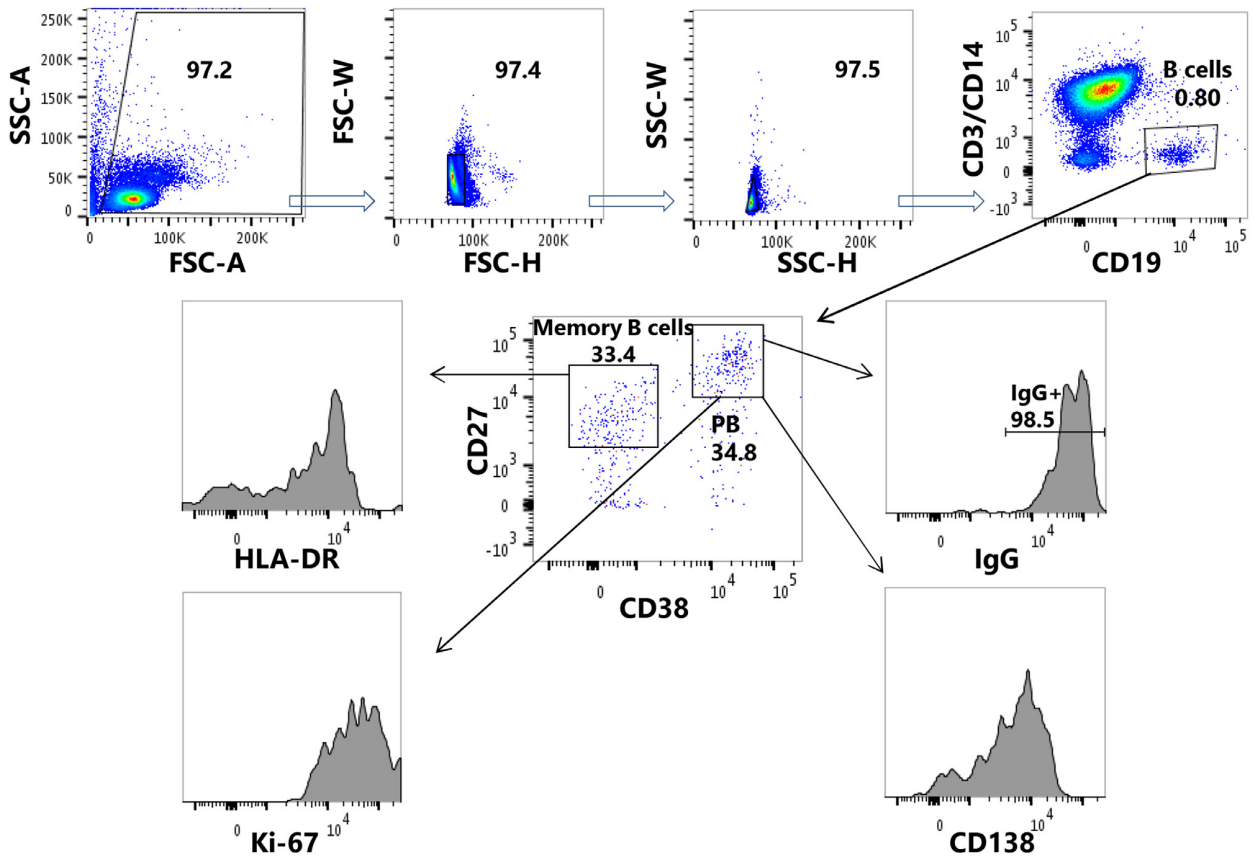

Fig. 1. Gating strategy. We devised a gating strategy to identify single lymphocytes expressing CD19, CD27, CD38, CD138, HLA-DR, IgG and/or Ki-67. Cells expressing CD3 or CD14 were excluded in a dump channel.

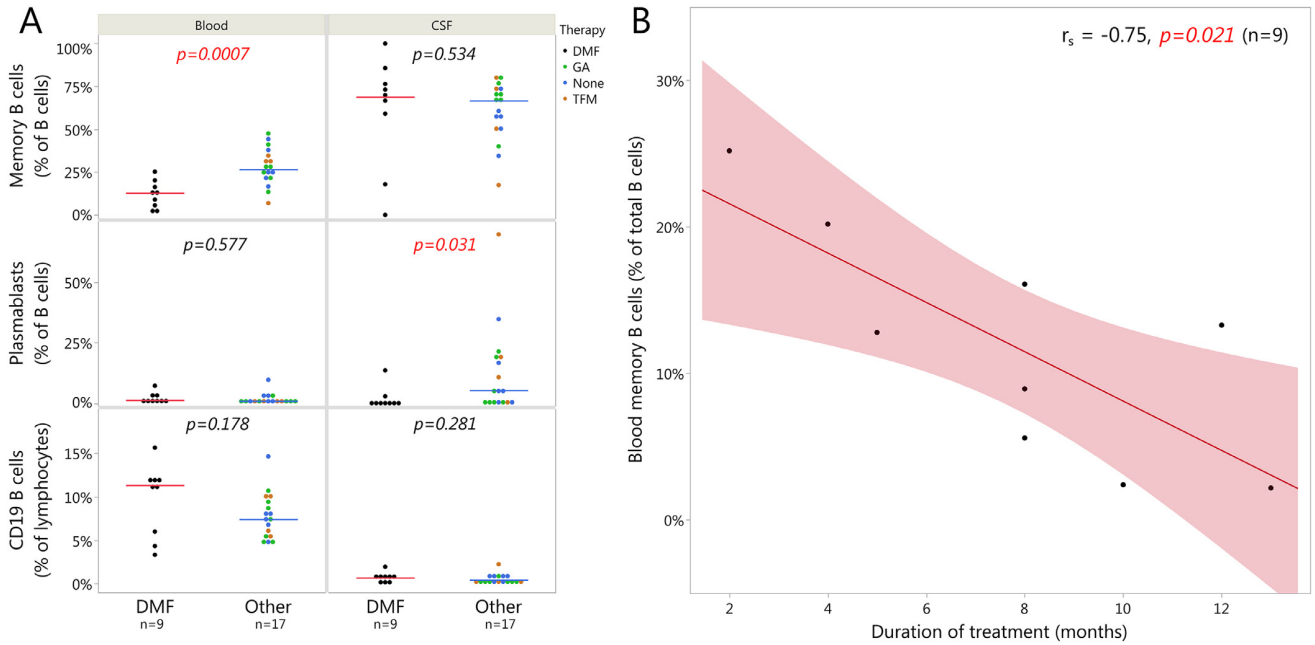

Fig. 2. DMF preferentially reduces the frequency of memory B cells in blood and plasmablasts in the CSF. (A) Proportion of $CD19^+CD27^+CD38^-$ memory B cells and $CD19^+CD27^+CD38^+$ plasmablasts of $CD19^+$ B cells, and proportion of $CD19^+$ B cells of lymphocytes in blood and CSF. Each symbol represents the cell frequencies in a given individual, and the bars depict the median. (B) Proportion of memory B cells in DMF treated patients, in linear fit with treatment duration (boundaries depict 95% confidence interval). DMF, dimethyl fumarate; GA, glatiramer acetate; TFM, teriflunomide.

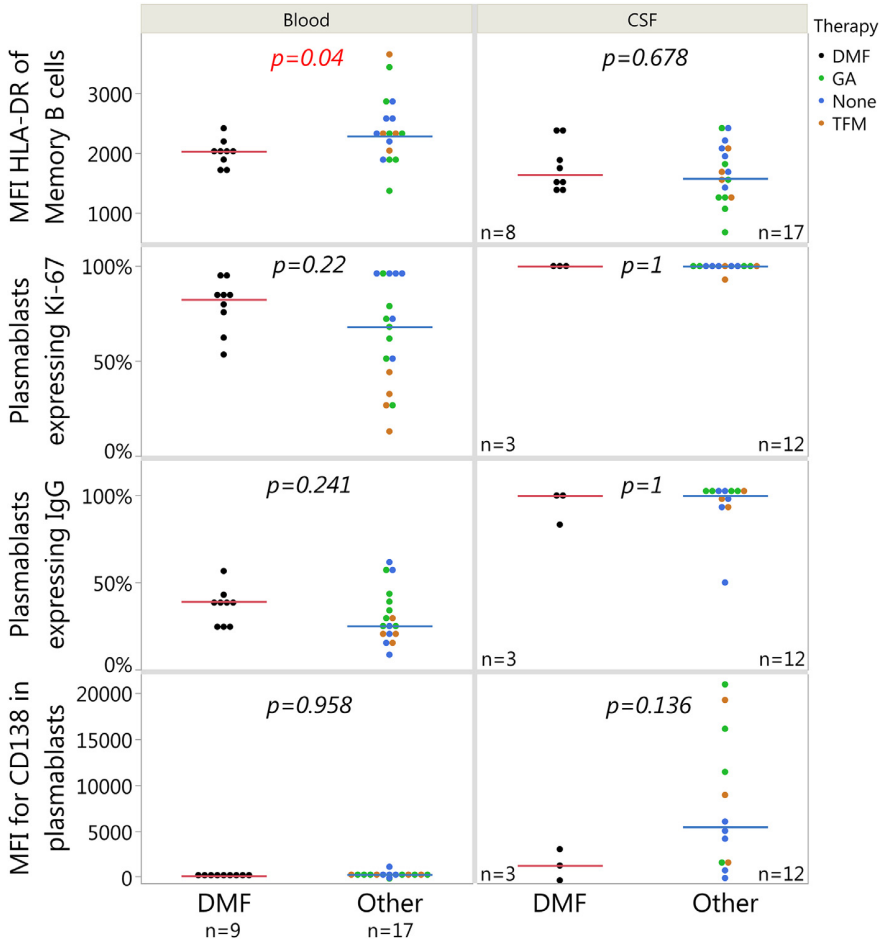

Fig. 3. DMF reduces HLA-DR expression among memory B cells in blood. MFI of HLA-DR for $CD19^+CD27^+CD38^-$ memory B cells, proportion of $CD19^+CD27^+CD38^+$ plasmablasts expressing Ki-67 and IgG, and MFI of CD138 for plasmablasts. Each symbol represents the cell frequencies or MFI in a given individual, and the bars depict the median. DMF, dimethyl fumarate; GA, glatiramer acetate; TFM, teriflunomide.

(68.9% [0–100] in DMF-treated vs 66.7% [17.4–80] in other MS-patients, $p = 0.534$, Fig. 2A). There were no differences between the two groups in the proportion of total $CD19^+$ B cells in blood or CSF (Fig. 2A). Including only DMF-treated and untreated patients in the analyses yielded similar results (Fig. S1 B).

3.4. DMF reduces HLA-DR expression among memory B cells in blood

To further characterize the B-cell subsets, we examined antigen-presenting potential (HLA-DR), IgG expression, proliferation status (Ki-67), and the expression of the differentiation marker CD138. In patients treated with DMF, we found that blood $CD19^+CD27^+CD38^-$ memory B cells express lower levels of the HLA class II molecule HLA-DR (median fluorescence intensity (MFI) 2025 [1702–2410] vs 2279 [1360–3649], $p = 0.04$, Fig. 3). The majority of blood plasmablasts expressed Ki-67 and IgG, and there were no significant differences between the patient groups (Fig. 3). We found overall low levels of CD138 expression among blood plasmablasts.

In the CSF, the HLA-DR expression among $CD19^+CD27^+CD38^-$ memory B cells was similar in both groups (MFI 1634 [1337–2391] vs 1570 [666–2414], $p = 0.68$). Virtually all intrathecal $CD19^+CD27^+CD38^+$ plasmablasts in both patient groups expressed Ki-67 and the majority expressed IgG (100% [83.3–100] vs 100% [50–100], Fig. 3). In most patients in both groups we found that CSF plasmablasts expressed moderate to high levels of CD138 (MFI 1223 [−392–2998] vs MFI 5437 [−142–20,911]). There were no significant differences for these variables between the patient groups (Fig. 3).

3.5. DMF treatment did not influence intrathecal IgG production

Since DMF-treated patients exhibited preferential reductions of $CD19^+CD27^+CD38^+$ antibody-secreting cells in CSF, we compared the intrathecal IgG production among DMF-treated patients ($n = 10$) with that among untreated patients ($n = 7$). There were no differences in IgG or albumin levels or indices of these, also indicating a similar blood–brain barrier integrity (Table 1).

4. Discussion

This cross-sectional study demonstrates that while DMF-treatment causes a time-dependent reduction in $CD19^+CD27^+CD38^-$ memory B cells in blood, it leads to a depletion of $CD19^+CD27^+CD38^+$ plasmablasts in the CSF. Our findings in blood are in agreement with recent publications (Smith et al., 2017; Longbrake et al., 2017; Li et al., 2017; Lundy et al., 2016), and the present work demonstrates how the peripheral effects of DMF translate into the CSF. These data point to a possible B-cell mediated mechanism of action for DMF, in addition to the previously discussed pluripotent immunomodulatory effects (Deeks, 2016).

The almost immediate effect of anti-CD20 treatment in MS is thought to be mediated by a reduction of B cells participating in antigen presentation and/or cytokine production (Funaro et al., 2016; Kinzel

and Weber, 2016). Accordingly, the intrathecal IgG production does not seem to be affected by the treatment in the short run (Hauser et al., 2017; Cross et al., 2006). Memory B cells express HLA class II molecules and are potent antigen-presenting cells (Kurosaki et al., 2015). Interestingly, we found that blood $CD19^+CD27^+CD38^-$memory B cells express lower levels of HLA-DR in DMF-treated than in untreated MS patients, suggesting that memory B cells in these patients are less efficient in presenting antigens. One could speculate that a reduced amount of memory B cells, with additionally reduced expression of HLA class II molecules, may result in less maturation and development of $CD19^+CD27^+CD38^+$antibody-secreting cells in the CSF. This possibility is supported by the dynamic exchange of B cells between the CSF and periphery (Obermeier et al., 2011; Stern et al., 2014; von Budingen et al., 2012; Johansen et al., 2015). However, a not mutually exclusive possibility is that the observed alterations in the composition of CSF B cells could be due to a local intrathecal effect of MMF.

Despite depletion of $CD19^+CD27^+CD38^+$ plasmablasts in the CSF of DMF-treated patients, we did not observe a reduced intrathecal IgG production. This could be due to persistent secretion from end-differentiated plasma cells protected within tertiary lymphoid tissue in the meninges of MS patients (Pikor et al., 2016). In line with this thought, we found that all antibody-secreting cells in the CSF express high levels of Ki-67, compatible with recently derived proliferating plasmablast. Interestingly, a similar persistence of intrathecal IgG synthesis has been observed in patients receiving anti-CD20 therapies (Hauser, 2015). In accordance with the present findings, no difference in circulating IgG, IgA, or IgM in blood of DMF treated patients has been observed, indicating that end differentiated plasma cells could be protected from the effects of the drug also in the periphery in a short-term perspective (Longbrake et al., 2017).

The strength of this study is the comparison of CSF B cell subsets between two groups of MS patients similar in clinical and demographic characteristics. This was made possible by slight different treatment strategies between the two clinical departments contributing to the study. Samples from both hospitals were transported directly to the same external laboratory and processed identically, and the findings are not influenced by differences in inflammatory activity. Although we cannot exclude that differences in treatment durations could have influenced the results, treatment durations were long enough to allow full immunological effect in the majority of patients receiving DMF and other DMTs.

This study has several limitations. First, the number of patients is small. Given the risk of lumbar puncture headache, as well as rare but more serious risks such as infection, bleeding and herniation, we cannot perform lumbar puncture solely for the purpose of studying drug effects. While properly understanding the mechanism of action of DMF in MS patients is important, such studies must due to the above reasons be part of studies on disease mechanisms, which was the primary aim of this study (Lossius et al., 2017). This is therefore an exploratory study, the *p*-values were not corrected for multiple testing, and the results need to be reproduced in an independent study. Second, the control group is heterogeneous from a treatment standpoint, which potentially could confound our results. Nevertheless, as the sub-analysis with untreated controls ($n = 7$) demonstrated similar results, and lymphocyte depletion and reduced memory B cell population in blood are analogue to previous reports (Smith et al., 2017; Longbrake et al., 2017; Li et al., 2017; Lundy et al., 2016)' we believe our findings have merit. While reduction in blood plasmablasts similar to what we observed in CSF have not been extensively described, a recent interim analysis of the PROCLAIM study demonstrated a decline in blood plasmablasts that had a delayed onset compared to memory B cell depletion (von Hehn et al., 2017). This delay, in addition to the relatively low proportions of circulating plasmablasts in blood compared to CSF of MS patients can potentially have hidden this phenomenon in studies with shorter timeframes. Lastly, as our data did not contain markers for IgD, we were unable to differentiate between class-switched and unswitched memory B cells. A recent publication limited to blood found that both populations are affected similarly, with a corresponding increase in $CD27^-IgD^+$ naïve B cells (Nakhaei-Nejad et al., 2018). New studies as to how these subpopulations are distributed in the CSF could also enlighten whether the effects of DMF are mainly peripheral or intrathecal.

5. Conclusion

This is the first study on the effects of DMF treatment on B cells in CSF, suggesting that while memory B cells are reduced in blood, plasmablasts are preferentially depleted in CSF. These findings, which need to be verified in an independent study, support the hypothesis that DMF mediates positive effects through B-cell modulation.

Funding

The study was supported by the South-Eastern Norway Regional Health Authority (grant 2016079) and the Norwegian Research Council (grant 250864/F20).

Conflict of interests

RH has received speaker honoraria from Merck and Roche, and unrestricted research grants from Biogen and Novartis. TH has received unrestricted research grants or speaker honoraria from Biogen, Merck, Novartis, Sanofi Genzyme and Teva. AL has received speaker honoraria from Roche, and unrestricted research grants from Sanofi Genzyme. JP and FV declare no conflict of interest.

Author contributions

Study concept and design: A.L., F.V., R.H., T.H.; data acquisition and/or analysis: A.L., J.P., R.H.; drafting the manuscript A.L., R.H.. All authors revised the manuscript for intellectual content.

Supplementary materials

Supplementary material associated with this article can be found, in the online version, at doi:10.1016/j.msard.2018.08.032.

References

Bar-Or, A., Calabresi, P.A., Arnold, D., et al., 2008. Rituximab in relapsing-remitting multiple sclerosis: a 72-week, open-label, phase I trial. Ann. Neurol. 63, 395–400. https://doi.org/10.1002/ana.21363.

von Budingen, H.C., Kuo, T.C., Sirota, M., et al., 2012. B cell exchange across the blood-brain barrier in multiple sclerosis. J. Clin. Invest. 122, 4533–4543. https://doi.org/10.1172/jci63842.

Cepok, S., Rosche, B., Grummel, V., et al., 2005. Short-lived plasma blasts are the main B cell effector subset during the course of multiple sclerosis. Brain J. Neurol.y 128, 1667–1676. https://doi.org/10.1093/brain/awh486.

Cross, A.H., Stark, J.L., Lauber, J., et al., 2006. Rituximab reduces B cells and T cells in cerebrospinal fluid of multiple sclerosis patients. J. Neuroimmunol. 180, 63–70. https://doi.org/10.1016/j.jneuroim.2006.06.029.

Deeks, E.D., 2016. Dimethyl fumarate: a review in relapsing-remitting MS. Drugs 76, 243–254. https://doi.org/10.1007/s40265-015-0528-1.

Edwards, K., Penner, N., Rogge, M., et al., 2016. A pharmacokinetic study of delayed-release dimethyl fumarate to evaluate cerebrospinal fluid penetration in patients with secondary progressive multiple sclerosis. ePosters EP1501. Mult. Scler.s J. 22 (3_suppl), 706–827. https://doi.org/10.1177/1352458516663067.

Eggers, E.L., Michel, B.A., Wu, H., et al., 2017Eggers. Clonal relationships of CSF B cells in treatment-naive multiple sclerosis patients. JCI Insight 2 (22), e92724. https://doi.org/10.1172/jci.insight.92724.

Funaro, M., Messina, M., Shabbir, M., et al., 2016. The role of B cells in multiple sclerosis: more than antibodies. Discov. med. 22, 251–255.

Hauser, S.L., Bar-Or, A., Comi, G., et al., 2017. Ocrelizumab versus Interferon Beta-1a in Relapsing Multiple Sclerosis. N. Engl. J. Med. 376, 221–234.

Hauser, S.L., 2015. The Charcot lecture | beating MS: a story of B cells, with twists and turns. Mult. Scler. 21, 8–21. https://doi.org/10.1177/1352458514561911.

von Hehn, C., Mehta, D., Prada, C., et al., 2017. Interim results of an open-label study to assess the effects of delayed-release dimethyl fumarate on lymphocyte subsets and immunoglobulins in patients with relapsing-remitting multiple sclerosis. In: Poster 380 presented at American Academy of Neurology - 69th Annual Meeting, Session P5,

MS and CNS Inflammatory Disease, April 27. Accessed online May 25, 2018 at http://submissions.mirasmart.com/Verify/AAN2017/Submission/Temp/radFD3DA.pdf
Johansen, J.N., Vartdal, F., Desmarais, C., et al., 2015. Intrathecal BCR transcriptome in multiple sclerosis versus other neuroinflammation: equally diverse and compartmentalized, but more mutated, biased and overlapping with the proteome. Clin. immunol. 160, 211–225. https://doi.org/10.1016/j.clim.2015.06.001.
Kappos, L., Li, D., Calabresi, P.A., et al., 2011. Ocrelizumab in relapsing-remitting multiple sclerosis: a phase 2, randomised, placebo-controlled, multicentre trial. Lancet 378, 1779–1787. https://doi.org/10.1016/s0140-6736(11)61649-8.
Kinzel, S., Weber, M.S., 2016. B Cell-directed therapeutics in multiple sclerosis: rationale and clinical evidence. CNS Drugs 30, 1137–1148. https://doi.org/10.1007/s40263-016-0396-6.
Kowarik, M.C., Grummel, V., Wemlinger, S., et al., 2014. Immune cell subtyping in the cerebrospinal fluid of patients with neurological diseases. J. Neurol. 261, 130–143. https://doi.org/10.1007/s00415-013-7145-2.
Kurosaki, T., Kometani, K., Ise, W., 2015. Memory B cells. Nat. Rev. Immunol. 15, 149–159. 2015/02/14, doi:10.1038/nri3802.
Lehmann-Horn, K., Kinzel, S., Weber, M., 2017. Deciphering the Role of B Cells in multiple sclerosis—towards specific targeting of pathogenic function. Int. J. Mol. Sci. 18, 2048.
Li, R., Rezk, A., Ghadiri, M., et al., 2017. Dimethyl fumarate treatment mediates an anti-inflammatory shift in Bcell subsets of patients with multiple sclerosis. J. Immunol. 198, 691–698. https://doi.org/10.4049/jimmunol.1601649.
Longbrake, E.E., Cantoni, C., Chahin, S., et al., 2017. Dimethyl fumarate induces changes in B- and T-lymphocyte function independent of the effects on absolute lymphocyte count. Mult. Scler. 1352458517707069, doi:10.1177/1352458517707069.
Lossius, A., Tomescu-Baciu, A., Holmoy, T., et al., 2017. Selective intrathecal enrichment of G1m1-positive B cells in multiple sclerosis. Ann. Clin. Transl.l Neurol. 4, 756–761. https://doi.org/10.1002/acn3.451.
Lundy, S.K., Wu, Q., Wang, Q., et al., 2016. Dimethyl fumarate treatment of relapsing-remitting multiple sclerosis influences B-cell subsets. Neurol.(R) Neuroimmunol. Neuroinflamm. 3, e211. https://doi.org/10.1212/nxi.0000000000000211.
Nakhaei-Nejad, M., Barilla, D., Lee, C.-H., et al., 2018. Characterization of lymphopenia in patients with MS treated with dimethyl fumarate and fingolimod. Neurol. – Neuroimmunol. Neuroinflamm. 5. https://doi.org/10.1212/nxi.0000000000000432.
Obermeier, B., Lovato, L., Mentele, R., et al., 2011. Related B cell clones that populate the CSF and CNS of patients with multiple sclerosis produce CSF immunoglobulin. J. Neuroimmunol. 233, 245–248. https://doi.org/10.1016/j.jneuroim.2011.01.010.
Penner, N., Zhu, B., Woodward, C., et al., 2016. Penetration of dimethyl fumarate into cerebrospinal fluid and brain: a pharmacokinetic and tissue distribution study in monkeys. Poster Session 1, P672. Mult. Scler. J.l 22 (3_suppl), 88–399. 277, doi:10.1177/1352458516663081.
Pikor, N.B., Prat, A., Bar-Or, A., et al., 2016. Meningeal tertiary lymphoid tissues and multiple sclerosis: a gathering place for diverse types of immune cells during CNS autoimmunity. Front. immunol. 6. Mini Review, doi:10.3389/fimmu.2015.00657
Polman, C.H., Reingold, S.C., Banwell, B., et al., 2011. Diagnostic criteria for multiple sclerosis: 2010 revisions to the McDonald criteria. Annals of neurology 69, 292–302. 2011/03/10, doi:10.1002/ana.22366
Smith, M.D., Martin, K.A., Calabresi, P.A., et al., 2017. Dimethyl fumarate alters B-cell memory and cytokine production in MS patients. Ann. clin. transl neurol. 4, 351–355. https://doi.org/10.1002/acn3.411.
Stern, J.N., Yaari, G., Vander Heiden, J.A., et al., 2014. B cells populating the multiple sclerosis brain mature in the draining cervical lymph nodes. Sci. Transl. Med. 6, 248ra107. https://doi.org/10.1126/scitranslmed.3008879.
Teunissen, C.E., Petzold, A., Bennett, J.L., et al., 2009. A consensus protocol for the standardization of cerebrospinal fluid collection and biobanking. Neurology 73 (22), 1914–1922. https://doi.org/10.1212/WNL.0b013e3181c47cc2.